

Referee #4 and Referee #5

Referee #4

Although this paper has improved from its first iteration, it is still poorly written and requires major revision before it is in acceptable form.

My main complaints are the writing is very unclear in distinguishing behavior reproduced by the model and behavior that is actually observed. There are also numerous logical inconsistencies. For example, there are sentences where something is stated emphatically, and then controverted in the same paragraph.

While I have skimmed the prior reviews, as a new reviewer, I have consciously tried to put them aside and treat this as new submission (there are just too many comments to sort out whether earlier reviewers comments have been appropriately dealt with – I am focusing more on the quality of the revised paper). As such, some of my comments may seem redundant (probably a good indication comments by other reviewers were not fully addressed).

Below I include point by point issues throughout the paper, some of which are minor grammatical things and other which are major flaws.

In particular, the paper should make an effort to explain clearly to the reader why a particular forcing is causing a particular behavior. As a total made up example of how it should read: Warmer temperatures in the model induce more hydrofracturing in the model, causing more frequent calving, which accelerates terminus retreat. As just mentioned, this only mean to illustrate how something should be stated. The way such a statement would read in the current manuscript is. Climate produced more terminus retreat (see SI). Readers should not have to refer to the SI to get the gist of what is being said (the SI should have the details of the model, not the main results.)

Authors: Significant improvements have been made in the manuscript and SI such that any comments raised have been carefully addressed and resolved. Most of the text in SI has been moved to the main manuscript to ease reading and increase consistency. Any inconsistencies in the manuscript have been tracked and resolved. The quality of the writing has certainly improved and the difference between modelled results and what is deduced from the observations has become clear now.

Point by point answer is given below.

Specific Comments:

P1L28 “We find that most of the JI retreat during 27 1990-2014 is driven by ocean forcing and bed geometry.” This is more or less what the model shows, but as noted in the paper there are other effects (e.g., meltwater in crevasses) that are not modelled. So a more accurate statement would be

“In our simulations most of the JI retreat during 27 1990-2014 is driven by ocean forcing and the glaciers subsequent response, which is largely governed by bed geometry. Other processes not included in the model (e.g., melt water driving hydrofracture) may also be important.”

Authors: Done.

P2L2 “We identify two major accelerations that are consistent with observations of changes in 2 glacier terminus.” This paper is not identifying any accelerations. Instead the text should say “Our model simulates two major accelerations....”

Authors: Done.

P2L7 “And as the slope steepened inland” This is totally unclear. I think what is meant is “as the terminus retreated over a reverse bed slope into deeper water....”

Authors: Agree. Done.

P2L8 “Our model provides evidence that the 1998 and 2003 flow accelerations are most likely initiated by the bed geometry.” This is an example of what I mean by logistical inconsistency. The bed is not doesn’t initiate anything. Instead it governs the response to the ocean or other forcing that initiates (triggers) the retreat.

Authors: Agree. The statement is replaced with:

“Our model provides evidence that the 1998 and 2003 flow accelerations are most likely initiated by ocean forcing but JIs subsequent dynamic response is determined by its own bed geometry.”

P2L9 “reproduce” would be a better word than “capture”

Authors: Done.

P12 “Both modelled and observed results suggest that JI has been losing mass at an accelerated 12 rate, and that JI continued to accelerate throughout 2014.” Other papers have already shown this and this is not a new finding of this paper. Instead it should say something like “Our model is able to simulate the previously observed increase in mass loss through 2014”

Authors: Done.

P2L16 There is some ambiguity here between ice loss due to discharge and net ice loss (difference between discharge and smb). At a minimum it should say “net ice loss” since discharge has not doubled. Would make sense to include a reference to Enderlyn et al, 2014 here as it is the most current estimate.

Authors: Done.

P2L25 “Joughin et al, 2004” would be the better reference here because it was the first to covers this time period.

Authors: Done.

P3L12 “reduction in resistance (buttressing) at the marine front through thinning or retreat of the floating tongue of the glacier.” Much of the time it is the retreat of the grounded (not floating terminus).

Authors: Agree. The statement is changed to:

“One process is a reduction in resistance (buttressing) at the marine front through thinning or retreat of the glacier termini.”

P3L28 “climatic forcing and oceanic boundary conditions.” The ocean in large part determine climate. I think there are many places below where climate is used where “atmospheric is actually what is meant. In this case both are forcing – so “ocean and atmospheric forcing” makes this separation clearer.

Authors: Agree. The statement here, and in other locations, is changed to “atmospheric forcing”.

e.g.

“Our modelling approach is based on a regional equilibrium simulation and a time-integration over the period 1990 to 2014, where the grounding lines and the calving fronts are free to evolve under ocean and monthly atmospheric forcing.”

P4L21 “thickness in the JI basin is computed as the difference between surface and bedrock elevation, which implies that at the beginning of our equilibrium simulation JI’s terminus is considered to be grounded.” Part of the time Jakobshavn has had a long extended ice tongue, and part of the time it has had a short (<few km) or non-existent tongue (i.e., vertical calving face). There should be a clearer discussion in the main text as to how these two types (vertical vs. horizontal melting). Also in the case mentioned here, what does it mean to be “grounded” (is there melting or not, is there basal friction or not). This is an important aspect of the model and it should clearly stated.

Authors:

- For **what does it mean to be “grounded”** we have added
“(i.e. no ice floating tongue exists)”
- For **how these two types (vertical vs. horizontal melting)** we have added

“Following this melting parametrization, the highest melt rates are modelled in the proximity of the glacier grounding lines and decrease with elevation such that the lowest melt rates are closer to the central to frontal area of the modelled ice shelves. At the grounding line, the sub-grid scheme (Albrecht et al., 2011; Feldmann et al., 2014) interpolates the sub-shelf melt rate, allowing for a smooth transition between floating and grounded ice. For a completely grounded terminus (i.e. no ice floating tongue exists) the melt parametrization is applied only at the grounding line position.”

However, do not that during the forward runs the terminus is never completely grounded!

P5L27 “The calving law is known to yield realistic calving” “appears to” rather than “is known” is a better way to put it.

Authors: Done.

P6L3 “which” should be changed to “that”

Authors: Done.

Section 2.1.3 There is a lot of detail here, yet the section says very little about how the ocean is represented in the model. A clear description of what the model does is in order (some of the detailed equations could go in the supplement).

Authors: Done. Section 2.1.3 in the new version of the manuscript has been widely rewritten. The way the ocean is represented in the model is clear now. The detailed equations have been moved to the supplement.

“We use a simple parametrization for ice shelf melting where the melting effect of the ocean is based on both sub-shelf ocean temperature and salinity (Martin et al., 2011). To accommodate this parametrization, several changes have been made to PISM at the sub-shelf boundary (Winkelmann et al., 2011). First, the ice temperature at the base of the shelf (the pressure-melting temperature) is calculated from the Clausius-Clapeyron gradient and the elevation at the base of the shelf, and then the temperature is applied as a Dirichlet boundary condition in the conservation of energy equation.

Secondly, basal melting and refreezing is incorporated through a sub-shelf mass flux used as a sink/source term in the mass-continuity equation. This mass flux from shelf to ocean (Beckmann and Goosse, 2003) is computed as a heat flux between the ocean and ice and represents the melting effect of the ocean due to both temperature and salinity (Martin et al., 2011).

We start our simulations with a constant ocean water temperature (T_o) of -1.7°C , which here represents the mean surface ocean temperature in the grid cells adjacent to the JI terminus. In the heat flux parametrization, the ocean temperature at the ice shelf base is computed as the difference between the input ocean temperature and a virtual temperature that represents the freezing point temperature of ocean water below the ice shelf (Fig. S4). The freezing point temperature is calculated based on the elevation at the base of the shelf and the ocean water salinity. As a consequence of these constraints, as the glacier retreats and/or advances, both the pressure-melting temperature and the heat flux between the ocean and ice evolve alongside the modelled glacier ice shelf geometry. The ocean water salinity ($S_o=35$ psu) is kept constant in time and space as the model does not capture the salinity gradient from the base of the ice shelf through layers of low and high salinity. A previous study conducted by Mengel and Levermann (2014) using the same model established that the sensitivity of the melt rate to salinity is negligible.

Following this melting parametrization, the highest melt rates are modelled in the proximity of the glacier grounding lines and decrease with elevation such that the lowest melt rates are closer to the central to frontal area of the modelled ice shelf. At the grounding line, the sub-grid scheme (Albrecht et al., 2011; Feldmann et al., 2014) interpolates the sub-shelf melt rate, allowing for a smooth transition between floating and grounded ice. For a completely grounded terminus (i.e. the case when no ice floating tongue exists), the melt parametrization is applied only at the grounding line position.”

P8Section 3: While I realized the parameters are in a table, something more descriptive about what processes are represented by the parameter space should be included.

Authors: Done.

“This section is organized in two main subsections. Sect. 3.1 introduces the results obtained relative to observations, and Sect 3.2 focuses mainly on the limitations of the model that need to be considered before a final conclusion can be drawn. A short introduction to the different simulations and preparatory experiments performed is given below.

A total number of fifty simulations with different sets of parameters (excluding preparatory and additional experiments on the 1 km) are performed on a 2 km grid. We alter the parameters controlling the ice dynamics (e.g. the flow enhancement factor, the exponent of the pseudo-plastic basal resistance model, the till effective fraction overburden, etc.) but also parameters related with ice shelf melt, ocean temperature, and calving (i.e. the ice thickness threshold in the basic calving mechanism). These parameters are modified only during the regional JI runs such that the model reproduces the frontal positions and the ice mass change observations at JI during the period 1990-2014 (Fig. 2) and 1997-2014 (Fig. 4), respectively. From these results, we present the parameterization that best captures the full observed evolution of JI during the period 1990–2014. The values of the ice sheet model parameters used, together with their underlying equations and the ice sheet model sensitivity to parameters controlling ice dynamics, basal processes, ice shelf melt, and ocean temperature, are further illustrated in the supplementary material (SI).”

P8L26” The first speedup is caused by a retreat...” Change to “The first speedup PRODUCED BY THE SIMULATION is caused by a retreat....

Authors: Done.

P9L4 “Starting in 1992 we obtain a good fit between modelled and observed frontal 4 positions.” Try “Starting in 1992, the modelled and observed terminus positions agree well.”

Authors: Done.

P9L7 “From 1993 a stronger seasonal 7 velocity signal begins to emerge in our simulation that continues and intensifies in 8 magnitude during 1994 and 1995” It looks like there is sub-annual variability, not necessarily seasonal variability (i.e., the period of the variation is not necessarily close to annual).

Authors: Done.

P9L14 “The modelled velocities for 1992 and 1995 are consistent with observed” There are only limited velocities during this time and they show constant winter velocity. Since you have just noted sub-annual variability, which observations are too sparse to confirm or refute, you need to be clearer here about what the agreement is (for example you mean-annual velocity may agree well with the 1992 and 1995 data).

Authors: Done.

“Modelled mean-annual velocities for 1992 and 1995 are consistent with observed velocities for the same period (Joughin et al., 2008; Vieli et al., 2011).”

P9L24 “of the terminus in 1997-1998” add “ice tongue’s” before terminus to remind readers it was floating.

Authors: Done.

P928These findings are corroborated both by observations 28 (SI, Fig. S15) and modelling results (Fig. 3). Although thinning appears to have 29 increased in our model during three continuous years we find little additional 30 speedup during the period prior to 1998 (Figs. 2, 6, and S7). Since you have just mentioned both observations and model results in the earlier part of the paragraph, it would be clearer to say “The modelled behavior agrees well with the observations of the observed behavior [CITE REFS]. Rather than “we find little additional 30 speedup during the period prior to 1998” Although thinning appears to have 29 increased in our model during three continuous years , it produced only minor additional speedup during the period prior to 1998 (Figs. 2, 6, and S7).

Authors: Done.

“The modelled behaviour agrees well with observations of the observed behaviour (Krabill et al., 2004). Although thinning appears to have increased in our model during three continuous years, it produced only minor additional speedup during the period prior to 1998 (Figs. 2, 6, and 7).”

P9L31 Change “According to...” to “In our...” The way it sounds as written, you are speculating that this is what actually happened, based on inference from the model. A better way to state this would be: In our simulation, JI’s speed increased in the summer of 1998 by ~ 80% relative to the summer of 1992 (Fig. 3), at which time the grounding line position starting starts to retreat thereafter (Figs. 2, 6, and S7). Observations (cite luckman) do not show this level of speedup and there are no observations of the grounding line position at this time with which to assess our model performance.

Authors: Done.

P10L3 “between 1999 and 2002 is in our simulation characterized by a temporal uniform 3 flow, with no episodes of significant terminus retreat” This is not an accurate statement of the behavior shown in figure 3, particularly at “S1”. There is not much apparent trend, but the speed is varying substantially with time.

Authors: Done. The statement is removed.

P10L12 “In the late summer of 2003, an increase in flow velocity is observed (Fig. 3),” don’t use the word “observed” for your model, its too confusing since there are many references to actual observations.

Try “In the late summer of 2003, the simulated flow velocity increases....”

Authors: Done.

P10L16 “By December 2003 the terminus has retreated back to the position of the 16 grounding line” Would be better to say something like “By December 2003 the modeled ice tongue has completely disintegrated so that the terminus is grounded.

Authors: Done.

P10L17 Add “simulated” before retreat.

Authors: Done.

P10L20 “During the final breakup of the ice tongue, JI reached unprecedented 21 flow rates, which in our simulation are as high as 20 km a-1” During the final breakup of the ice tongue, the simulation produces speeds high as 20 km a-1(substantially higher than the sparse observations from that time[REF]).

Authors: We don't have any observations during 2003 and 2004. For 2004 there are no available observations (not even by Joughin et al.) The sparse available observations for 2003 available in Joughin et al 2012 (see e.g., Joughin et al. 2012 – Fig. 4) are from early 2003 (before the breaking of the floating tongue) and an eye ball comparison suggests that they more or less agree with our modelled velocities.

Furthermore, our S1-S6 points are much closer to the terminus when compared to the M points from e.g. Joughin et al 2012, Fig.1 (M6-M20). As such, one should not expect that our modelled velocities in S1-S6 will completely match figures in Joughin et al. from e.g., 2003 or thereafter.

Therefore, we have added:

*“During the final breakup of the ice tongue, the simulation produces speeds high as 20 km a-1 (~ 120% increase relative to 1998). The modelled velocities decreased to 16 km a-1 (~ 80% increase relative to 1998) in the subsequent months and remain substantially higher **than the sparse observations from that time (Joughin et al., 2012)).**”*

L10L23 “The velocities...” insert “modelled”

Authors: Done.

P10L24 replace “seasonal” with “sub-annual”

Authors: Done.

P10L25 replace “observed at” with “modelled for” (This is a good example where the text is written such its hard to tell modelled from observed behavior – be very clear when you are describing the model, when you are describing data, and when there is and isn't good agreement between the two).

Authors: Done.

P10L32 “seasonal” -> “sub-annual”

Authors: Done.

P11L1 “the terminus remained close to the grounding line” add “(i.e., the terminus remained grounded or only a small floating ice tongue existed)”

Authors: Done.

P11L7 “In terms of seasonality, our results suggest that most of the seasonal signal in the model is climate driven (see SI, Sect. 1.4 and Fig. S12).” For a concluding sentence, I shouldn't have to go see these

other sections. Basically I really don't really know here what is meant by "climate driven", especially since the "seasonal" variation don't seem seasonal. Elsewhere in the paper a better explanation is given, which is that the coarseness of the grid induce much of this variability (i.e., 4km² calving events).

Authors: The whole section has been adjusted to ease reading. This particular part has been rewritten as:

"In terms of seasonality, the only seasonal signal in the model is introduced by the monthly atmospheric forcing applied (Sect. 2). However, the modelled sub-annual variability in terms of terminus retreat and velocities does not always follow a seasonal signal (Fig. 3)." In the new version of the manuscript we have made a clear separation between seasonal induced signal and sub-seasonal variability:

In our model, the atmospheric forcing applied can influence JI's dynamics only through changes in surface mass balance (SMB) (i.e., accumulation and ablation) (Fig. S2). While these changes in ice thickness affect both the SIA and the SSA (Sect. 2.1), the effect in the SIA is very weak as the driving stresses are not affected by a few meters of difference in thickness induced by SMB variability. In the SSA, the coupling is achieved via the effective pressure term in the definition of the yield stress (see SI, Sect. 1.2 for detailed equations). The effective pressure is determined by the ice overburden pressure (i.e., ice thickness) and the effective thickness of water in the till, where the latter is computed by time-integrating the basal melt rate. This effect is much stronger and favours the idea that in our model some seasonal velocity peaks could potentially be influenced by the climatic forcing applied (Figs. S10 and S15).

We study the sensitivity of the model to atmospheric forcing by performing a simulation where we keep the atmospheric forcing constant (mean 1960-1990 temperature and SMB). By comparing this simulation with a simulation that includes full atmospheric variability (monthly temperature and SMB) we see that in terms of terminus retreat and velocities the modelled sub-annual variability does not always correlate with the observed seasonal signal (Fig. S15). In particular, the simulations suggest that to only a relatively small degree some of the variability appears to be influenced by the atmospheric forcing applied (Figs. S2, S10 and S15), which also represents the only seasonal input into the model. Some of the greater than seasonal frequency could be an issue with resolution in the model. We examined this sensitivity by performing additional runs at a higher spatial resolution. Simulations on a 1 km grid did show some improvement with respect to surface speed sub-annual variability (Fig. S13), suggesting that in our model the stress redistribution might be sensitive to the resolution of the calving event. However, given the short period spanned by the simulations, the stress redistribution does not change the overall modelled results, as seen in Figs. S11 and S12. Although we acknowledge that some of the variability is due to the grid resolution, part of it may also be related to unmodeled physical processes acting at the terminus. We suggest that additional contributions to the seasonality, e.g. from ice mélange or seasonal ocean temperature variability, which are not included in our model could potentially influence the advance and retreat of the front at seasonal scales (Fig. S15). For example, the ice mélange can prevent the ice at the calving front from breaking off and could therefore reduce the calving rates. Consequently, the introduction of an ice mélange parametrization will probably help to minimize some of the sub-annual signal modelled in our simulations. Similarly, seasonal ocean temperature variability can influence ice mélange formation and/or clearance and the melt rates at the glacier front and can accentuate seasonal glacier terminus and grounding line retreat and/or advance. However, at this point we find it difficult to determine the relative importance of each process."

L11L18 Remove all reference to the elastic loading, it really add nothing to the paper. Figure 4 does a nice job of making the point that your reproducing the mass loss. The loading stuff doesn't add anything new and just adds unnecessary complexity to the paper.

Authors: The loading does add useful value because it tells something about the distribution of the mass, information which is not provided by the mass loss.

Note for example, Sect. 3.1.2:

“Both model and observations consistently suggest large uplift rates near the JI front (20 mm a^{-1} for station KAGA) and somewhat minor uplift rates ($\sim 5 \text{ mm a}^{-1}$) at distances of $>100\text{km}$ from the ice margin.”

L12L20 “The glacier terminus in 20 1990s is known to have been floating” so remind us again why its not floating in the model (e.g., Figure 6).

Authors: The whole paragraph has been rewritten:

“As introduced in Sect. 2, our approach here is to adjust the terminus in the JI region to simulate the 1990s observed front position and surface elevation based on 1985 aerial photographs (Csatho et al., 2008). The glacier terminus in 1990s was floating (Csatho et al., 2008; Motyka et al. 2011). Motyka et al. (2011) calculated the 1985 hydrostatic equilibrium thickness of the south branch floating tongue from smoothed surface DEMs and obtained a height of 600 m near the calving front and 940 m near the grounding zone. In this paper, however, we compute the thickness as the difference between the surface elevation and the bed topography, and allow the glacier to evolve its own terminus geometry during the equilibrium simulation. Preparatory experiments have shown that in our model (disregarding its initial geometry floating/ grounded terminus) JI attains equilibrium with a grounding line position that stabilizes close to the 1990s observed terminus position. According to observations, JI is characterized in 1990 by a large floating tongue ($> 10 \text{ km}$; e.g. Motyka et al., 2011) that we are not able to simulate during the equilibrium runs. In our model (Fig. 6), the glacier starts to develop a large floating tongue ($\sim 10 \text{ km}$) in 1999. Starting in 2000, the floating tongue is comparable in length and thickness with observations and the model is able to simulate, with a high degree of accuracy, its breakup that occurred in late summer 2003 and the subsequent glacier acceleration. Observations of terminus positions (Sohn et al., 1998; Csatho et al., 2008) suggest that over more than 40 years, between 1946 and 1992, JIs terminus stabilized in the proximity of the 1990's observed terminus position. Furthermore, during 1959 and 1985 the southern tributary was in balance (Csatho et al., 2008). This suggests that, during the equilibrium and at the beginning of the forward simulations, we are forcing our model with climatic conditions that favoured the glacier to remain in balance. This may explain our unsuccessful attempts to simulate prior to 1998 a floating tongue comparable in length and thickness with observations, and suggests that for simulating the large floating tongue that characterized JI during this period, future studies should consider to start modelling JI before the glacier begins to float in the late 1940s (Csatho et al., 2008).”

L12L20 “but details 21 regarding its thickness are not known.” There are lots of lidar lines on the tongue in this period, from which thickness can be inferred (with some uncertainty).

Authors: The statement has been deleted.

L12L26 “thickness as the difference between the surface elevation and the bed. This implies that our 26 simulations start with a grounded terminus.”

Our choice is to allow the glacier to evolve its own terminus geometry. See also the explanation above.

Why is this being done. If the terminus is grounded, how can the ocean force the glacier in a realistic way. As mentioned above, what basal traction is used (loss of this traction will have an effect on the speedup, which didn't occur on true tongue since it was floating).

Authors: During the forward simulations the glacier is never grounded (Fig. 6)! The terminus is grounded only at the beginning of the equilibrium simulation. Calving (Sect. 2.1.2) can only occur when the thickness of the tongue is lower than approx. 500 m. This has been better explained in the new version of the manuscript.

L29 As expected, the difference in 29 geometry results in modelled basal melt rates slightly larger than those obtained by Motyka et al. (2011).

Motyka et al, had something like a m/day, over an area of roughly 5x15 km², you have an ocean melt rate that is applied to just a calving face. You purport to be reproducing behavior well pre-1999, but only then has a floating ice tongue developed. Your simplistic assumption is introducing all sorts of unrealistic forcing (i.e., ungrounding of 5x15 km section, instead of loss of an isolated pinning point or sidewall traction on a floating ice shelf).

Authors: The terminus is grounded only at the beginning of the equilibrium simulation. During the forward simulations the glacier is never grounded (Figs. 2 and 6)! While we do agree there should be a difference between a relatively small and large floating tongue, the redistribution of the stress should still follow a similar trend. Note that the acceleration modelled in 1998 is generated by a retreat of the ice tongue and is consistent with observations.

Further, Motyka et al 2011 provides also yearly average for 1984-1985 and the increase for 1997 relative to 1984-1985.

We added:

“Relative to other studies, e.g. Motyka et al. (2011), our melt rate for 1998 is ~2 times larger (Table S3). While we choose here to compare the two melt rates in order to offer a scale perspective, we acknowledge the difference in geometry between the two studies. Furthermore, our basal melt rates include both melting along the base of the shelf and in the proximity of the grounding line. In our model, the melt rates at the grounding line are higher than the melt rates modelled closer to the centre of the shelf (Sect. 2.1.3).”

P13L1 “the model is able to simulate with much accuracy its breakup that occurred in late summer 1 2003 and the subsequent glacier acceleration.”

This statement can hardly hold true since you modeled something completely different during this period than was actually the case (grounded terminus vs floating ice tongue).

Authors: The terminus is not grounded in 2003! It starts developing a **large** floating tongue in 2000. Even in 1998, the terminus is not fully grounded!! In fact, the terminus is never fully grounded during the forward run. The only moment when the terminus is fully grounded is at the start of the regional equilibrium simulation. Please see Fig. 2 or 6.

We added:

“Starting 2000, the floating tongue is comparable in length and thickness with observations and the model is able to simulate with much accuracy its breakup that occurred in late summer 2003 and the subsequent glacier acceleration.”

P13L3 add “modelled” before “the retreat”

Authors: Done.

P13L4 “The terminus and the grounding line retreat does not cease after 2010” Modelled or observed????

Authors: Observed. Done.

P13L7 “suggesting that additional feedbacks and/or 7 forcings must continue to disturb the glacier.”

This statement is too strong. It could just be that the bed rock in the model is wrong or the model has other deficiencies, which you acknowledge below. Change to “suggesting that additional feedbacks and/or forcings may affect the glacier. Alternatively, it may represent missing physics, inaccuracies in atmospheric/oceanic conditions, or other various limitations (e.g. bed topography model constraints and 10 grid resolution; see SI, Sect. 1.3 for more details).

Authors: Done.

P14L11 add “,” before “which”

Authors: Done.

P14L13 Change “climate” to “atmosphere”

Authors: Done.

P14L15 “Our results suggest that most of the sub-annual signal in the 15 model is climate driven” This statement should be supported by more than a reference to the SI. It should include a description of what the processes are important and why forcing on annual time-scale produces more rapid variation.

Authors: Done. The paragraph has been rewritten. We have included in the main manuscript (Sect. 3.2):

„We study the sensitivity of the model to atmospheric forcing by performing a simulation where we keep the atmospheric forcing constant (mean 1960-1990 temperature and SMB). By comparing this simulation with a simulation that includes full atmospheric variability (monthly temperature and SMB) we see that in terms of terminus retreat and velocities the modelled sub-annual variability does not always correlate with the observed seasonal signal (Fig. 3). In particular, the simulations suggest that only to a relatively small

degree some of the variability appears to be influenced by the atmospheric forcing applied (Figs. S2, S10 and S15), which also represents the only seasonal input in the model. Some of the greater than seasonal frequency could be an issue with resolution in the model. We examined this sensitivity by doing additional runs at higher resolution. Simulations on 1 km did show some improvement with respect to surface speed sub-annual variability (Fig. S13), suggesting that in our model the stress redistribution might be sensitive to the resolution of the calving event. Although some of the variability may be due to the grid resolution, part of it may also be related with missing physical processes at the terminus. We suggest that additional contributions to the seasonality from, e.g. ice mélange or seasonal ocean temperature variability, which are not included in our model, could potentially influence the advance and retreat of the front at seasonal scales. For example, the ice mélange can prevent the ice at the calving front from breaking off and could therefore reduce the calving rates. Consequently, the introduction of an ice mélange parametrization will probably help to minimize some of the sub-annual signal observed in our simulations. Similarly, seasonal ocean temperature variability can influence the ice mélange formation and/or clearance and the melt rates at the glacier front and can accentuate seasonal glacier terminus and grounding line retreat and/or advance. However, at this point we find it difficult to determine the relative importance of each process.”

P14L18: “and a simulation with constant climatic forcing (mean 1960-1990 temperature and SMB) 18 indicates that the two accelerations, in 1998 and 2003, are related to bed geometry and ocean 19 melt.” What was it about these two simulations that led to this conclusion (remind us with words or at least call out a result in figure if one exists).

Authors: The statement in this form is confusing and has been removed due to redundancy.

Moreover, page 14 is one long paragraph dealing with multiple subjects. Break it up.

Authors: Done.

P14L20: “Furthermore, our results show that some seasonal velocity peaks could potentially be 20 influenced by the climatic forcing applied (see Figs. S9 and S12(A,B))” This statement seems to relate to the L15 statement I commented on above. So why are the statements separated by a statement related to the long-term forcing (don’t ping pong back and forth, start with a theme, discuss it thoroughly, then move on to the next).

Authors: Done. It has been moved.

P14L24: “accelerations. The modelled sub-annual signal in terms of terminus retreat and velocities 24 does not always correlate with the observed signal, suggesting that potentially different 25 seasonal forcings (e.g. ice mélange variability, seasonal ocean temperature variability) may 26 influence the advance and retreat of the front at seasonal scales. The” Back to the seasonal cycle, with some explanation (I am not sure if buttresses early explanations or offers alternative).

Authors: It has been rewritten in the new version of the manuscript (Sect. 3.2):

“In particular, the simulations suggest that to only a relatively small degree some of the variability appears to be influenced by the atmospheric forcing applied (Figs. S2, S10 and S15), which also represents the only seasonal input into the model. Some of the greater than seasonal frequency could be an issue with resolution in the model. We examined this sensitivity by performing additional runs at a higher spatial resolution. Simulations on a 1 km grid did show some improvement with respect to surface speed sub-

annual variability (Fig. S13), suggesting that in our model the stress redistribution might be sensitive to the resolution of the calving event. However, given the short period spanned by the simulations, the stress redistribution does not change the overall modelled results, as seen in Figs. S11 and S12. Although we acknowledge that some of the variability is due to the grid resolution, part of it may also be related to unmodeled physical processes acting at the terminus. We suggest that additional contributions to the seasonality, e.g. from ice mélange or seasonal ocean temperature variability, which are not included in our model could potentially influence the advance and retreat of the front at seasonal scales (Fig. S15). For example, the ice mélange can prevent the ice at the calving front from breaking off and could therefore reduce the calving rates. Consequently, the introduction of an ice mélange parametrization will probably help to minimize some of the sub-annual signal modelled in our simulations. Similarly, seasonal ocean temperature variability can influence ice mélange formation and/or clearance and the melt rates at the glacier front and can accentuate seasonal glacier terminus and grounding line retreat and/or advance. However, at this point we find it difficult to determine the relative importance of each process.”

P14L30 “Furthermore, the 2 km resolution 30 used in this study may not be sufficient to accurately model the seasonal retreat and advance 31 of the front. The smallest calving event in our model is 4 km², which is larger than most of the 32 calving events observed at JI (see SI, Sect. 1.3.1)”

Authors: Not included in the new version of the manuscript. Additional simulations on 1 km showed the resolution is not an issue. The trend, shape and even the overall magnitude of the velocities remains unchanged in a 1 km simulation (see Figs. S11, S12, S13). See also the answer to the comment below.

Now we are getting to what may be driving much of the issue – the poor resolution of the model. Given that 50-runs were done to pick the right model, it seems like some computational resources should be available to run the model at say 0.5 km to test out the sensitivity such large events. Although there have been 2by2km ice bergs, often this is when the ice is floating.

Authors: The statement has been removed. Although we see some improvement relative to sub-annual signal when the resolution is increased to 1 km (Fig. S13), figures S11 and S12 clearly show the resolution is not an issue in our model. The overall trend in velocities remains widely unchanged on 1 km showing that our results hold on 1 km as well.

Furthermore, a paper published recently (Aschwanden et al. 2016) which focuses solely on improving the shape of the flow shows that a resolution of 2 km is sufficient to resolve the valley geometry of JI. Here, we find the same. Furthermore, in comparison to other outlets, JI flows through a very large subglacial valley (~10-km wide).

P14 General comment. Start with something like this outline “We see such and such type of seasonal variability. Some of the greater than annual frequency could be an issue with resolution in the model. We examined this sensitivity by doing a few runs at higher resolution. Although some of the variability does appear to be due to this effect, some of it is due to physical processes. In particular, the model shows process A is important because ... It also shows process B could be important too. At this point we can’t precisely determine the relative importance of each process. Finally, there could be additional contributions to the seasonality from processes X, Y, and Z” (this likely should take more than one paragraph)

Then start with something like “At the decadal time scale,....something like the above where you discuss the relevant processes, with clear descriptions of the physics revealed by the model (fine put the details in the SI, but the reader should be able to go through and understand what is being said without resorting to the supplement, which is for the nitty gritty details modelers will want to see.

Authors: Done. Example from the main manuscript (Sect. 3.2):

“Some of the greater than seasonal frequency could be an issue with resolution in the model. We examined this sensitivity by performing additional runs at a higher spatial resolution. Simulations on a 1 km grid did show some improvement with respect to surface speed sub-annual variability (Fig. S13), suggesting that in our model the stress redistribution might be sensitive to the resolution of the calving event. However, given the short period spanned by the simulations, the stress redistribution does not change the overall modelled results, as seen in Figs. S11 and S12. Although we acknowledge that some of the variability is due to the grid resolution, part of it may also be related to unmodeled physical processes acting at the terminus. We suggest that additional contributions to the seasonality, e.g. from ice mélange or seasonal ocean temperature variability, which are not included in our model could potentially influence the advance and retreat of the front at seasonal scales (Fig. S15). For example, the ice mélange can prevent the ice at the calving front from breaking off and could therefore reduce the calving rates. Consequently, the introduction of an ice mélange parametrization will probably help to minimize some of the sub-annual signal modelled in our simulations. Similarly, seasonal ocean temperature variability can influence ice mélange formation and/or clearance and the melt rates at the glacier front and can accentuate seasonal glacier terminus and grounding line retreat and/or advance. However, at this point we find it difficult to determine the relative importance of each process.”

P15L4 Change “determine” to “determined”

Authors: Done.

P15L10 “and not by an increase in e.g. ocean temperature.” Change to “and not by an increase in variability in ocean temperature.

Authors: Done.

P15L17 “most likely responds to changes in ocean temperature that are sustained for longer time 17 periods (ADD PARENS WITH TIME SCALE DECADEAL, MULTIDECADAL??).

Authors: Done (decadal).

P15L21 “This generated” Add something after “this” such “this increase generated”

Authors: Done.

L15L19-27. Here you demonstrate that there is a sensitivity to temperature increases of ~1 deg over timescales of a few years. Yet your model reproduces the observed behavior with no variability. Could this be a consequence of the fact that you had 50 runs to choose from??

Authors: No. The ocean temperature forcing with 0.7 degrees increase from 1997 to 2014 produces mass change estimates and a retreat of the terminus that are far from being close to observations. For example in Gladish et al. 2015, the increase in ocean temp. at the fjord mouth from 1994 to 1997 is over 1 degree and continues to accelerates thereafter. This shows that the increase in ocean temperatures starting 1997 (eg. Gladish et al. 2015, temperatures measured at the fjord mouth) is not sustained by our model.

“Two additional experiments, where the input ocean temperature (T_o) was increased to $-1\text{ }^{\circ}\text{C}$ indicate that higher melt rates beneath the grounding line could potentially explain the retreat observed after 2010. In our first experiment, the input T_o was increased from $-1.7\text{ }^{\circ}\text{C}$ to $-1\text{ }^{\circ}\text{C}$ ($\sim 0.7\text{ }^{\circ}\text{C}$ relative to 1990) starting 1997. This temperature increase is consistent with observations of ocean temperature (Gladish et al., 2015) at the mouth of the Ilulissat fjord and generated in our simulation, for the period 1997-2014, an accelerated retreat of the front that does not correlate with observations (Fig. S8). Similarly, mass loss estimates from the simulations are significantly larger (by $\sim 50\%$; Fig. S7) than those calculated from airborne and satellite altimetry observations (Sect. 3.1.2). Overall, the experiment shows that an increase in ocean temperature that starts in 1997 and is sustained until 2014 generates modelled estimates for the period 1998-2014 that do not agree with observations. In the second experiment, T_o was increased to $-1\text{ }^{\circ}\text{C}$ starting in 2010 ($\sim +0.7^{\circ}\text{C}$ at the base of the shelf in 2010). For the period 2010-2014, our model predicted a faster retreat of the front that correlates well with observations (Fig. S8), and an increase of mass loss by $\sim 7\text{ Gt}$ (Fig. S7). This experiment shows that an increase in ocean temperature beginning in 2010 could potentially explain the retreat observed thereafter.”

As I expressed above, how can we believe you have the ocean forcing, when the ice tongue is not properly represented in the model (e.g., in 1998 melt is not applied to a 15-km long tongue). Even if ocean conditions were constant, there would be a lot of variability based on whether there is a tongue or a grounded terminus. Some of this is in the model, but given that Figure 6 shows ice tongue/terminus configurations vastly different than observed, how can we draw firm conclusions from the model????

Authors: The configuration is not vastly different than the observed one. Starting 2000 the geometry does agree with observations. Although there might be some differences in geometry before 2000 (geometry and reasoning explained in Sect. 3.2), we should still expect a similar response. Even before 2000, we still have a small floating tongue in the model and the terminus is never fully grounded during the forward simulations! The fact that we are able to capture the 2 accelerations within the time frame and magnitude (Fig. 3) suggested by observations and that we widely match the observed terminus retreat (Fig. 2) is firm enough for us.

“As introduced in Sect. 2, our approach here is to adjust the terminus in the JI region to simulate the 1990s observed front position and surface elevation based on 1985 aerial photographs (Csatho et al., 2008). The glacier terminus in 1990s was floating (Csatho et al., 2008; Motyka et al. 2011). Motyka et al. (2011) calculated the 1985 hydrostatic equilibrium thickness of the south branch floating tongue from smoothed surface DEMs and obtained a height of 600 m near the calving front and 940 m near the grounding zone. In this paper, however, we compute the thickness as the difference between the surface elevation and the bed topography, and allow the glacier to evolve its own terminus geometry during the equilibrium simulation. Preparatory experiments have shown that in our model (disregarding its initial geometry floating/ grounded terminus) JI attains equilibrium with a grounding line position that stabilizes close to the 1990s observed

terminus position. According to observations, JI is characterized in 1990 by a large floating tongue (> 10 km; e.g. Motyka et al., 2011) that we are not able to simulate during the equilibrium runs. In our model (Fig. 6), the glacier starts to develop a large floating tongue (~ 10 km) in 1999. Starting in 2000, the floating tongue is comparable in length and thickness with observations and the model is able to simulate, with a high degree of accuracy, its breakup that occurred in late summer 2003 and the subsequent glacier acceleration. Observations of terminus positions (Sohn et al., 1998; Csatho et al., 2008) suggest that over more than 40 years, between 1946 and 1992, JIs terminus stabilized in the proximity of the 1990's observed terminus position. Furthermore, during 1959 and 1985 the southern tributary was in balance (Csatho et al., 2008). This suggests that, during the equilibrium and at the beginning of the forward simulations, we are forcing our model with climatic conditions that favoured the glacier to remain in balance. This may explain our unsuccessful attempts to simulate prior to 1998 a floating tongue comparable in length and thickness with observations, and suggests that for simulating the large floating tongue that characterized JI during this period, future studies should consider to start modelling JI before the glacier begins to float in the late 1940s (Csatho et al., 2008).

The geometry of the terminus plays an important role in parameterizing ice shelf melting, and therefore our pre-1999 geometry will influence the magnitude of the basal melt rates (Sect. 2.1.3). The difference in geometry results in modelled basal melt rates that are larger for the period 1999-2003, when JI begins to develop a large floating tongue and when the calving front was already largely floating. Relative to other studies, e.g. Motyka et al. (2011), our melt rate for 1998 is ~2 times larger (Table S3). While we choose here to compare the two melt rates in order to offer a scale perspective, we acknowledge the difference in geometry between the two studies. Furthermore, our basal melt rates include both melting along the base of the shelf and in the proximity of the grounding line. In our model, the melt rates at the grounding line are higher than the melt rates modelled closer to the centre of the shelf (Sect. 2.1.3). "

P16L5 "change, and GPS derived elastic uplift of the crust (Figs. 3 and 5)." Again remove this part as it adds an unnecessary constraint (if you got the observed mass changes right, then you don't need this).

Authors: The modelled uplift provides information about the distribution of the mass. This information is not provided by the overall mass loss.

e.g.

"Both model and observations consistently suggest large uplift rates near the JI front (20 mm a⁻¹ for station KAGA) and somewhat minor uplift rates (~ 5 mm a⁻¹) at distances of >100km from the ice margin."

P16L6 "Our results suggest that most of the JI retreat during 1990-2014 is ocean and bed geometry 6 driven "Its not really driven by geometry – rather the glacier response to ocean or other forcing is function of its bed geometry. Given the above discussion about how melt is applied – its not really that ocean forcing is well established as a major factor.

Authors: Changed to:

"Our results suggest that most of the JI retreat during 1990-2014 is driven by ocean forcing, and bed geometry and the glacier subsequent response, which is largely governed by its own bed geometry."

P16L7 “and that the overall variability in the modelled horizontal velocities is a response to 7 variations in terminus position.” It should be noted this confirms earlier work that reached this same conclusion”

Authors: We added:

“In agreement with previous studies (e.g. Joughin et al. 2012), our simulations suggest that the overall variability in the modelled horizontal velocities is a response to variations in terminus position.”

P16L7 “The seasonal variability observed in our simulations is climate driven.” Like the discussion this is very weak (again, do you mean atmospheric forcing)” Should be worded more like “The seasonal variability observed in our simulations is likely is driven by processes related to atmospheric forcing (e.g., mélange variability, melt induced hydrofracture ...).

Authors: Changed to:

“In our model, the seasonal variability is likely driven by processes related to the atmospheric forcing applied (e.g. temperature and SMB variability), which in fact represents the only seasonal input used in the model. A greater than seasonal frequency is seen in our simulations is attributed to grid resolution and missing seasonal scale processes (e.g., ice mélange variability or seasonal ocean temperature variability) in the model. Sensitivity experiments performed on a 1 km grid did not show significant improvement with respect to ice thickness (Fig. S11) or surface speed (i.e. shape of the flow and overall magnitude; Fig. S12).”

Page16L16 “provides evidence” should be “reproduces”

Authors: Done.

Page16L19 “During this period, JI attained unprecedented velocities reaching as high as 20 km a-1.” This is a model result not a statement about what JI did. Should be rewritten as “During this period in the simulation, JI attained unprecedented velocities reaching as high as 20 km a-1, which are considerably higher than observed speeds for this period (CITE PAPERS).

Authors: We don't have any observations during 2003 and 2004. For 2004 there are no available observations (not even by Joughin et al.) The sparse available observations for 2003 available in Joughin et al 2012 (see e.g., Joughin et al. 2012 – Fig. 4) are from early 2003 (before the break-up of the floating tongue) and an eye ball comparison suggests that they more or less agree (within 1-2 km yr⁻¹) with our modelled velocities. Furthermore, our S1-S6 points are much closer to the terminus when compared to the M points for e.g. Joughin et al 2012, Fig.1 (M6-M20).

Therefore, it is changed to:

“During this period, JI attained in our simulation unprecedented velocities reaching as high as 20 km a⁻¹.”

P16L21 “Over the last decade, as the slope steepened inland, sustained high 21 flow rates were observed at JI.” This isn't really a finding of the model as worded (it restates earlier findings), so cut or make relevant to this study (e.g, the model confirms this finding).

Authors: Deleted.

L16L29 “In our model, the terminus retreat is mostly driven by the 29 sub-shelf melting parametrization applied. Thus, our results suggest that ocean forcing is the 30 principal driver for the retreat observed over the last 2 decades.” This seems much stronger a statement about the ocean’s role than is provided in the main text (not to mention the problems with how the melt is applied).

Authors: The statement has been deleted.

L1631 “Further, our model provides evidence that the rapid accelerations of JI in 1998 and 2003 could be triggered by the bed geometry and internal glacier dynamics, and not by a sudden increase in e.g. ocean temperature.” This more or less contradicts the rather strong statement in the model above. Whatever the forcing (ocean or atmospheric), the sensitivity of the glaciers response is governed by the bed geometry (its not a case of ocean/atmosphere or bed). If the ocean is responsible one of two things likely happened.

1) Constant ocean forcing over a long period led to gradual thinning, which caused the glacier (like many others) to eventually retreat of its bedrock high and snap back. This seems more like what your model indicates given you used a steady forcing.

Authors: We agree and as the statement was rather confusing it was not included in the new version of the manuscript.

We have added (L12L13):

“This constant ocean forcing at the terminus leads, in our simulation, to gradual thinning of JI and favours its retreat without any shift (e.g. increase) in ocean temperature.”

2) The glacier was in a position of precarious stability on a bedrock high and ocean or atmospheric forcing triggered a retreat (your sensitivity studies indicate this could have happened, but the actual simulations).

Gladish et al. 2015 (Table 3) suggests an increase in ocean temp. at the fjord mouth from 1990 to 1997 of 1.22 deg Celsius (e.g. 1990 to 1997 of ~0.7 deg Celsius) which is sustained, with some fluctuations, until the end of 2013. What the experiment with 0.7 degree increase from 1997 to 2014 show is that the assumption no. 2 is not valid. A similar increase generated in our model mass change estimates and a retreat of the terminus that is very far from being close to observations.

References

Aschwanden, A., M. A. Fahnestock and M. Truffer. 2016. "Complex Greenland outlet glacier flow captured". Nature Communications 7 (10524). doi: 10.1038/ncomms10524.

Referee #5

General statement

With the manuscript “Modelled glacier dynamics over the last quarter of a century at Jakobshavn Isbræ”, Muresan et al. use numerical modeling to simulate the behavior of Jakobshavn Isbræ between 1990 and 2014 and compare their simulations with observations of ice front position changes and mass loss from the glacier. They conclude that bedrock elevation and ocean forcings have mainly controlled the evolution of the grounding line and calving from positions over the last twenty-five years and that most of the seasonal signal is driven by climate forcings. This manuscript aims to understand the processes and mechanisms that have triggered the destabilization of Jakobshavn Isbræ, and to reproduce its evolution since the 1990's. This is a very complex topic that many previous studies have already partially addressed.

The subject of the study and the approach are compelling but they are many limitations and inconsistencies between the different sections. For example, the main text states that using a grid with a 2 km resolution probably impacts the results while the supplementary material states that using a 1 km resolution grid does not alter the results.

Authors: We have addressed all these inconsistencies between the main manuscript and SI. Most of the text in the SI has been edited and moved in the main manuscript to ease reading. Any inconsistencies in the manuscript have been tracked and resolved.

The text is also sometimes poorly written and it took me several readings to actually figure out how the ocean forcing was used, or to understand the conclusions regarding the impact of the climate forcing on ice dynamics.

Authors: The quality of the writing has been improved. The ocean parametrization has been reformulated (see the new Sect. 2.1.3) and the climate forcing and its impact on ice dynamics have been better described (see the new Sect. 3.2).

Several statements are not supported by any results (i.e. p.11 l.8, the seasonal signal is climate driven) while strong conclusions are made from these statements.

Authors: New figures have been added to the main manuscript (Fig. 7) and SI (Fig. S7, S8, S11, S12, S13) to further sustain our statements and conclusions. The whole paragraph (p.11 l.8, the seasonal signal is climate driven) and like many others in Sect. 3.2 have been rewritten and made clear for the readers.

Finally, the values provided in Table S3 for the melt rates seem excessively high (1387 m/yr in 2000, there is just no way there can be any ice shelf with these kind of values).

Authors: Yes we agree. There should not be any shelf with such high melt rates **along its base**. However, in our model the melt rates from Table S3 include both melt rates at the shelf base and grounding line. In our model the melt rates are much higher in the proximity of the grounding line. This has become clear in the new version of the manuscript as Sect. 2.1.3 reads:

“Following this melting parametrization, the highest melt rates are modelled in the proximity of the glacier grounding lines and decrease with elevation such that the lowest melt rates are closer to the central to frontal area of the modelled ice shelf.”

Table S3 caption reads now:

“Table S3. Yearly modelled basal melt rates. The basal melt rates include here melt rates modelled along the base of the shelf and in the proximity of the grounding line position.”

The parameterization for the ocean forcing seem is a major control of the evolution of the glacier, and there is no analysis of its impact except for a few sentences at the end of the discussion that are not supported by any material.

Authors: Figures (S7 and S8) have been added to the supplement.

All the comments above are also raised in the point by point comments. Supporting material (e.g. text from the new version of the manuscript) that highlights our improvements has been included in the answers given below.

Major comments

As mentioned above, the impact of the grid resolution is not clearly investigated and explained. This could be a major limitation of the model, as calving events of 4 km² have a very large impact on ice dynamics. This problem is rarely mentioned in the limitations of the model (not in the abstract p.2 l.11 or the conclusions p.16 l.15 for example). Furthermore, the supplementary material suggests that using a 1 km grid would not make a big difference by running an additional stress balance simulation. Would that be similar for transient runs? I understand that there are some limitations that prevented the authors to do the simulations with a 1 km resolution, but this is a major limitation.

Authors: Yes, that would be similar for transient runs (see Figs. S11 and S12). The impact of the grid resolution has been now better investigated in Sect. 3.2 in terms of ice thickness, surface velocities and sub-annual signal. For this reason additional simulations using a 1 km resolution have been performed and supporting figures have been added in the SI (the new figs. S11, S12, S13). In terms of modelled ice thickness and surface velocities we see no improvement with increasing resolution and this is clearly illustrated by figures S11 and S12.

Some improvement is seen in terms of the sub-annual signal (Fig. S13) but the trend, the magnitude and the shape of the flow remain unchanged with a 2 or a 1 km resolution. Fig. S11 and S12 certainly show, that our results held also on a 1 km resolution and the grid used in this study is not a major limitation. We do not intend or do not wish to perfectly capture the seasonal signal but the overall trend in velocities which remains unchanged disregarding the resolution used.

Furthermore, a paper published recently (Aschwanden et al. 2016) which focuses solely on improving the shape of the flow shows that a resolution of 2 km is sufficient to resolve the valley geometry of JI. Here, we find the same. Note that in comparison to other outlets, JI flows through a very large subglacial valley (~10-km wide).

We have added (Sect. 3.2):

“Regarding the grid resolution, simulations performed on 1 km did not show significant improvement with respect to ice thickness (Fig. S11) or surface speed (e.g. trend, magnitude and shape of the flow; Fig. S12).”

“Some of the greater than seasonal frequency could be an issue with resolution in the model. We examined this sensitivity by doing additional runs at higher resolution. Simulations on 1 km did show some improvement with respect to surface speed sub-annual variability (Fig. S13), suggesting that in our model the stress redistribution might be sensitive to the resolution of the calving event. Although some of the variability may be due to the grid resolution, part of it may also be related with missing physical processes at the terminus.”

(Conclusion):

“A greater than seasonal frequency is seen in our simulations is attributed to grid resolution and missing seasonal scale processes (e.g., ice mélange variability or seasonal ocean temperature variability) in the model. Sensitivity experiments performed on a 1 km grid did not show significant improvement with respect to ice thickness (Fig. S11) or surface speed (i.e. shape of the flow and overall magnitude; Fig. S12).”

Furthermore, it is surprising to see that the vertical resolution is 20 m, resulting in 200 vertical layers, while the horizontal grid is 310 by 213.

Authors: We do not find that surprising. Preparatory experiments have shown that our model performs significantly better when a high vertical resolution is used. A model with coarse vertical resolution is significantly inferior to a model with high vertical resolution and we find that the vertical resolution is equally important as the horizontal resolution is. Note, that our simulations on 2km and 1km did not show overall improvement with increasing resolution in the horizontal plane for ice thickness and horizontal velocities.

The grounding line is said to evolve within the grid cells according to Feldmann et al. [2014]. However, figures showing grounding line position do not show continuous advance and retreat of the grounding line, but rather jumps between a few positions spaced by relatively large distances (fig. S7A and fig. S12C for example). How do the authors explain this surprising behavior that usually happen when no sub-grid parameterization is used?

Authors: The advance and retreat of the grounding line is continue (see Fig. 7 and Fig. S8). The large jumps in 1998 and 2000 are more or less consistent with an increase in melt rate (Table S3) and are probably caused by the bed topography and the increase in basal melt. Preparatory experiments have shown that its position (the simulated grounding line position) is strongly dependent on topography (via the parameterization of basal resistance, eqs. in SI), on the melt rate at the base of shelf, and on the velocities in the shelf.

Furthermore, the experiments in Feldmann et al. are performed on an artificial bed geometry. This is far from being an equivalent comparison, especially regarding JIs rough bed topography.

As mentioned above, the melt rates provided in table S3 are extremely high, especially between 1998 and 2003. This should at least be mentioned and explained.

Authors: Done. The geometry and the melt rates are better discussed in sect. 3.2. They are also mentioned in the conclusion.

We added (Sect. 3.2):

“As introduced in Sect. 2, our approach here is to adjust the terminus in the JI region to simulate the 1990s observed front position and surface elevation based on 1985 aerial photographs (Csatho et al., 2008). The glacier terminus in 1990s was floating (Csatho et al., 2008; Motyka et al. 2011). Motyka et al. (2011) calculated the 1985 hydrostatic equilibrium thickness of the south branch floating tongue from smoothed surface DEMs and obtained a height of 600 m near the calving front and 940 m near the grounding zone. In this paper, however, we compute the thickness as the difference between the surface elevation and the bed topography, and allow the glacier to evolve its own terminus geometry during the equilibrium simulation. Preparatory experiments have shown that in our model (disregarding its initial geometry floating/ grounded terminus) JI attains equilibrium with a grounding line position that stabilizes close to the 1990s observed terminus position. According to observations, JI is characterized in 1990 by a large floating tongue (> 10 km; e.g. Motyka et al., 2011) that we are not able to simulate during the equilibrium runs. In our model (Fig. 6), the glacier starts to develop a large floating tongue (~ 10 km) in 1999. Starting in 2000, the floating tongue is comparable in length and thickness with observations and the model is able to simulate, with a high degree of accuracy, its breakup that occurred in late summer 2003 and the subsequent glacier acceleration. Observations of terminus positions (Sohn et al., 1998; Csatho et al., 2008) suggest that over more than 40 years, between 1946 and 1992, JIs terminus stabilized in the proximity of the 1990’s observed terminus position. Furthermore, during 1959 and 1985 the southern tributary was in balance (Csatho et al., 2008). This suggests that, during the equilibrium and at the beginning of the forward simulations, we are forcing our model with climatic conditions that favoured the glacier to remain in balance. This may explain our unsuccessful attempts to simulate prior to 1998 a floating tongue comparable in length and thickness with observations, and suggests that for simulating the large floating tongue that characterized JI during this period, future studies should consider to start modelling JI before the glacier begins to float in the late 1940s (Csatho et al., 2008).

The geometry of the terminus plays an important role in parameterizing ice shelf melting, and therefore our pre-1999 geometry will influence the magnitude of the basal melt rates (Sect. 2.1.3). The difference in geometry results in modelled basal melt rates that are larger for the period 1999-2003, when JI begins to develop a large floating tongue and when the calving front was already largely floating. Relative to other studies, e.g. Motyka et al. (2011), our melt rate for 1998 is ~2 times larger (Table S3). While we choose here to compare the two melt rates in order to offer a scale perspective, we acknowledge the difference in geometry between the two studies. Furthermore, our basal melt rates include both melting along the base of the shelf and in the proximity of the grounding line. In our model, the melt rates at the grounding line are higher than the melt rates modelled closer to the centre of the shelf (Sect. 2.1.3).”

(Conclusion):

“In 1990, JI had a large floating tongue (> 10 km; e.g. Motyka et al., 2011) that we are not able to simulate during the equilibrium runs. In our model (Fig. 6), the glacier starts to develop a floating tongue comparable with observations in 1999. Starting in 2000, the floating tongue is consistent in length and thickness with observations and the model is able to simulate its breakup (that occurred in late summer 2003) and the subsequent glacier acceleration. The difference between observed and modelled pre-1999 geometry results in relatively large basal melt rates for the period 1997-2003 (Fig. S10).”

This is an ocean parameterization more than an ocean forcing.

Authors: Agree. Ocean forcing has been widely changed to ocean parametrization.

The description of the calving should be clarified: there seems to be two criterions used, one based on the eigencalving parameterization, and the second one based on the ice thickness.

Authors: Done. See Sect. 2.1.2 (see also answer to comment below).

How are they combined? Also the description mentions (p.5) that ice is removed at a rate of at most one grid cell per time step and sub-grid scale ice front advance and retreat are used.

Authors: Rewritten. See Sect. 2.1.2 and Sect. 3.2.

“In our model, the eigen calving law has priority over the basic calving mechanism. That is to say, the second calving law used (the basic calving mechanism) removes any ice at the calving front not calved by the eigen calving parametrization, thinner than 500 m in the equilibrium simulations and 375 m in the forward runs. “

“The eigen calving style cannot resolve individual calving events, and, thus, the introduction of the basic calving mechanism was necessary in order to accurately match observed front positions. Preparatory experiments have shown that overall calving is mostly driven in our model by the basic calving mechanism used, and that the eigen calving parametrization is more important in modelling sub-annual to seasonal fluctuations of the terminus.”

However the smallest calving event is said to be 2 by 2 km (one grid cell)?

Authors: The statement has been removed. It should have been “the largest”. The sensitivity of the sub-annual signal to grid resolution has been rewritten in the new version of the manuscript:

“Some of the greater than seasonal frequency could be an issue with resolution in the model. We examined this sensitivity by performing additional runs at a higher spatial resolution. Simulations on a 1 km grid did show some improvement with respect to surface speed sub-annual variability (Fig. S13), suggesting that in our model the stress redistribution might be sensitive to the resolution of the calving event. However, given the short period spanned by the simulations, the stress redistribution does not change the overall modelled results, as seen in Figs. S11 and S12. Although we acknowledge that some of the variability is due to the grid resolution, part of it may also be related to unmodeled physical processes acting at the terminus.”

What is the difference between these two processes?

Authors: The eigen calving is physically based, while the basic calving mechanism is calving any ice (no physical ground) smaller than a given threshold. This has been explained now in Sect. 2.1.2.

“Along the ice shelf calving front, we superimpose a physically based calving (eigen calving) parametrization (Winkelmann et al., 2011; Levermann et al., 2012) and a basic calving mechanism (Albrecht et al., 2011) that removes any floating ice at the calving front thinner than a given threshold at a maximum rate of one grid cell per time step. The average calving rate (c) is calculated as the product of the principal components of the horizontal strain rates ($\dot{\epsilon}_{\pm}$), derived from SSA velocities, and a proportionality constant parameter (k) that captures the material properties relevant for calving:

$$c = k\dot{\epsilon}_{+}\dot{\epsilon}_{-} \quad \text{for } \dot{\epsilon}_{\pm} > 0. \quad (1)$$

The strain rate pattern is strongly influenced by the geometry and the boundary conditions at the ice shelf front (Levermann et al. (2012)). The proportionality constant, k , is chosen such that the ice front variability is small (Leverman et. al., 2012). This physically based calving law appears to yield realistic calving front positions for various types of ice shelves having been successfully used for modelling calving front positions in entire Antarctica simulations (Martin et al., 2011) and regional east Antarctica simulations (Mengel and Levermann, 2014). In contrast to Antarctica, known for its large shelves and shallow fjords, the GrIS is characterized by narrow and deep fjords, and JI is no exception. The strain rate pattern in the eigen calving parametrization performs well only if fractures in glacier ice can grow, and calving occurs only if these rifts intersect (i.e. possible only for relatively thin ice shelves). In our model, the eigen calving law has priority over the basic calving mechanism. That is to say that the second calving law used (the basic calving mechanism) removes any ice at the calving front not calved by the eigen calving parametrization thinner than 500 m in the equilibrium simulations and 375 m in the forward runs. “

From sect. 3.2:

“The eigen calving style cannot resolve individual calving events, and, thus, the introduction of the basic calving mechanism was necessary in order to accurately match observed front positions. Preparatory experiments have shown that overall calving is mostly driven in our model by the basic calving mechanism used, and that the eigen calving parametrization is more important in modelling sub-annual to seasonal fluctuations of the terminus.”

The eigenvalue calving has been tested on Antarctica, where large ice shelves spread in all directions. Greenland has very narrow fjords with almost no lateral velocities, which makes the across flow strain rate very small and noisy. How does this impact the results?

Authors: In terms of calving this will not alter the results. If the eigen calving will not perform, the basic calving mechanism is there to backup. Preparatory experiments showed that most of the calving is not done through eigen calving but rather through the basic calving mechanism.

“The eigen calving style cannot resolve individual calving events, and, thus, the introduction of the basic calving mechanism was necessary in order to accurately match observed front positions. Preparatory

experiments have shown that overall calving is mostly driven in our model by the basic calving mechanism used, and that the eigen calving parametrization is more important in modelling sub-annual to seasonal fluctuations of the terminus."

One of the conclusions is that climate forcing drives the seasonal (sub-annual) evolution of the front position, grounding line position and ice dynamics. However, the only climate forcing happens through SMB changes. This impacts the ice thickness and driving stress, but the changes are really small and these processes happen on much longer time scales. How can changes in SMB only trigger these large changes on very short time scales? This should be better demonstrated in the paper.

Authors: This has been rewritten and better described in the new version of the manuscript. The climate forcing should have been atmospheric forcing. In the new version of the manuscript we have made a clearer separation between seasonal signal and sub-annual signal.

From Sect. 3.2:

"In our model, the atmospheric forcing applied can influence JI 's dynamics only through changes in surface mass balance (SMB) (i.e., accumulation and ablation) (Fig. S2). While these changes in ice thickness affect both the SIA and the SSA (Sect. 2.1), the effect in the SIA is very weak as the driving stresses are not affected by a few meters of difference in thickness induced by SMB variability. In the SSA, the coupling is achieved via the effective pressure term in the definition of the yield stress (see SI, Sect. 1.2 for detailed equations). The effective pressure is determined by the ice overburden pressure (i.e., ice thickness) and the effective thickness of water in the till, where the latter is computed by time-integrating the basal melt rate. This effect is much stronger and favours the idea that in our model some seasonal velocity peaks could potentially be influenced by the climatic forcing applied (Figs. S10 and S15).

We study the sensitivity of the model to atmospheric forcing by performing a simulation where we keep the atmospheric forcing constant (mean 1960-1990 temperature and SMB). By comparing this simulation with a simulation that includes full atmospheric variability (monthly temperature and SMB) we see that in terms of terminus retreat and velocities the modelled sub-annual variability does not always correlate with the observed seasonal signal (Fig. S15). In particular, the simulations suggest that to only a relatively small degree some of the variability appears to be influenced by the atmospheric forcing applied (Figs. S2, S10 and S15), which also represents the only seasonal input into the model. Some of the greater than seasonal frequency could be an issue with resolution in the model. We examined this sensitivity by performing additional runs at a higher spatial resolution. Simulations on a 1 km grid did show some improvement with respect to surface speed sub-annual variability (Fig. S13), suggesting that in our model the stress redistribution might be sensitive to the resolution of the calving event. However, given the short period spanned by the simulations, the stress redistribution does not change the overall modelled results, as seen in Figs. S11 and S12. Although we acknowledge that some of the variability is due to the grid resolution, part of it may also be related to unmodeled physical processes acting at the terminus. We suggest that additional contributions to the seasonality, e.g. from ice mélange or seasonal ocean temperature variability, which are not included in our model could potentially influence the advance and retreat of the front at seasonal scales (Fig. S15). For example, the ice mélange can prevent the ice at the calving front from breaking off and could therefore reduce the calving rates. Consequently, the introduction of an ice mélange parametrization will probably help to minimize some of the sub-annual signal modelled in our simulations.

Similarly, seasonal ocean temperature variability can influence ice mélange formation and/or clearance and the melt rates at the glacier front and can accentuate seasonal glacier terminus and grounding line retreat and/or advance. However, at this point we find it difficult to determine the relative importance of each process.”

The enhancement factor chosen is equal to 0.6 for the SSA. This is a very surprising value as enhancement factors are usually greater than 1. For Greenland, the calibrated values are between 3 and 6 [Cuffey and Paterson, 2010]. How can this value be explained?

Preparatory experiments showed that the model performs better when we use an enhancement factor for the SSA of 0.6. First, in our model we use a hybrid scheme in which SSA is used both for simulating slowly moving grounded ice in the interior part of the ice sheet, and for simulating fast-flowing outlet glacier and ice shelf systems. We are obliged to keep a balance between the two. Second, the values from Cuffey and Paterson are based on whole Greenland simulations, not on a particular glacier. Third, for this particular study, the value of the SSA factor is less relevant for the period 1990-2014 as we keep the same value both during the equilibrium and the forward simulations.

p.9 l.12: the authors mention that the high melt rate is responsible for the flow acceleration, and that their model is able to reproduce the acceleration. However the model does not include any process to include this high melt so it seems that the ability to reproduce the acceleration is likely to be just a coincidence.

Authors: We added in Sect. 3.2:

*“In the SSA, the coupling is done via the effective pressure term in the definition of the yield stress (see SI, Sect. 1.2 for detailed equations). The effective pressure is determined by the ice overburden pressure (i.e., ice thickness) and **the effective thickness of water in the till, where the latter is computed by time-integrating the basal melt rate**. This effect is much stronger and favours the idea that in our model some seasonal velocity peaks could potentially be influenced by the climatic forcing applied (Figs. S10 and S15).”*

Fig. S7 is very informative of the general behavior of the model and is a good summary of the evolution of the glacier. It should be added to the main text.

Authors: Done.

Minor comments

p.1 l.25: “an attempt” is a surprising word. The model should simply describe results.

Authors: “an attempt” is removed.

p.1 l.26: “ocean parametrization” would be more accurate than “ocean forcing”

Authors: Changed.

p.2 l.6: A sentence should not start with “And”.

Authors: "And" is removed.

p.2 l.9: the bed geometry is not changing and does not initiate any change. Also, the floating ice does not care about bed elevations as it is already floating.

Authors: Changed.

p.2 l.10: Consider changing "slight failing" to "limitation".

Authors: Done.

p.2 l.12: Observations do not "suggest", they are measurements that show the evolution.

Authors: "Suggest" has been removed.

p.3 l.4-9: I would only mention flow line models to describe their results.

Authors: Done. L4-9 has been removed.

p.3 l.11: "One process"

Authors: Done.

p.3 l.12: "thinning and/or retreat"

Authors: Done.

p.3 l.25: "to model and understand the recent behaviour of JI": that sounds really ambitious.

Authors: Understand has been removed.

p.3 l.27: "in which the grounding lines ..."

Authors: Done.

p.4 l.2: "Ice sheet model"

Authors: Done.

p.4 l.6: "SIA-SSA": acronyms should be defined before being used. References should also be added for these stress balance approximations.

Authors: Done.

p.4 l.5-9: Not clear, should be rephrased

Authors: Done. The paragraph has been rephrased.

p.4 l.20: what year is used for the altimetry observations?

Authors: Changed accordingly.

“The terminus position and surface elevation in the Jakobshavn region are based on 1985 aerial photographs (Csatho et al., 2008).”

p.4 l.27: at this point of manuscript, the reader has no clue why RACMO results should be interpolated on a 2 by 2 km grid.

Authors: Removed.

p.5 l.1: “grounding line parametrization”. Consider adding also “initialization procedure” or something equivalent in the section title.

Authors: Done.

p.5 l.8: What year is used for the other terminus positions?

Authors: We added Bamber et al. (2013).

p.5 l.14-18: Not clear, rephrase.

Authors: Has been rephrased.

p.5 l.20: How is the value of k chosen?

Authors: We added:

“The proportionality constant, k, is chosen such that the ice front variability is small (Leverman et. al., 2012).”

p.6 l.1: What is “LI”?

Authors: A linear interpolation scheme; added to the manuscript.

“The parameterization of the grounding line position is based on a linear interpolation scheme (the “LI” parameterization; Gladstone et al., 2010) extended to two horizontal dimensions (x,y).”

p.6 l.17: Should add one sentence to describe the parameterization in Feldmann et al. [2014].

Authors: The parameters are nicely discussed in Pattyn et al. [2013] and Feldmann et al [2014]. We have added them as a reference.

“In the three-dimensional Marine Ice Sheet Model Intercomparison Project (Mismip3d) experiments, PISM was used to model reversible grounding line dynamics with results consistent with full-Stokes models (Pattyn et al. (2013); Feldmann et al., 2014; see parameters therein)”

p.6 l.21: “regularly spaced layers within the ice”: Are the vertical layers of uniform thickness (20 m as stated earlier) or regularly spaced between the bed and surface elevations?

Authors: “and a vertical resolution of 20 m” is removed. They are regularly spaced between the bed and surface elevations.

The “vertical resolution of 20 m” corresponds to a statement from a previous version of the manuscript where we made reference to a “computational domain that does not extend farther than 4000m above the bed”. This implied that the maximum vertical resolution was 20 m.

p.6 l.27-29: Rephrase

Authors: Rephrased as:

“The 2 km model simulation reaches equilibrium after 200 years with an ice volume of $0.25 \cdot 10^6 \text{ km}^3$ (or a 3.6 % increase relative to the adjusted (see Sect. 2.1.1) input dataset from Bamber et al. (2013)).”

p.6 l.30: Is the vertical resolution 10 or 20 m?

Authors: See comment above. During the forward runs we use 400 regularly spaced layers within the ice, which for a maximum domain of 4000 m will correspond to roughly 10 m. Has been rewritten as:

“Further, using our equilibrium simulations with a 2 km horizontal grid and 400 regularly spaced layers within the ice, we simulate forward in time (hindcast) [...]”

p.6 l.31: “integrate” → “simulate”

Authors: Done.

p.6 l.32: It is not really coupling if it is one way, but rather forcing.

Authors: Done. Has been changed to forcing.

p.7 l.8: “sub-shelf ice temperature”: Not clear. Is this sub-shelf ocean temperature or ice shelf temperature?

Authors: Rephrased in the new version of the manuscript:

“ice temperature at the base of the shelf”

p.7 l.25: The description of the ocean forcing is not clear. I read it several times and I am still not sure what is used.

Authors: We improved the ocean parametrization, Sect. 2.1.3, as following:

“We use a simple parametrization for ice shelf melting where the melting effect of the ocean is based on both sub-shelf ocean temperature and salinity (Martin et al., 2011). To accommodate this parametrization, several changes have been made to PISM at the sub-shelf boundary (Winkelmann et al., 2011). First, the ice temperature at the base of the shelf (the pressure-melting temperature) is calculated from the Clausius-Clapeyron gradient and the elevation at the base of the shelf, and then the temperature is applied as a Dirichlet boundary condition in the conservation of energy equation.

Secondly, basal melting and refreezing is incorporated through a sub-shelf mass flux used as a sink/source term in the mass-continuity equation. This mass flux from shelf to ocean (Beckmann and Goosse, 2003) is

computed as a heat flux between the ocean and ice and represents the melting effect of the ocean due to both temperature and salinity (Martin et al., 2011).

We start our simulations with a constant ocean water temperature (T_o) of -1.7°C , which here represents the mean surface ocean temperature in the grid cells adjacent to the JI terminus. In the heat flux parametrization, the ocean temperature at the ice shelf base is computed as the difference between the input ocean temperature and a virtual temperature that represents the freezing point temperature of ocean water below the ice shelf (Fig. S4). The freezing point temperature is calculated based on the elevation at the base of the shelf and the ocean water salinity. As a consequence of these constraints, as the glacier retreats and/or advances, both the pressure-melting temperature and the heat flux between the ocean and ice evolve alongside the modelled glacier ice shelf geometry. The ocean water salinity ($S_o=35$ psu) is kept constant in time and space as the model does not capture the salinity gradient from the base of the ice shelf through layers of low and high salinity. A previous study conducted by Mengel and Levermann (2014) using the same model established that the sensitivity of the melt rate to salinity is negligible.

Following this melting parametrization, the highest melt rates are modelled in the proximity of the glacier grounding lines and decrease with elevation such that the lowest melt rates are closer to the central to frontal area of the modelled ice shelf. At the grounding line, the sub-grid scheme (Albrecht et al., 2011; Feldmann et al., 2014) interpolates the sub-shelf melt rate, allowing for a smooth transition between floating and grounded ice. For a completely grounded terminus (i.e. the case when no ice floating tongue exists), the melt parametrization is applied only at the grounding line position.”

p.7 l.28: What does “indirectly” mean?

Authors: Not included in the new version of the manuscript. The ocean parametrization section has been rewritten.

p.8 l.21: “between 1990 and 2014”

Authors: Done.

p.8 l.26: “approximately 2 to 4 km”: so just one or two grid cells!

Authors: Yes.

p.8 l.29: “ new oceanic and atmospheric conditions”: what is new here? I thought the same RACMO data were used.

Authors: In the forward runs the forcing is monthly compared with the equilibrium runs where we used yearly mean 1960-1990. Has been changed to:

“It is probably a modelling artefact as the geometry obtained during the regional equilibrium simulation is forced with monthly atmospheric forcing and new oceanic conditions.”

p.9 l.5: “Disregarding” → “Apart from”

Authors: Done.

p.10 l.3: “temporally”

Authors: The sentence is no included in the new version of the manuscript.

p.10 l.9: “the front continuous in 2002”: rephrase

Authors: Moved to p11.l.7 and rephrased as:

“In our simulation, this retreat of the terminus triggers a decrease of resistive stresses at the terminus (Figs. 7 and S9).”

p.10 l.19: “had thinned”

Authors: Done.

p.10 l.24: “JI remained”

Authors: Done.

p.10 l.26: “in 2004 onward”: rephrase

Authors: Rephrased to : “after 2003”.

p.11 l.8: How is the seasonal signal driven by climate? What processes are responsible of such variations? Investigating the different processes included in the model should allow to better answer these questions.

Authors: The seasonal and the sub-seasonal signal has been better investigated and described in Sect. 3.2.

“In our model, the atmospheric forcing applied can influence JI’s dynamics only through changes in surface mass balance (SMB) (i.e., accumulation and ablation) (Fig. S2). While these changes in ice thickness affect both the SIA and the SSA (Sect. 2.1), the effect in the SIA is very weak as the driving stresses are not affected by a few meters of difference in thickness induced by SMB variability. In the SSA, the coupling is achieved via the effective pressure term in the definition of the yield stress (see SI, Sect. 1.2 for detailed equations). The effective pressure is determined by the ice overburden pressure (i.e., ice thickness) and the effective thickness of water in the till, where the latter is computed by time-integrating the basal melt rate. This effect is much stronger and favours the idea that in our model some seasonal velocity peaks could potentially be influenced by the climatic forcing applied (Figs. S10 and S15).

We study the sensitivity of the model to atmospheric forcing by performing a simulation where we keep the atmospheric forcing constant (mean 1960-1990 temperature and SMB). By comparing this simulation with a simulation that includes full atmospheric variability (monthly temperature and SMB) we see that in terms of terminus retreat and velocities the modelled sub-annual variability does not always correlate with the observed seasonal signal (Fig. S15). In particular, the simulations suggest that to only a relatively small degree some of the variability appears to be influenced by the atmospheric forcing applied (Figs. S2, S10 and S15), which also represents the only seasonal input into the model. Some of the greater than seasonal frequency could be an issue with resolution in the model. We examined this sensitivity by performing additional runs at a higher spatial resolution. Simulations on a 1 km grid did show some improvement with

respect to surface speed sub-annual variability (Fig. S13), suggesting that in our model the stress redistribution might be sensitive to the resolution of the calving event. However, given the short period spanned by the simulations, the stress redistribution does not change the overall modelled results, as seen in Figs. S11 and S12. Although we acknowledge that some of the variability is due to the grid resolution, part of it may also be related to unmodeled physical processes acting at the terminus. We suggest that additional contributions to the seasonality, e.g. from ice mélange or seasonal ocean temperature variability, which are not included in our model could potentially influence the advance and retreat of the front at seasonal scales (Fig. S15). For example, the ice mélange can prevent the ice at the calving front from breaking off and could therefore reduce the calving rates. Consequently, the introduction of an ice mélange parametrization will probably help to minimize some of the sub-annual signal modelled in our simulations. Similarly, seasonal ocean temperature variability can influence ice mélange formation and/or clearance and the melt rates at the glacier front and can accentuate seasonal glacier terminus and grounding line retreat and/or advance. However, at this point we find it difficult to determine the relative importance of each process.”

p.11 l.8: How does the acceleration propagate inland?

Authors: We added:

“In agreement with previous studies (e.g. Joughin et al. 2012), our results suggest that the overall variability in the modelled horizontal velocities is a response to variations in terminus position (Fig. 7). In our simulation, the retreat of the front reduced the buttressing at the terminus and generated a dynamic response in the upstream region of JI which finally led to flow acceleration. In contrast, when the front advanced the modelled flow slowed as the resistive stresses at the terminus were reinforced. This buttressing effect tends to govern JI’s behaviour in our model. Regarding the overall terminus retreat, our simulations suggest that it is mostly driven by the sub-shelf melting parametrization applied (Figs. S5 and S15). Although the heat flux supplied to the shelf evolves in time based on the modelled terminus geometry, the input ocean temperature is kept constant throughout the simulations. This constant ocean forcing at the terminus leads, in our simulation, to gradual thinning of JI and favours its retreat without any shift (e.g. increase) in ocean temperature. In terms of seasonality, the only seasonal signal in the model is introduced by the monthly atmospheric forcing applied (Sect. 2). However, the modelled sub-annual variability in terms of terminus retreat and velocities does not always follow the seasonal signal (Fig. 3). We investigate this higher than seasonal variability in Sect. 3.2.”

p.11 l.21: How large is the uplift?

Authors: 20 mm a⁻¹ for KAGA and in the 5 mm a⁻¹ for the other stations. We added:

“Both model and observations consistently suggest large uplift rates near the JI front (20 mm a⁻¹ for station KAGA) and somewhat minor uplift rates (~ 5 mm a⁻¹) at distances of >100km from the ice margin.”

p.12 l.4: “physically based”

Authors: Done.

p.12 l.8: The eigencalving is combined with the thickness criterion. How much of the calving is due to each of these mechanisms? As the flow is parallel to the fjord, the second value eigenvalue is close to zero and therefore this mechanism is likely not to modify the position of the front.

Authors: Regarding the comment above, we added (Sect. 3.2):

*“Determining terminus positions by using the superposition of a physically based calving (eigencalving) parametrization (Winkelmann et al., 2011; Levermann et al., 2012) and a basic calving mechanism (Albrecht et al., 2011) is motivated by the model’s ability to maintain realistic calving front positions (Levermann et al., 2012). The eigen calving style cannot resolve individual calving events and so the introduction of the basic calving mechanism was necessary in order to accurately match observed front positions. **Preparatory experiments have shown that overall calving is mostly driven in our model by the basic calving mechanism used, and that the eigen calving parametrization is more important in modelling sub-annual to seasonal fluctuations of the terminus.**”*

Also, the superposition of the two calving mechanism have been better described in sect 2.1.2.

p.13 l.4: “The terminus and the grounding line retreats do not ...”

Authors: Done.

p.13 l.5: “suggest”

Authors: Done.

p.13 l.6: “overdeepening”

Authors: Done.

p.13 l.20: “bed sill by 100 m”

Authors: Done.

p.13 l.22: What do the authors mean by “equivalent”?

Authors: Similar with the experiment performed by Vieli et al. and described at lines 19-21. We have added:

“In an equivalent experiment (Viel et al., 2011) performed [...]”

p.13 l.30: “Surface melt above average was already ...”

Authors: Done.

p.14 l.8: “related to the 2012 ...”

Authors: Done.

p.14 l.16: again, it is not clear how SMB forcing can cause sub-annual changes

Authors: We added:

*“In our model, the atmospheric forcing applied can influence *JI*’s dynamics only through changes in surface mass balance (SMB) (i.e., accumulation and ablation) (Fig. S2). While these changes in ice thickness affect both the SIA and the SSA (Sect. 2.1), the effect in the SIA is very weak as the driving stresses are not affected by a few meters of difference in thickness induced by SMB variability. In the SSA, the coupling is achieved via the effective pressure term in the definition of the yield stress (see SI, Sect. 1.2 for detailed equations). The effective pressure is determined by the ice overburden pressure (i.e., ice thickness) and the effective thickness of water in the till, where the latter is computed by time-integrating the basal melt rate. This effect is much stronger and favours the idea that in our model some seasonal velocity peaks could potentially be influenced by the climatic forcing applied (Figs. S10 and S15).”*

p.14 l.31: “the 2 km resolution ... may not be sufficient”: the supplementary material says pretty much the opposite.

Authors: Done. Additional simulation on 1km did not show significant improved with increasing resolution relative to ice thickness and surface velocities. The statement has been removed.

p.15 l1. “Concerning” → “Regarding”

Authors: Done.

p.15 l.18-27: Additional figures should help support these conclusions.

Authors: Done. See Fig. S7 and S8.

p.16 l.15: Another major limitation is the coarse mesh, that should also be discussed here.

Authors: Done. However, additional simulation on 1km did not show significant improved with increasing resolution relative to ice thickness and surface velocities. This has been discussed in Sect. 3.2. ,

“Regarding the grid resolution, simulations performed on 1 km did not show significant improvement with respect to ice thickness (Fig. S11) or surface speed (e.g. trend, magnitude and shape of the flow; Fig. S12).”

“We examined this sensitivity by performing additional runs at a higher spatial resolution. Simulations on a 1 km grid did show some improvement with respect to surface speed sub-annual variability (Fig. S13), suggesting that in our model the stress redistribution might be sensitive to the resolution of the calving event. However, given the short period spanned by the simulations, the stress redistribution does not change the overall modelled results, as seen in Figs. S11 and S12. Although we acknowledge that some of the variability is due to the grid resolution, part of it may also be related to unmodeled physical processes acting at the terminus.”

and mentioned in the final conclusion

“A greater than seasonal frequency is seen in our simulations is attributed to grid resolution and missing seasonal scale processes (e.g., ice mélange variability or seasonal ocean temperature variability) in the model. Sensitivity experiments performed on a 1 km grid did not show significant improvement with respect to ice thickness (Fig. S11) or surface speed (i.e. shape of the flow and overall magnitude; Fig. S12). “

Fig.1 caption: replace “polygon” by “rectangle”. “Khan et al. (2014)”

Authors: Done.

Fig.2: Eight different years are shown (not seven). By the way, why not show the results every year? How are these years picked?

Authors: For this 2-D display we choose to include only the years where there is change i.e., in flow acceleration, advance/retreat of the terminus etc. as known from observations. Old Fig. S7, new fig.7 in the main text shows (monthly) terminus and grounding line positions, ice thickness and velocities from 1994-2014 along the flowline in Fig. 1C.

Fig.3: How is the thickness adjusted? This should also appear in the text.

Authors: Done.

Fig.4: The grey error bar is hard to distinguish on the figure. Caption I.5-7 should be rephrased.

Authors: Done, caption I.5-7 has been rephrased:

“The green curve represents the modelled ice dynamics mass change (i.e., modelled mass change minus SMB change).”

Fig. S1 (bottom right): Only three curves appear, if some are superimposed, it should be mentioned in the caption.

Authors: Done. Fig. S1 caption reads:

“In the right bottom plot, the curves for $F_{melt}=0.01$ and $F_{melt}=0.1$ are superimposed.”

Also the range of values used for F_{melt} seems inconsistent with the values listed in Table S2.

Authors: Table S2 has been updated.

References

Aschwanden, A., M. A. Fahnestock and M. Truffer. 2016. “Complex Greenland outlet glacier flow captured”. Nature Communications 7 (10524). doi: 10.1038/ncomms10524.

Modelled glacier dynamics over the last quarter of a century at Jakobshavn Isbræ

Ioana S. Muresan¹, Shfaqat A. Khan¹, Andy Aschwanden², Constantine Khroulev², Tonie Van Dam³, Jonathan Bamber⁴, Michiel R. van den Broeke⁵, Bert Wouters^{4,5}, Peter Kuipers Munneke⁵, and Kurt H. Kjær⁶

[1]{Department of Geodesy, DTU Space, Technical University of Denmark, Kgs. Lyngby, Denmark}

[2]{Geophysical Institute, University of Alaska Fairbanks, Fairbanks, Alaska, USA}

[3]{University of Luxembourg, Faculty of Science, Technology and Communication (FSTC), Engineering Research Unit, Luxembourg}

[4]{University of Bristol, School of Geographical Sciences, Bristol, England}

[5]{Institute for Marine and Atmospheric research Utrecht (IMAU), Utrecht University, The Netherlands}

[6]{Centre for GeoGenetics, Natural History Museum of Denmark, University of Copenhagen, Copenhagen, Denmark}

Correspondence to: I. S. Muresan (iomur@space.dtu.dk)

Abstract

Observations over the past two decades show substantial ice loss associated with the speedup of marine terminating glaciers in Greenland. Here we use a regional 3-D outlet glacier model to simulate the behaviour of Jakobshavn Isbræ (JI) located in west Greenland. Our approach ~~represents an attempt~~ is to model and understand the recent behaviour of JI with a physical process-based model. Using atmospheric forcing and ~~oceanic forcing~~ an ocean parametrization we tune our model to reproduce observed frontal changes of JI during 1990–2014. ~~We find that~~ In our simulations most of the JI retreat during 1990–2014 is driven by ~~ocean forcing~~ the

ocean parametrization used, and bed geometry and the glacier's subsequent response, which is largely governed by bed geometry. Our results suggest that the overall variability in modelled horizontal velocities is a response to variations in terminus position. ~~We identify~~ The model simulates two major accelerations that are consistent with observations of changes in glacier terminus. The first event occurred in 1998, and was triggered by a retreat of the front and moderate thinning of JI prior to 1998. The second event, which started in 2003 and peaked in the summer 2004, was triggered by the final breakup of the floating tongue. This breakup reduced the buttressing at the JI terminus that resulted in further thinning. ~~And as~~ As the slope steepened inland, the terminus retreated over a reverse bed slope into deeper water over the last decade, sustained high velocities have been observed at JI over the last decade. Our model provides evidence that the 1998 and 2003 flow accelerations are most likely initiated by the ocean parametrization used but JI's subsequent dynamic response was govern by its own bed geometry. ~~However, our model is not able to capture the~~ The observed 2010-2012 terminus retreat is not reproduced in our simulations. We attribute this slight failing limitation to either inaccuracies in basal topography, or to misrepresentations of the climatic and oceanic forcings that were applied. ~~Both modelled and observed results suggest that JI has been losing mass at an accelerated rate, and that JI continued to accelerate throughout 2014. Nevertheless, the model is able to simulate the previously observed increase in mass loss through 2014.~~

1 Introduction

The rate of net ice mass loss from Greenland's marine terminating glaciers has more than doubled over the past two decades (Rignot et al., 2008; Moon et al., 2012; Shepherd et al., 2012, Enderlin et al., 2014). Jakobshavn Isbræ, located mid-way up on the west side of Greenland, is one of the largest outlet glaciers in terms of drainage area as it drains ~6 % of the Greenland Ice Sheet (GrIS) (Krabill et al., 2000). Due to its consistently high ice flow rate and seasonally varying flow speed and front position, the glacier has received much attention over the last two decades (Thomas et al., 2003; Luckman and Murray, 2005; Holland et al., 2008; Amundson et al., 2010; Khan et al., 2010; Motyka et al., 2011; Joughin et al., 2012; Gladish et al., 2015a; Gladish et al., 2015b). Measurements from synthetic aperture radar suggest that the ice flow speed of JI doubled between 1992 and 2003 (Joughin et al., 2008, 2004). More recent measurements show a steady increase in the flow rate over the

1 glacier's faster-moving region of $\sim 5\%$ per year (Joughin et al., 2008). The speedup coincides
2 with thinning of up to 15 m a^{-1} between 2003 and 2012 near the glacier front (Krabill et al.,
3 2004; Nielsen et al., 2013) as observed from airborne laser altimeter surveys. The steady
4 increase in the flow rate and glacier thinning suggest a continuous dynamic drawdown of
5 mass, and they highlight JIs importance for the GrIS mass balance.

6 Over the past decade, we have seen significant improvements in the numerical modelling of
7 glaciers and ice sheets (e.g. Price et al., 2011; Vieli and Nick, 2011; Winkelmann et al., 2011;
8 Larour et al., 2012; Pattyn et al., 2012; Seroussi et al., 2012; Aschwanden et al., 2013; Nick et
9 al., 2013; Mengel and Levermann, 2014)- ~~and Some of these models include regional scale~~
10 ~~glacier models that are based on a flow line approach (Nick et al., 2009; Parizek and Walker,~~
11 ~~2010), and which model the one or two dimensional dynamic behaviour of the glacier~~
12 ~~considered. Flow line models are computationally efficient and are valuable for~~
13 ~~understanding the basic processes. However, three dimensional models are more appropriate~~
14 ~~in areas of flow divergence/convergence and/or where lateral stresses are important.~~

15 ~~In the last decade,~~ several processes have been identified as controlling the observed speedup
16 of JI (Nick et al., 2009; Van der Veen et al., 2011; Joughin et al., 2012). One processes is a
17 reduction in resistance (buttressing) at the marine front through thinning ~~and/or~~ retreat of the
18 ~~floating tongue of the~~ glacier termini. But the details of the processes triggering and
19 controlling thinning and retreat remain elusive. Accurately modelling complex interactions
20 between thinning, retreat, and acceleration of flow speed as observed at JI, is challenging. Our
21 knowledge of the mechanisms triggering these events is usually constrained to the period
22 covered by observations. The initial speedup of JI occurred at a time when the satellite and
23 airborne observations were infrequent and therefore insufficient to monitor the annual to
24 seasonal evolution of glacier geometry and speed.

25 Here, we use a high-resolution, three-dimensional, time-dependent regional outlet glacier
26 model that has been developed as part of the Parallel Ice Sheet Model (PISM; please refer to
27 Sect. 2.1 The ice sheet model) (The PISM Authors, 2014) to investigate the dynamic
28 evolution of JI between 1990 and 2014. While previous 3-D modelling studies have mostly
29 concentrated on modelling individual processes using stress perturbations (e.g. Van der Veen
30 et al., 2011, Joughin et al. 2012), the present aims to model ~~and understand~~ the recent
31 behaviour of JI with a process-based model. Our modelling approach is based on a regional
32 equilibrium simulation and a time-integration over the period 1990 to 2014, where-in which

the grounding lines and the calving fronts are free to evolve under the ocean parametrization and the monthly climatic forcing atmospheric and oceanic boundary conditions forcing applied.

2 Methods and forcing

2.1 ~~The ice~~ ice sheet model

The ice sheet model used in this study is PISM (stable version 0.6). PISM is an open source, parallel, three-dimensional, thermodynamically coupled and time dependent ice sheet model (Bueler and Brown, 2009; ~~Winkelmann et al., 2011;~~ The PISM Authors, 2014). ~~The ice dynamic model is the “SIA+SSA hybrid” model, uses the superposition of the non-sliding shallow ice approximation (SIA; Hutter, 1983) and the shallow shelf approximation (SSA; Weis et al., 1999) for simulating slowly moving grounded ice in the interior part of the ice sheet, and the SSA for simulating fast-flowing outlet glacier and ice shelf systems (Winkelmann et al., 2011). with the non-sliding shallow ice approximation (SIA). for simulating slowly moving grounded ice in the interior part of the ice sheet. For simulating fast flowing outlet glacier and ice shelf systems (Bueler and Brown, 2009) we use the shallow shelf approximation (SSA). The~~ This superposition of SIA and SSA ~~(the “SIA+SSA” hybrid model)~~ sustains a smooth transition between non-sliding, bedrock frozen ice and sliding, fast-flowing ice, and has been shown to reasonably simulate the flow of both grounded and floating ice (Winkelmann et al., 2011). For conservation of energy, PISM uses an enthalpy scheme (Aschwanden et al., 2012) that accounts for changes in temperature in cold ice (i.e., ice below the pressure melting point) and for changes in water content in temperate ice (i.e., ice at the pressure melting point).

2.1.1 Input data

We use the bed topography from Bamber et al. (2013). The 1 km bed elevation dataset for all of Greenland was derived from a combination of multiple airborne ice thickness surveys and satellite-derived elevations during 1970–2012 ~~(see Supplementary information (SI), Sect. 4.3.2). The dataset has an improved resolution, particularly along the ice sheet margin. In the region close to the outlet of JI, data from an 125 m CReSIS DEM (that includes all the data collected in the region by CReSIS between 1997 and 2007) have been used to improve the accuracy of the dataset. Errors in bed elevation range from 10 m to 300 m, depending on the distance from an observation and the variability of the local topography (Bamber et al., 2013).~~

The terminus position and surface elevation in the Jakobshavn region are based on 1985 aerial

1 photographs ~~and existing satellite altimetry observations~~ (Csatho et al., 2008). Ice thickness in
2 the JI basin is computed as the difference between surface and bedrock elevation, ~~which~~
3 ~~implies that at the beginning of our equilibrium simulation JI's terminus is considered to be~~
4 ~~grounded~~. The model of the geothermal flux is adopted from Shapiro and Ritzwoller (2004).
5 We use input fields of near-surface air temperature and surface mass balance (SMB) from the
6 regional climate model RACMO2.3 (Noël et al., 2015) (~~see SI, Figs S2 and S3~~). The version
7 used in this study is produced at a spatial resolution of ~ 11 km and covers the period from
8 1958 to 2014. ~~The original dataset of 11 km grid is interpolated to 2 x 2 km grids using~~
9 ~~bilinear interpolation. Any further grid refinements are performed using bilinear interpolation~~
10 ~~for climatic datasets and a second order conservative remapping scheme (Jones, 1999) for bed~~
11 ~~topography.~~

12 **2.1.2 Initialization procedure, bBoundary conditions, calving and** 13 **grounding line parametrization**

14 In our model, the three-dimensional ice enthalpy field, basal melt, modelled amount of till-
15 pore water, and lithospheric temperature are obtained from an ice-sheet-wide paleo-climatic
16 spin-up. The paleo-climatic spin-up follows the initialization procedure described by
17 Bindshadler et al. (2013) and Aschwanden et al. (2013). We start the spin-up on a 10 km
18 grid, and then we refine to 5 km at -5ka. It is important to note that during the paleo-climatic
19 initialization the terminus is held fixed to the observed 1990 position in the JI region, and to
20 the ~~present-day~~ position from Bamber et al., 2013 elsewhere.

21 In the regional outlet glacier model of PISM, the boundary conditions are handled in a 10 km
22 strip positioned outside of the JI's drainage basin and around the edge of the computational
23 domain (Fig. 1B). In this strip, the input values of the basal melt, the amount of till-pore
24 water, ice enthalpy, and lithospheric temperature (Aschwanden et al., 2013) are held fixed and
25 applied as Dirichlet boundary conditions in the conservation of energy model (The PISM
26 Authors, 2014). We start our regional JI runs with an equilibrium simulation on a horizontal
27 grid with 5 km spacing. The enthalpy formulation models the mass and energy balance for
28 the three-dimensional ice fluid field based on 200 regularly spaced layers within the ice. The
29 temperature of the bedrock thermal layer is computed up to a depth of 1000 m with 50
30 regularly spaced layers. The first step is to obtain a 5 km regional equilibrium model for JI
31 using constant mean climate (i.e. repeating the 1960-1990 mean air temperature and surface
32 mass balance; see Sect. 2.1.1). We consider that equilibrium has been established when the

ice volume in the regional domain changes by less than 1% in the final 100 model years. Grid refinements are made from 5 km (125×86) to 2 km (310×213) after 3000 years. The 2 km simulation reaches equilibrium after 200 years with an ice volume of $0.25 \cdot 10^6 \text{ km}^3$ (or a 3.6 % increase relative to the input dataset from Bamber et al. (2013)). Further, using our equilibrium simulations with a 2 km horizontal grid and 400 regularly spaced layers within the ice, we simulate forward in time (hindcast) from 1990 to 2014 by imposing monthly fields of SMB and 2 m air temperatures through a one-way forcing scheme. For simulations performed on a 1 km horizontal grid, the exact same procedure is used with the mention that in the regional equilibrium run an additional grid refinement from 2 km to 1 km is made after 200 years. The length of the 1 km regional equilibrium simulation is 100 years.

In our regional model, all boundaries (calving fronts, grounding lines, upper and lower surfaces) are free to evolve in time both during the regional equilibrium and the forward simulations. Along the ice shelf calving front, we apply the superposition of a physically based calving (eigencalving) parametrization (Winkelmann et al., 2011; Levermann et al., 2012) and ~~a basic calving mechanism an ice thickness condition~~ (Albrecht et al., 2011) that removes at a rate of at most one grid cell per time step, any floating ice at the calving front thinner than a given threshold ~~(see SI Sect. 1, Table S2 for its specific value)~~. The average calving rate (c) is calculated as the product of the principal components of the horizontal strain rates ($\dot{\epsilon}_{\pm}$), derived from SSA velocities, and a proportionality constant parameter (k) that captures the material properties relevant for calving:

$$c = k \dot{\epsilon}_{+} \dot{\epsilon}_{-} \quad \text{for } \dot{\epsilon}_{\pm} > 0. \quad (1)$$

The strain rate pattern is strongly influenced by the geometry and the boundary conditions at the ice shelf front (Levermann et al. (2012)). The proportionality constant, k , is chosen such that the ice front variability is small (Leverman et. al., 2012). This physically based calving law appears to yield realistic calving front positions for various types of ice shelves being successfully used for modelling calving front positions in whole Antarctica simulations (Martin et al., 2011) and regional east Antarctica simulations (Mengel and Levermann, 2014). In contrast to Antarctica, known for its large shelves and shallow fjords, the GrIS is characterized by narrow and deep fjords, and JI makes no exception. The strain rate pattern in the eigen calving parametrization performs well only if fractures in glacier ice can grow, and calving occurs only if these rifts intersect (i.e. possible only for relatively thin ice shelves).

In our model, the eigen calving law has priority over the basic calving mechanism. That is to say, the second calving law used (the basic calving mechanism) removes any ice at the calving front not calved by the eigen calving parametrization, thinner than 500 m in the equilibrium simulations and 375 m in the forward runs. Therefore, the creation of the conditions under which calving can finally occur (e.g., floating ice shelf), relies solely on the parametrization for ice shelf melting (Sect. 2.1.3). A partially-filled grid cell formulation (Albrecht et al., 2011), which allows for sub-grid scale retreat and advance of the ~~front-ice shelf front~~ is used to connect the calving rate computed by the ~~eigen~~-calving parametrizations ~~is connected~~ with the mass transport scheme at the ice shelf terminus. This sub-grid scale retreat and advance of the shelf allows for realistic spreading rates, important for the eigen calving parametrization. The subgrid interpolation is performed only when a floating terminus exists. In both situations (i.e., floating or grounded terminus) the stress boundary conditions are applied at the calving front and in the discretization of the SSA equations (Winkelmann et al., 2011). The retreat and advance of the front through calving is restricted to at most one grid cell length per adaptive time step. The calving law is known to yield realistic calving front positions for various types of ice shelves being successfully used for modelling calving front positions in whole Antarctica simulations (Martin et al., 2011) and regional east Antarctica simulations (Mengel and Levermann, 2014).

The parameterization of the grounding line position is based on a linear interpolation scheme (the “LI” parameterization; ~~(Gladstone et al., 2010)~~ extended to two horizontal dimensions (x, y) and is not subject to any boundary conditions. This sub-grid treatment of the grounding line interpolates the basal shear stress in x, y based on the spatial gradient between cells below and above the grounding line, and allows for a smooth transition of the basal friction from grounded to floating ice (Feldmann et al., 2014). At each time step the grounding line position is determined by a mask ~~which~~ that distinguishes between grounded and floating ice using a flotation criterion based on the modelled ice thickness (Winkelmann et al., 2011):

$$b(x, y) = -\frac{\rho_i}{\rho_o} H(x, y) \quad (2)$$

~~where (x, y) give the horizontal dimension,~~ where ρ_i is the density of the ice, ρ_o is the density of the ocean water and H represents the ice thickness. Therefore, the grounding line migration is influenced by the ice thickness evolution, which further depends on the velocities computed from the stress balance. The superposition of SIA and SSA, which implies that the SSA velocities are computed simultaneously for the shelf and for the sheet, ensures that the stress

transmission across the grounding line is continuous and that buttressing effects are included. In the [three-dimensional Marine Ice Sheet Model Intercomparison Project \(Mismip3d\)](#) experiments, `_PISM` was used to model reversible grounding line dynamics with results consistent with full-Stokes models ([Pattyn et al. \(2013\)](#); [Feldmann et al., 2014](#); [see parameters therein](#)). ~~However, we~~ We have not performed the Mismip3d experiments for our particular parameter settings and therefore, the accuracy of the modelled grounding line migration is solely based on the results presented in [Feldmann et al. \(2014\)](#).

~~We start our regional JI runs with an equilibrium simulation on a 125×86 horizontal grid with 5 km spacing and a vertical resolution of 20 m. The enthalpy formulation models the mass and energy balance for the three dimensional ice fluid field based on 200 regularly spaced layers within the ice. The temperature of the bedrock thermal layer is computed up to a depth of 1000 m with 50 regularly spaced layers. The first step is to obtain a 5 km regional equilibrium model for JI using constant mean climate (i.e. repeating the 1960–1990 mean air temperature and surface mass balance; see 2.1.1 Input data). We consider that equilibrium has been established when the ice volume in the regional domain changes by less than 1% in the final 100 model years. Grid refinements are made from 5 km (125×86) to 2 km (310×213) after 3000 years. The length of the simulation with the 2 km grid is 200 years. The model reaches equilibrium with an ice volume of $0.25 \cdot 10^6 \text{ km}^3$ (or a 3.6 % increase relative to the input dataset from [Bamber et al. \(2013\)](#) adjusted to simulate, 1990’s metrics; see Sect. 2.1.1). Further, using our equilibrium simulations with a 2 km horizontal grid and a 10 m vertical grid, we integrate forward in time (hindcast) from 1990 to 2014 by imposing monthly fields of SMB and 2 m air temperatures through a one-way coupling scheme. The calving fronts and grounding lines are free to evolve in time both during the regional equilibrium and the forward simulation.~~

2.1.3 Parameterization for ice shelf melting

We use a simple parametrization for ice shelf melting where the melting effect of the ocean is based on both sub-shelf ocean temperature and salinity ([Martin et al., 2011](#)). ~~At the base of the ice shelf, the sub-shelf~~ To accommodate this parametrization several changes have been made in PISM at the sub-shelf boundary ([Winkelmann et al., 2011](#)). First, the ice temperature at the base of the shelf (the pressure-melting temperature) (T_{pm}) is set calculated based on the Clausius-Clapeyron gradient and the elevation at the base of the shelf to the pressure-melting

temperature_i and is applied as a Dirichlet boundary condition in the conservation of energy equation. ~~The sub-shelf ice temperature holds the following form:~~

$$T_{pm} = 273.15 + \beta_{ee} z_b \quad (3)$$

~~where $\beta_{ee} = 8.66 \times 10^{-4} \text{ K m}^{-1}$ represents the Clausius-Clapeyron gradient and z_b represents the elevation at the base of the ice shelf.~~

~~Secondly, basal melting and refreezing is incorporated through a~~ The sub-shelf mass flux ~~is~~ used as a sink/source term in the mass-continuity equation. This mass flux from shelf to ocean ~~(S) follows~~ (Beckmann and Goosse, 2003) ~~and~~ is computed as a heat flux (Q_{heat}) between the ocean and ice, ~~that and~~ represents the melting effect of the ocean through both temperature and salinity (Martin et al., 2011) ~~).~~

$$S = \frac{Q_{heat}}{L_t \rho_i} \quad (4)$$

$$Q_{heat} = \rho_o c_{po} \gamma_T F_{melt} (T_o - T_f) \quad (5)$$

~~where $L_t = 3.35 \times 10^5 \text{ J kg}^{-1}$ is the latent heat capacity of ice, $c_{po} = 3974 \text{ J (kg K)}^{-1}$ is the specific heat capacity of the ocean mixed layer, $\gamma_T = 10^{-4} \text{ m s}^{-1}$ is the thermal exchange velocity, F_{melt} is a model parameter (see SI, Table S2), T_o is the ocean water temperature and T_f is the virtual temperature. This virtual temperature represents the freezing temperature of ocean water at the depth z_b below the ice shelf and has the form:~~

$$T_f = 273.15 + 0.0939 - 0.057 S_o + 7.64 \times 10^{-4} z_b \quad (6)$$

~~where S_o is the salinity of the ocean.~~

We start our simulations with a constant ocean water temperature (T_o) of -1.7 °C, which here represents the mean surface ocean temperature in the grid cells adjacent to the JI terminus. In the heat flux parametrization, the ocean temperature at the ice shelf base is computed as the difference between the input ocean temperature and a virtual temperature that represents the freezing point temperature of ocean water below the ice shelf. The freezing point temperature is calculated based on the elevation at the base of the shelf and the ocean water salinity. In consequence, as the glacier retreats and/or advances, both the pressure-melting temperature and the heat flux between ocean and ice evolve alongside the modelled glacier ice shelf geometry. which is further scaled by the ice shelf melting parametrization spatially and temporally based on the depth below the ice shelf (geometry) and the ocean water salinity (see

1 ~~also SI, Fig. S4). Therefore, the sub-shelf melt rates are dependent on the ice shelf thickness~~
2 ~~and indirectly to the bed topography depth. We choose to keep the~~ The ocean water salinity
3 ($S_o = 35$ psu) is kept constant in time and space as the model does not capture the salinity
4 gradient from the base of the ice shelf through layers of low and high salinity. ~~However, a~~
5 previous study conducted by Mengel and Levermann (2014) using the same model
6 established that the sensitivity of the melt rate to salinity is negligible.

7 Following this melting parametrization, the highest melt rates are modelled in the proximity
8 of the glacier grounding lines and decrease with elevation such that the lowest melt rates are
9 closer to the central to frontal area of the modelled ice shelf. At the grounding line, the sub-
10 grid scheme (Albrecht et al., 2011; Feldmann et al., 2014) interpolates the sub-shelf melt
11 rates, allowing for a smooth transition between floating and grounded ice. For a completely
12 grounded terminus (i.e. no ice floating tongue exists) the melt parametrization is applied only
13 at the grounding line position.

15 3 Results and discussion

16 Sect. 3 is organized in two main subsections. Sect. 3.1 introduces the results obtained relative
17 to observations and Sect 3.2 focuses mainly on the limitations of the model that need to be
18 considered before a final conclusion is drawn. A short introduction for the different
19 simulations and preparatory experiments performed is given below.

20 ~~We perform~~ A total number of fifty simulations with different sets of parameters (excluding
21 preparatory and additional experiments on 1 km and 500 m) are performed on a 2 km
22 resolution. We alter parameters controlling ice dynamics (e.g. the flow enhancement factor,
23 the exponent of the pseudo-plastic basal resistance model, the till effective fraction
24 overburden) but also parameters related with ice shelf melt, ocean temperature and calving
25 (e.g. the ice thickness threshold in the basic calving mechanism). ~~The~~ These parameters are
26 altered only during the regional JI runs. ~~We calibrated the parameters~~ such that the model
27 reproduces the frontal positions (Fig. 2) and the ice mass change observations (Fig. 4, please
28 refer to Sect. 3.1.2 Ice mass change) at JI during the period 1990-2014 (Fig. 2) -and 1997-
29 2014 (Fig. 4), respectively. From these results, we present here the parameterization that best
30 captures the full evolution of JI during the period 1990–2014 ~~(see SI, Sect. 1.1 for the values~~
31 of the ice sheet model parameters). The values of the ice sheet model parameters used and
32 ~~The~~ the sensitivity to parameters controlling ice dynamics, basal processes, ice shelf melt and

ocean temperature ~~are discussed~~are illustrated in SI, Sect. 1.2. ~~the supplementary material (SI). The evolution of the main driver variables for the atmosphere and the ocean are further described in SI, Sect. 1.2.5.~~

~~We calibrated the parameters such that the model reproduces the frontal positions (Fig. 2) and the ice mass change observations (Fig. 4, please refer to Sect. 3.1.2 Ice mass change) at JI during the period 1990–2014 and 1997–2014, respectively.~~

3.1 Observations vs. modelling results

3.1.1. Annual scale variations in velocities, terminus and grounding line positions

We investigate the processes driving the dynamic evolution of JI and its variation in velocity between 1990 ~~and~~ –2014 with a focus on the initial speedup of JI and the 2003 breakup of the ice tongue. The overall pattern observed in our simulations suggests a gradual increase in velocities that agrees well with observations (Joughin et al., 2014) (Fig. 3). Three distinct stages of acceleration are identified in Fig. 3 (see also Movie 1) and discussed in detail below.

- **1990–1997**

The first speedup produced by the simulation is caused by a retreat of the front position by approximately 2 to 4 km between 1990 and 1991. There is no observational evidence that this retreat actually occurred. It is probably a modelling artefact as the geometry obtained during the regional equilibrium simulation is forced with ~~new oceanic and atmospheric conditions~~monthly atmospheric forcing and new oceanic conditions. This acceleration (Fig. 3) is caused by a reduction in buttressing due to a reduction in lateral resistance (Van der Veen et al., 2011), which is generated by the gradual retreat of the front, and which triggers a dynamic response in the upstream region of JI.

Starting in 1992, ~~the modelled and observed terminus positions agree well. we obtain a good fit between modelled and observed frontal positions. Disregarding~~ Apart from the acceleration in 1991–1992, no significant seasonal fluctuation in flow rate is modelled during this period. These results are consistent with observations (Echelmeyer et al., 1994). From 1993 a stronger ~~seasonal~~ sub-annual velocity signal begins to emerge in our simulation that continues and intensifies in

magnitude during 1994 and 1995. The departure in 1995 from the normal seasonal invariance in velocity seems to be in our model influenced by the ~~climate~~ atmospheric forcing (see SI, Figs. S2, S9, and S12(A, B)). This indicates that, as suggested by Luckman and Murray (2005), the 1995 anomalously high melt year (see Figs. S2 and S3) may have potentially contributed to JIs retreat and flow acceleration during this period. ~~The modelled~~ Modelled mean-annual velocities for 1992 and 1995 are consistent with observed velocities for the same period (Joughin et al., 2008; Vieli et al., 2011). In 1996 and 1997, the frontal extent and the grounding line position remain relatively stable (Figs. 2 and 6), and no significant seasonal fluctuation in ice flow rate is modelled. These model results agree well with observations, which indicate that the glacier speed was relatively constant during this period (Luckman and Murray, 2005).

• 1998–2002

According to observations (Joughin et al., 2004; Luckman and Murray, 2005; Motyka et al., 2011; Bevan et al., 2012), the initial acceleration of JI occurred in May-August 1998, which coincides with our modelled results. In our simulation, the 1998 acceleration is generated by a retreat of the ice tongue's terminus in 1997-1998, which may be responsible for reduction in buttressing (see Movie 1 and SI, Fig. S7). Thinning, both near the terminus and inland (up to 10 km away from the 1990 front position), starts in our model in the summer of 1995 and continues to accelerate after 1998 (Figs. 3 and 6). The modelled behavior agrees well with the observed behaviour (Krabill et al., 2004). These findings are corroborated both by observations (SI, Fig. S15) and modelling results (Fig. 3). Although thinning appears to have increased in our model during three continuous years, ~~we find littleit produced only minor~~ additional speedup during the period prior to 1998 (Figs. 2, 6, and S7). ~~According to-~~ In our simulation, JI's speed increased in the summer of 1998 by ~ 80% relative to the summer of 1992 (Fig. 3-), at which time the grounding line position starts to retreat thereafter (Figs. 2, 6, and S7). Our model suggests a retreat of the grounding line position starting in 1998 that accelerates thereafter (Figs. 2, 6, and S7). Observations (Luckman and Murray, 2005) do not show this level of speedup and there are no observations of the grounding line position at this time with which to assess our model performance.

~~The period between 1999 and 2002 is in our simulation characterized by a temporal uniform flow, with no episodes of significant terminus retreat.~~ Overall modelling results suggest an advance of the terminus between 1999 and 2000 and a retreat of the southern tributary between 2000 and 2002 by ~4 km, which correlates with existing observations (Thomas, 2004). This retreat of the terminus triggers in our simulation a decrease of resistive stresses at the terminus (see SI, Figs. S7 and S8). Concurrent with the 1998-~~2001-2002~~ terminus retreat, the grounding line retreats in our model by ~6 km (Figs. 2 and 6). ~~Calving and thinning near the front continuous in 2002 and results in decrease in resistive stresses at the terminus (see SI, Figs. S7 and S8).~~

• 2003–2014

In the late summer of 2003, ~~an increase in flow velocity is observed~~the simulated flow velocity increases (Fig. 3), ~~which is driven~~This acceleration of JI is driven in our simulations by the final breakup of the ice tongue (see Figs. 2 and 6). The period, 2002-2003, is characterized in our model by substantial retreat of the front (~4-6 km) and the grounding line (~4 km), which starts in June 2002 and continues throughout 2003. By ~~December 2003 the terminus has retreated back to the position of the grounding line (see Figs. 2 and 6).~~ The simulated retreat that occurred in 2003 and the loss of large parts of the floating tongue caused a major decrease in resistive stresses near the terminus (see Figs. 2, 6, 7 and S9)~~(see SI, Figs. S7 and S8)~~. By 2004 the glacier ~~has had~~ thinned significantly, both near the front, and further inland in response to a change in the near-terminus stress field (Figs. 3 and 6). During the final breakup of the ice tongue, ~~JI the simulation produces reached unprecedented flow rates, which in our simulation are speeds as~~ high as 20 km a^{-1} (~ 120% increase relative to 1998).~~.-~~ The modelled velocities decreased to 16 km a^{-1} (~ 80% increase relative to 1998) in the subsequent months and remained substantially higher than the sparse observations from that time (e.g. Joughin et al., 2012,-)). ~~and JI remains relatively stable with high seasonal fluctuations.~~ The high velocities ~~observed~~ modelled at JI after the loss of its floating tongue are further sustained in our simulation by the thinning that occurred ~~in 2004 onward~~ after 2003 (see Fig. 3), which continues to steepen the slopes near the terminus (see Fig. 6), and by a seasonal driven (sub-annual scale) -retreat and advance of the front. This thinning is

combined in the following years with a reduction in surface mass balance due to increased melting and runoff (van den Broeke et al., 2009; Enderlin et al., 2014, Khan et al., 2014). The period 2004-2014 is characterized in our simulation by relatively uniform velocity peaks with strong ~~seasonal~~ sub-annual variations (Fig. 3). During this period, only a small floating ice tongue is modelled and the terminus remained relatively stable~~the terminus remained close to the grounding line,~~ with no episodes of significant retreat.

In agreement with previous studies (e.g. Joughin et al. 2012), our results suggest that the overall variability in the modelled horizontal velocities is a response to variations in terminus position (see SI, Fig. S7 and Sect. 1.4 for more details). In our simulation, the retreat of the front reduced the buttressing at the terminus and generated a dynamic response in the upstream region of JI which finally lead to flow acceleration. In contrast, when the front advanced the modelled flow slowed as the resistive stresses at the terminus were reinforced. This buttressing effect tends to govern JI's behaviour in our model. Concerning t~~The overall terminus retreat, our model suggests that it~~ is mostly driven ~~in our model~~ by the sub-shelf melting parametrization applied (see SI, Sect. 1.2.5 and Figs. S5, S12). Although, the heat flux supplied to the shelf evolves in time based on the modelled terminus geometry, the input ocean temperature is kept constant throughout the simulations. This constant ocean forcing at the terminus lead in our simulation to gradual thinning of JI and favoured its retreat without any additional increase in ocean temperature. The terminus retreat is mostly driven in our model by the sub-shelf melting parametrization applied (see SI, Sect. 1.2.5 and Figs. S5, S12). In terms of seasonality, our results suggest that most of the seasonal signal in the model is climate driven (see SI, Sect. 1.4 and Fig. S12). In terms of seasonality, the only seasonal signal in the model is introduced by the monthly atmospheric forcing applied. The modelled sub-annual variability in terms of terminus retreat and velocities does not always follow a seasonal signal (Fig. 3). We investigate this higher than seasonal variability in Sect. 3.2.

Ice mass change

Figure 4 shows observed and modelled mass change for the period 1997 to 2014. We estimate the observed rate of ice volume change from airborne and satellite altimetry over the same period and convert to mass change rate (see SI, Sect. 2 for more details). Overall there is good agreement between modelled and observed mass change (see Fig. 4), and our results are in agreement with other similar studies (Howat et al., 2011; Nick et al., 2013). Dynamically

driven discharge is known to control Jakobshavn's mass loss between 2000-2010 (Nick et al., 2013). The modelled cumulative mass loss is 269 Gt, of which 93% (~251 Gt) is ~~determined to be~~ dynamic in origin while the remaining 7% (~18 Gt) is attributed to a decrease in SMB (see Fig. 4). Further, the present-day unloading of ice causes the Earth to respond elastically. Thus, we can use modelled mass changes to predict elastic uplift. We compare modelled changes of the Earth's elastic response to changes in ice mass to uplift observed at four GPS sites (see Fig. 5 and SI, Sect. 3). Both model and observations consistently suggest large uplift rates near the JI front (20 mm a⁻¹ for station KAGA) and somewhat minor uplift rates (~ 5 mm a⁻¹) of few mm a⁻¹ at distances of >100km from the ice margin.

Although the terminus has ceased to retreat in our simulations after 2009 (see Fig. 6 and SI, Fig. S7), the modelled mass loss, and most important the dynamic mass loss, has continued to accelerate (see Fig. 4). Our results show (SI, Figs. S7 and S8) that during this period the mass change is mostly driven by the sub-annual terminus retreat and advance, which continues to generate dynamic changes at JI through seasonal (sub-annual scale) reductions in resistive stresses.

3.2 Feedback mechanisms, forcings and limitations

Representing the processes that act at the marine boundary (i.e. calving and ocean melt) are ~~significantly~~ important for understanding and modelling the retreat/advance of marine terminating glaciers like JI. Determining terminus positions by using the superposition of a physically based calving (eigencalving) parametrization (Winkelmann et al., 2011; Levermann et al., 2012) and a basic calving mechanism (Albrecht et al., 2011) ~~a physical based calving law with horizontal strain rates (see Sect. 2.1.2)~~ is motivated by the model's ability to maintain realistic calving front positions (Levermann et al., 2012). The eigen calving style cannot resolve individual calving events and so the introduction of the basic calving mechanism was necessary in order to accurately match observed front positions. Preparatory experiments have shown that overall calving is mostly driven in our model by the basic calving mechanism used, and that the eigen calving parametrization is more important in modelling sub-annual to seasonal fluctuations of the terminus. Our simulations suggest that the superposition of these two calving mechanisms ~~Although, the calving law was designed and primarily used for modelling large ice shelves specific to the Antarctic ice sheet, our results show that the calving law also performs well for~~

1 ~~the narrow, and~~ deep fjords characterized by JI (see Fig. 2). The benefit of using such a
2 combination of calving laws is that it can evolve the terminus position with time and thus,
3 ~~potential~~ calving feedbacks are not ignored. As the terminus retreats, the feedback between
4 calving and retreat generates dynamic changes due to a reduction in lateral shear and resistive
5 stresses (~~see SI, Figs. S7 and S8~~Fig. 7). In a simulation in which the terminus position is kept
6 fixed to the 1990s position, the velocity peaks are uniform (i.e. no acceleration is modelled
7 except for some small seasonal related fluctuations generated by the ~~climatic-atmospheric~~
8 forcing applied) and the mass loss remains relatively small (~ 70 Gt). Therefore, consistent
9 with Vieli et al. (2011), we find that this feedback between calving and retreat is highly
10 important in modelling JI's dynamics.

11 As introduced in Sect. 2.1.2, our approach here is to adjust the terminus in the JI region to
12 simulate the 1990s observed front position and surface elevation based on 1985 aerial
13 photographs ~~and available satellite altimetry observations~~ (Csatho et al., 2008). The glacier
14 terminus in 1990s ~~is known to have been~~was floating (Csatho et al., 2008; Motyka et al.
15 2011), ~~but details regarding its thickness are not known~~. Motyka et al. (2011) calculated the
16 1985 hydrostatic equilibrium thickness of the south branch floating tongue from smoothed
17 surface DEMs and obtained a height of 600 m near the calving front and 940 m near the
18 grounding zone. In this paper however, ~~we choose to use a more simplistic approach in which~~
19 we compute the thickness as the difference between the surface elevation and the bed
20 topography, and allow the glacier to evolve its own terminus geometry during the equilibrium
21 simulation. This implies that our simulations start with a grounded terminus. Preparatory
22 experiments have shown that in our model (disregarding its initial geometry floating/
23 grounded terminus) JI attains equilibrium with a grounding line position that stabilizes close
24 to the 1990s observed terminus position. According to observations, JI is characterized in
25 1990 by a large floating tongue (> 10 km; e.g. Motyka et al., 2011) that we are not able to
26 simulate during the equilibrium runs. In our model (Fig. 6), the glacier starts to develop a
27 large floating tongue (~ 10 km) in 1999. Starting 2000, the floating tongue is comparable in
28 length and thickness with observations and the model is able to simulate with much accuracy
29 its breakup that occurred in late summer 2003 and the subsequent glacier acceleration.
30 Observations of terminus positions (Sohn et al., 1998; Csatho et al., 2008) suggest that over
31 more than 40 years, between 1946 and 1992, JI's terminus stabilized in the proximity of the
32 1990's observed terminus position. Furthermore, during 1959 and 1985 the southern tributary
33 was in balance (Csatho et al., 2008). This suggests that, during the equilibrium and at the

beginning of the forward simulations, we are forcing our model with climatic conditions that favoured the glacier to remain in balance. This may explain our unsuccessful attempts to simulate prior to 1998 a floating tongue comparable in length and thickness with observations, and suggests that for simulating the large floating tongue that characterized JI during this period, future studies should consider to start modelling JI before the glacier begins to float in the late 1940s (Csatho et al., 2008).

The geometry of the terminus plays an important role in parameterizing ice shelf melting, and therefore our ~~choice pre-1999 geometry could directly affect~~ influences the magnitude of the basal melt rates (see SI, Sect. 1.2.8). ~~As expected, the~~ The difference in geometry results in modelled basal melt rates ~~slightly larger than those obtained by Motyka et al. (2011) for the period 1999-2003, when JI begins to develop a large floating tongue and when the calving front was already largely floating. As shown in Fig. 6, the glacier starts to develop a large floating tongue in 1999 and the model is able to simulate with much accuracy its breakup that occurred in late summer 2003 and the subsequent glacier acceleration. Relative to other studies, e.g. Motyka et al. (2011), our melt rate for 1998 is ~2 times larger (Table S3). While we choose here to compare the two melt rates in order to offer a scale perspective, we acknowledge the difference in geometry between the two studies. Furthermore, our basal melt rates include both melting along the base of the shelf and in the proximity of the grounding line. In our model, the melt rates at the grounding line are higher than the melt rates modelled closer to the centre of the shelf (Sect. 2.1.3).~~

Starting in 2010 the modelled retreat of the terminus did not correlate well with observations (see Fig. 2). The observed terminus and the grounding line retreats ~~does~~ not cease after 2010. Further, observed front positions (Joughin et al., 2014) suggests that by summer 2010 JI was already retreating over the sill and on the overdeepening indicated by the red star in Fig. 6. The observed retreat is not reproduced in our simulations (see Fig. 6) suggesting that additional feedbacks and/or forcings ~~must continue to disturb~~ may affect the glacier. ~~These feedbacks may not be well represented (e.g. missing physics, inaccuracies in climatic or oceanic conditions) or simply may not be captured by the model due to various limitations (e.g. bed topography model constraints and grid resolution; see SI, Sect. 1.3 for more details). Alternatively, it may represent missing physics, inaccuracies in atmospheric/oceanic conditions, or other various limitations (e.g. bed topography model constraints and grid~~

1 ~~resolution).~~ ~~As detailed in SI, Sect. 1.3.2, the~~ Their particular influence for our model is
2 detailed below.

3 The basal topography of JIs channels represents a large source of uncertainty. Ji is a marine
4 terminating glacier whose bedrock topography is characterized by a long and narrow channel
5 with deep troughs that contribute to its retreat and acceleration, e.g. once the grounding line
6 starts to retreat on a down-sloping bed, the flow increases, leading to further retreat and
7 acceleration. The timing and the magnitude of these retreats are dependent on bed topography
8 and the glacier width changes (Jamieson et al., 2012; Enderlin et al., 2013). ~~The terminus~~
9 ~~retreat is mostly driven in our model by the sub-shelf melting parametrization that we applied~~
10 ~~(see SI, Fig. S4) that is highly dependent on the bed geometry.~~ Accurate modelling of the
11 grounding line behaviour is, therefore, crucial for JIs dynamics as its retreat removes areas of
12 flow resistance at the base and may trigger unstable retreat if the glacier is retreating into
13 deeper waters. The grounding line behaviour is crucial for the dynamics of marine outlet
14 glaciers, as its migration removes areas of flow resistance at the base and may trigger unstable
15 retreat if the glacier is retreating into deeper waters. In our simulation the grounding line
16 position shows stabilization stabilizes downstream of the sill after 2005 (see Fig. 2 and Fig.
17 6), which is in accordance with previous modelling studies (Vieli et al., 2001, Vieli et al.,
18 2011). ~~The grounding line behaviour is crucial for the dynamics of marine outlet glaciers, as~~
19 ~~its migration removes areas of flow resistance at the base and may trigger unstable retreat if~~
20 ~~the glacier is retreating into deeper waters.~~ Vieli et al. (2011) found that by artificially
21 lowering the same bed sill ~~with-by~~ 100 m, the grounding line eventually retreats and triggers a
22 catastrophic retreat of 80 km in just over 20 years. Similar to Vieli et al. (2011), the grounding
23 line ~~in our simulation~~ does not manage to retreat in our simulation upstream over the shallow
24 sill. In an equivalent experiment (Vieli et al., 2011) ~~-but~~ performed with our model, lowering
25 the bed sill by 100 m, did not result in a retreat of the grounding line over the sill. Regarding
26 the grid resolution, simulations performed on 1 km did not show significant improvement
27 with respect to ice thickness (Fig. S11) or surface speed (e.g. trend, magnitude and shape of
28 the flow; Fig. S12).

29 From a climatic perspective, the summer of 2012 was characterized by exceptional surface
30 melt, covering 98% of the entire ice sheet surface, including the high elevation Summit region
31 (Nghiem et al., 2012; Hanna et al., 2014). Overall, the 2012 melt-season was two months
32 longer than the 1979–2011 mean and the longest recorded in the satellite era (Tedesco et al.,

1 2013). Furthermore, the summer of 2012 was preceded by a series of warm summers (2007,
2 2008, 2010 and 2011) (Hanna et al., 2014). ~~Over the~~ Surface melt above average ~~surface melt~~
3 was already recorded in May-June 2012 (see Fig. 3 from NSIDC (2015)) when most of the
4 2011-2012 winter accumulation melted and over 30% of the ice sheet surface experienced
5 surface melt.

6 An intense and long melt year leads to extensive thinning of the ice, and has the potential to
7 enhance hydrofracturing of the calving front due to melt water draining into surface crevasses
8 (MacAyeal et al., 2003; Joughin et al., 2013; Pollard et al., 2015) resulting in greater and/or
9 faster seasonal retreat and an increase in submarine melt at the terminus and the sub-shelf
10 cavity (Schoof, 2007; Stanley et al., 2011; Kimura et al., 2014; Slater et al., 2015).

11 The seasonal retreat of JIs terminus started relatively early in 2012, with a large calving event
12 having already occurred in June. While it seems difficult to attribute this particular calving
13 event solely to processes related ~~with to~~ the 2012 melt season, it does seem probable that the
14 series of warm summers (2007-2011) together with the 2012 exceptional melt season could
15 have enhanced hydrofracturing of the calving front ~~and consequently~~. In turn, this could have
16 induced a retreat of the terminus ~~which that~~ cannot be captured by the model (i.e. in its
17 present configuration the model does not account for the influence of meltwater runoff and its
18 role in the subglacial system during surface melt events). In our model, the ~~climatic~~
19 atmospheric forcing applied can influence JI's dynamics only through changes in surface
20 mass balance (SMB) (i.e., accumulation and ablation) (~~see SI, Sect. 1.2, 5~~Fig. S2). While
21 these changes in ice thickness affect both the SIA and the SSA, the effect in the SIA is very
22 weak as the driving stresses are not affected by a few meters of difference in thickness
23 induced by SMB variability. In the SSA, the coupling is done via the effective pressure term
24 in the definition of the yield stress (see SI, Sect. 1.2 for detailed equations). The effective
25 pressure is determined by the ice overburden pressure (i.e. ice thickness) and the effective
26 thickness of water in the till, where the latter is computed by time-integrating the basal melt
27 rate. This effect is much stronger and favours the idea that in our model some seasonal
28 velocity peaks could potentially be influenced by the climatic forcing applied (Figs. S10 and
29 S15).

30 ~~Our results suggest that most of the sub-annual signal in the model is climate driven (see SI,~~
31 ~~Sect. 1.4 and Fig. S12).~~ We study the sensitivity of the model to atmospheric forcing by
32 performing a simulation where we keep the atmospheric forcing constant (mean 1960-1990

temperature and SMB). By comparing this simulation with a simulation that includes full atmospheric variability (monthly temperature and SMB) we see that in terms of terminus retreat and velocities the modelled sub-annual variability does not always correlate with the observed seasonal signal (Fig. 3 S15). In particular, the simulations suggest that to only a relatively small degree some of the variability appears to be influenced by the atmospheric forcing applied (Figs. S2, S10 and S15), which also represents the only seasonal input into the model. A comparison between a simulation that includes the full climatic variability (monthly temperature and SMB from RACMO2.3) and a simulation with constant climatic forcing (mean 1960-1990 temperature and SMB) indicates that the two accelerations, in 1998 and 2003, are related to bed geometry and ocean melt. Furthermore, our results show that some seasonal velocity peaks could potentially be influenced by the climatic forcing applied. This suggests that even though the climate does not trigger and sustain long accelerations, the climate certainly does have the capacity to contribute and accentuate the processes that are responsible for these accelerations.

The modelled sub-annual signal in terms of terminus retreat and velocities does not always correlate with the observed signal. Some of the greater than seasonal frequency could be an issue with resolution in the model. We examined this sensitivity by doing additional runs at higher resolution. Simulations on a 1 km did show some improvement with respect to surface speed sub-annual variability (Fig. S13), suggesting that in our model the stress redistribution might be sensitive to the resolution of the calving event (Fig. 7). However, given the short period spanned by the simulations, the stress redistribution does not significantly affect the modelled results, as seen in Figs. S11 and S12. Although we acknowledge that some of the variability is due the grid resolution, part of it may be also related with unmodeled physical processes at the terminus. We suggest that additional contributions to the seasonality potentially different seasonal forcings (e.g. from ice mélange variability or seasonal ocean temperature variability), which are not included in our model, may could potentially influence the advance and retreat of the front at seasonal scales and so, the large sub-annual signal in our simulations. For example, the ice mélange can prevent the ice at the calving front from breaking off and could therefore reduce the calving rates. Consequently, the introduction of an ice mélange parametrization will probably help to minimize some of the sub-annual noise signal observed-modelled in our simulations (see Fig. 3). Seasonal ocean temperature variability can influence the ice mélange formation and/or clearance and the melt rates at the glacier front and can accentuate seasonal glacier terminus and grounding line

1 retreat and/or advance. However, at this point we can't precisely determine the relative
2 importance of each process.

3 ~~Furthermore, the 2 km resolution used in this study may not be sufficient to accurately model~~
4 ~~the seasonal retreat and advance of the front. The smallest calving event in our model is 4~~
5 ~~km², which is larger than most of the calving events observed at JI (see SI, Sect. 1.3.1).~~

6 Concerning Finally, regarding the ocean conditions, warm water temperatures in the fjord
7 were recorded in 2012. Besides a cold anomaly in 2010, which was sustained until early 2011,
8 the period 2008-2013 is characterized by high fjord waters temperatures - equal to or warmer
9 than those recorded in 1998-1999 (Gladish et al., 2015). In our model, the ice melt rates are
10 determined from the given conditions in temperature (-1.7 °C), and salinity (35 psu) of the
11 fjord waters, and the given geometry (see Sect. 2.1.3 and SI, Sect. 1.2.5). ~~Although, the~~
12 ~~ocean temperature is scaled based on a virtual temperature that depends on the geometry of~~
13 ~~the shelf, the 1998 and 2003 accelerations can be modelled without additional variability in~~
14 ~~ocean temperatures. Further our results suggest that these accelerations are most likely driven~~
15 ~~by internal glacier dynamics and bed geometry, and not by an increase in e.g. ocean~~
16 ~~temperature.~~ The fact that we are able to model JIs retreat with no variability in ocean
17 temperature suggests that the retreat and acceleration observed at JI are likely not caused by a
18 year to year variability in ocean temperatures. This conclusion agrees with the observational
19 study of Gladish et al. (2015) who analysed ocean temperature variability in the Ilulissat fjord
20 with JI variability and who found that after 1999 there was no clear correlation. Our results do
21 not, however, imply that the ocean influence in JI's retreat is negligible (see Fig. S5), but
22 rather that the glacier most likely responds to changes in ocean temperature that are sustained
23 for longer time periods, e.g. decadal time scales. Two additional experiments, where the input
24 ocean temperature (T_o) was increased to -1 °C indicate that higher melt rates beneath the
25 grounding line could potentially explain the retreat observed after 2010. In the first
26 experiment, the input T_o was increased from -1.7 °C to -1 °C ~~between 1997-2014~~ starting
27 1997 (~0.7 °C relative to 1990). ~~(Gladish et al., 2015).~~ This temperature increase is consistent
28 with observed ocean temperatures at the mouth of the Ilulissat fjord (Gladish et al., 2015) and
29 ~~This~~ generated in our simulation, for the period 1997-2014, an accelerated retreat of the front
30 that does not correlate with observations (Fig. S8), and mass loss estimates significantly
31 larger (by ~ 50 %; Fig. S7) than those calculated from airborne and satellite altimetry
32 observations (see SI, Sect. 2). Overall, the experiment shows that an increase in ocean

temperature that starts in 1997 and is sustained until 2014 generates modelled estimates for the period 1998-2014 that do not agree with observations. In the second experiment, T_o was increased to $-1\text{ }^{\circ}\text{C}$ ~~between 2010-2014~~ starting 2010 ($\sim +0.7^{\circ}\text{C}$ at the base of the shelf in 2010 ~~with $(T_o - T_i) \sim +0.7^{\circ}\text{C}$ at the base of the shelf in 2010~~), and generated in our simulation, for the period 2010-2014, a faster retreat of the front that correlates well with observations (Fig. S8), and an increase of mass loss by $\sim 7\text{ Gt}$ (Fig. S7). This experiment shows that an increase in ocean temperature beginning in 2010 could potentially explain the retreat observed thereafter.

4 Conclusions

In this study, a three-dimensional, time-dependent regional outlet glacier model is used to investigate the processes driving the dynamic evolution of JI and its seasonal variation in ice velocity between 1990 and 2014. Here, we attempt to ~~model and understand~~ simulate the recent behaviour of JI with a process-based model. The model parameters were calibrated such that the model reproduces observed frontal positions (Fig. 2) and ice mass change observations (Fig. 4) at JI over the periods 1990-2014 and 1997-2014, respectively. We obtain a good agreement of our model output with measured horizontal velocities, observed thickness change, and GPS derived elastic uplift of the crust (Figs. 3 and 5). Overall, the study shows progress in modelling the temporal variability of the flow at JI.

Our results suggest that most of the JI retreat during 1990-2014 is driven by the ocean parametrization, and the glacier subsequent response, which is largely governed by its own bed geometry. ~~ocean and bed geometry driven and that the~~ In agreement with previous studies (e.g. Joughin et al. 2012), our simulations suggest that the overall variability in the modelled horizontal velocities is a response to variations in terminus position. In our model, the seasonal variability is likely driven by processes related to the atmospheric forcing applied (e.g. temperature and SMB variability), which in fact represents the only seasonal input used in the model. A greater than seasonal frequency is seen in our simulations and is attributed to grid resolution and missing seasonal scale processes (e.g., ice mélange variability or seasonal ocean temperature variability) in the model. Sensitivity experiments performed on a 1 km grid did not show significant improvement with respect to ice thickness (Fig. S11) or surface speed (i.e. shape of the flow and overall magnitude; Fig. S12). The seasonal variability observed in our simulations is climate driven. In its present configuration, the model does not

~~account for seasonal ocean temperature and ice mélange variability that may influence the seasonal advance and retreat of the front.~~

~~JI is characterized in 1990 by a large floating tongue (> 10 km; e.g. Motyka et al., 2011) that we are not able to simulate during the equilibrium runs. In our model (Fig. 6), the glacier starts to develop a floating tongue comparable with observations in 1999. Starting 2000, the floating tongue is consistent in length and thickness with observations and the model is able to simulate its breakup that occurred in late summer 2003 and the subsequent glacier acceleration. The difference between observed and modelled pre-1999 geometry results in relatively large basal melt rates for the period 1997-2003.~~

~~Nevertheless, For the period 1990-2010,~~ the model is able to capture the overall retreat of the terminus and the trends in the observed velocities (see Figs. 2 and 3) ~~for the period 1990-2010. Finally, t~~The 2010-2012 observed terminus retreat (Joughin et al., 2014) is ~~-, however,~~ not reproduced in our simulations, likely due to inaccuracies in basal topography, or misrepresentations of the ~~elimatie—atmospheric forcing~~ and ~~oceanic—forcingsthe ocean parametrization used.~~ ~~Additional sensitivity experiments showed that an increase in ocean temperature of ~ 0.7 °C for the period 2010-2014 may trigger a retreat of the terminus that agrees well with observations (Figs. S7 and S8).~~

Our model ~~provides evidence for~~ reproduces two distinct flow accelerations in 1998 and 2003 that are consistent with observations. The first was generated by a retreat of the terminus and moderate thinning prior to 1998; the latter was triggered by the final breakup of the floating tongue. During this period, JI attained in our simulation unprecedented velocities reaching as high as 20 km a⁻¹. Additionally, the final breakup of the floating tongue generated a reduction in buttressing that resulted in further thinning. ~~Over the last decade, as the slope steepened inland, sustained high flow rates were observed at JI. Similar to previous studies (Nick et al., 2009; Vieli et al., 2011; Joughin et al. 2012), our results show that the dynamic changes observed at JI are triggered at the terminus (Figs. 7, S5, S15 and S17).~~

In accordance with previous studies (Thomas, 2004; Joughin et al., 2012), our findings suggest that the speed observed today at JI is a result of thinning induced changes due to reduction in resistive stress (buttressing) near the terminus correlated with inland steepening slopes (Figs. 6 and S7). Both model and observations suggest that JI has been losing mass at an accelerating rate and that the glacier has continued to accelerate through 2014 (Fig. 4). ~~Similar to previous studies (Nick et al., 2009; Vieli et al., 2011; Joughin et al. 2012), our~~

~~results show that the dynamic changes observed at JI are triggered at the terminus (SI, Figs. S5 and S6). In our model, the terminus retreat is mostly driven by the sub-shelf melting parametrization applied. Thus, our results suggest that ocean forcing is the principal driver for the retreat observed over the last 2 decades. Further, our model provides evidence that the rapid accelerations of JI in 1998 and 2003 could be triggered by the bed geometry and internal glacier dynamics, and not by a sudden increase in e.g. ocean temperature.~~

Author Contributions

I.S.M. was responsible for the numerical modelling part. J.B. provided the bed model. M.R.V.D.B. and P.K.M. provided climate data. S.A.K and B.W. provided observational data. I.S.M. and S.A.K created the figures and wrote the manuscript with contributions from A. A, J.B., T.V.D., M.R.V.D.B, B.W., P.K.M, K.K., and C.K.

Acknowledgements

Ioana S. Muresan is funded by the Forskningsraadet for Natur og Univers (grant no. 12-155118). Shfaqat A. Khan is supported by Carlsbergfondet (grant no. CF14-0145). Jonathan Bamber was part funded by UK NERC grant NE/M000869/1. Bert Wouters is funded by a Marie Curie International Outgoing Fellowship within the 7th European Community Framework Programme (FP7-PEOPLE-2011-IOF-301260). The development of PISM is supported by NASA grants NNX13AM16G and NNX13AK27G. We thank the editor, three anonymous reviewers for their valuable comments and suggestions to improve and clarify the manuscript, and Veit Helm for providing cryosat-2 data.

References

- Albrecht, T., M. Martin, M. Haseloff, R. Winkelmann, and A. Levermann. 2011. "Parameterization for subgrid-scale motion of ice-shelf calving fronts." *The Cryosphere* 5: 35–44. doi:10.5194/tc-5-35-2011.
- Amundson, J. M., M. Fahnestock, M. Truffer, J. Brown, M. P. Lüthi, and R. J. Motyka. 2010. "Ice mélange dynamics and implications for terminus stability, Jakobshavn Isbræ, Greenland." *Journal of Geophysical Research* 115: F01005. doi:10.1029/2009JF001405.
- Aschwanden, A., E. Bueler, C. Khroulev, and H. Blatter. 2012. "An enthalpy formulation for glaciers and ice sheets." *Journal of Glaciology* 58(209): 441–457. doi:10.5194/tcd-6-5069-2012. doi:10.3189/2012JoG11J088.
- Aschwanden, A., G. Aðalgeirsdóttir, and C. Khroulev. 2013. "Hindcast to measure ice sheet model sensitivity to initial states." *The Cryosphere* 7: 1083–1093. doi:10.5194/tcd-6-5069-2012.
- Bamber, J. L., J. A. Griggs, R. T. W. L. Hurkmans, J. A. Dowdeswell, S. P. Gogineni, I. Howat, J. Mouginot, J. Paden, S. Palmer, E. Rignot, and D. Steinhage. 2013. "A new bed elevation dataset for Greenland." *The Cryosphere* 7: 499–510. doi:10.5194/tc-7-499-2013.
- Beckmann, A., and H. Goosse. 2003. "A parameterization of ice shelf–ocean interaction for climate models." *Ocean Modeling* 5 (2): 157–170. doi:10.1016/S1463-5003(02)00019-7.
- Bevan, S. L., A. J. Luckman, and T. Murray. 2012. "Glacier dynamics over the last quarter of a century at Helheim, Kangerdlugssuaq and other major Greenland outlet glaciers." *The Cryosphere* 6: 923–937. doi:10.5194/tc-6-923-2012.
- Bindschadler, R. A., S. Nowicki, A. Abe-Ouchi, A. Aschwanden, H. Choi, J. Fastook, G. Granzow, et al. 2013. "Ice-Sheet Model Sensitivities to Environmental Forcing and Their Use in Projecting Future Sea Level (the SeaRISE Project)." *Journal of Glaciology* 59 (214): 195–224. doi:10.3189/2013JoG12J125.

1 Broeke, M. van den, J. Bamber, J. Ettema, Eric Rignot, E. Schrama, W. J. van de Berg, E. van
2 Meijgaard, I. Velicogna, and B. Wouters. 2009. "Partitioning recent Greenland mass loss."
3 *Science* 326 (5955): 984–986. doi:10.1126/science.1178176.

4 Bueler, E., and J. Brown. 2009. "Shallow shelf approximation as a 'sliding law' in a
5 thermodynamically coupled ice sheet model." *Journal of Geophysical Research* 114: F03008.
6 doi:10.1029/2008JF001179.

7 Csatho, B., T. Schenk, C. J. Van Der Veen and W. B. Krabill. 2008. "Intermittent thinning of
8 Jakobshavn Isbræ, West Greenland, since the Little Ice Age." *Journal of Glaciology* 54 (184):
9 131–144. doi: 10.3189/002214308784409035.

10 Echelmeyer, K.A., W.D. Harrison, C. Larson, and J.E. Mitchell. 1994. The role of the
11 margins in the dynamics of an active ice stream. *Journal of Glaciology* 40(136): 527–538.

12 Enderlin, E. M., I. M. Howat, and A. Vieli. 2013. "High sensitivity of tidewater outlet glacier
13 dynamics to shape." *The Cryosphere* 7: 1007–1015. doi: 10.5194/tc-7-1007-2013.

14 Enderlin, E. M., I. M. Howat, S. Jeong, M. J. Noh, J. H. van Angelen, and M. R. van den
15 Broeke. 2014. "An improved mass budget for the Greenland ice sheet." *Geophysical Research*
16 *Letters* 41: 866–872. doi:10.1002/2013GL059010.

17 Feldmann, J., T. Albrecht, C. Khroulev, F. Pattyn, and A. Levermann. 2014. "Resolution-dependent performance of grounding line
18 motion in a shallow model compared with a full-Stokes model according to the MISIMIP3d
19 intercomparison." *Journal of Glaciology* 60 (220): 353–360. doi:10.3189/2014JoG13J093.

20 Feldmann, J., Albrecht, T., Khroulev, C., Pattyn, F., and Levermann, A.: Resolution-
21 dependent performance of grounding line motion in a shallow model compared with a full-
22 Stokes model according to the MISIMIP3d intercomparison, *J. Glaciol.*, 60, 353–360,
23 doi:10.3189/2014JoG13J093, 2014.

24 Gladish, C. V., D. M. Holland, and C. M. Lee. 2015a. "Oceanic boundary conditions for
25 Jakobshavn Glacier. Part II: Provenance and sources of variability of Disko Bay and Ilulissat
26 icefjord waters, 1990–2011." *Journal of Physical Oceanography* 45: 33–63.
27 doi:dx.doi.org/10.1175/JPO-D-14-0045.1.

28 Gladish, C. V., D. M. Holland, A. Rosing-Asvid, J. W. Behrens, and J. Boje. 2015b. "Oceanic
29 boundary conditions for Jakobshavn Glacier. Part I: Variability and renewal of Ilulissat
30 icefjord waters, 2001–2014." *Journal of Physical Oceanography* 45: 3–32.
31 doi:dx.doi.org/10.1175/JPO-D-14-0044.1.

- Gladstone, R. M., A. J. Payne, and S. L. Cornford. 2010. "Parameterising the grounding line in flow-line ice sheet models." *The Cryosphere* 4: 605–19. doi:10.5194/tc-4-605-2010.
- Hanna, E., X. Fettweis, S. Mernild, J. Cappelen, M. Ribergaard, C. Shuman, K. Steffen, L. Wood, and T. Mote. 2014. "Atmospheric and oceanic climate forcing of the exceptional Greenland ice sheet surface melt in summer 2012." *International Journal of Climatology* 34 (4): 1022–1037. doi:10.1002/joc.3743.
- Holland, D. M., R. H. Thomas, B. de Young, M. H. Ribergaard, and B. Lyberth. 2008. "Acceleration of Jakobshavn Isbræ Triggered by Warm Subsurface Ocean Waters." *Nature Geoscience* 1: 659–664. doi:10.1038/ngeo316.
- Howat I. M., Y. Ahn, I. Joughin, M. R. van den Broeke, J. T. M. Lenaerts, and B. Smith. 2011. "Mass balance of Greenland's three largest outlet glaciers, 2000–2010." *Geophysical Research Letters* 38(12): L12501. doi: 10.1029/2011GL047565.
- Hutter K. 1983. "Theoretical Glaciology: Material Science of Ice and the Mechanics of Glaciers and Ice Sheets." D. Reidel Publishing Co. Tokyo, Terra Scientific Publishing Co. xxxii, 510 p.
- IPCC. 2013. "Climate Change 2013: The Physical Science Basis. Contribution of Working Group I to the Fifth Assessment Report of the Intergovernmental Panel on Climate Change." Cambridge University Press, Cambridge, United Kingdom and New York, NY, USA: 1535 pp. doi:10.1017/CBO9781107415324.
- Jamieson, S. S. R., A. Vieli, S. J. Livingstone, C. Ó Cofaigh, C. Stokes, C.-D. Hillenbrand, and J. A. Dowdeswell. 2012. "Icestream stability on a reverse bed slope". *Nature Geoscience* 5 :799–802. doi:10.1038/NGEO1600.
- Jones, P. W. 1999. "First- and Second-Order Conservative Remapping Schemes for Grids in Spherical Coordinates". *Monthly Weather Review* 127 (9): 2204–2210. doi: http://dx.doi.org/10.1175/1520-0493(1999)127<2204:FASOCR>2.0.CO;2.
- Joughin, I., W. Abdalati, and M. Fahnestock. 2004. "Large fluctuations in speed on Greenland's Jakobshavn Isbræ glacier." *Nature* 432: 608–610. doi:10.1038/nature03130.
- Joughin, I., I. M. Howat, M. Fahnestock, B. Smith, W. Krabill, R. B. Alley, H. Stern, and M. Truffer. 2008. "Continued evolution of Jakobshavn Isbrae Following Its Rapid Speedup." *Journal of Geophysical Research* 113: F04006. doi:10.1029/2008JF001023.

1 Joughin, I, B. E. Smith, I. M. Howat, T. Scambos, and T. Moon. 2010. “Greenland Flow
2 Variability from Ice-Sheet-Wide Velocity Mapping”. *Journal of Glaciology* 56 (197): 415-
3 430. doi:10.3189/002214310792447734.

4 Joughin, I., I. Howat, B. Smith, and T. Scambos. 2011. “MEaSURES Greenland Ice Velocity:
5 Selected Glacier Site Velocity Maps from InSAR”. Boulder, Colorado, USA: NASA DAAC
6 at the National Snow and Ice Data Center. doi:10.5067/MEASURES/CRYOSPHERE/nsidc-
7 0481.001.

8 Joughin, I., B. E. Smith, I. M. Howat, D. Floricioiu, R. B. Alley, M. Truffer, and M.
9 Fahnestock. 2012. “Seasonal to decadal scale variations in the surface velocity of Jakobshavn
10 Isbræ, Greenland: Observation and model-based analysis.” *Journal of Geophysical Research*
11 117: F02030. doi:10.1029/2011JF002110.

12 Joughin, I., S. B. Das, G. E. Flowers, M. D. Behn, R. B. Alley, M. A. King, B. E. Smith, J. L.
13 Bamber, M. R. van den Broeke, and J. H. van Angelen. 2013. “Influence of ice-sheet
14 geometry and supraglacial lakes on seasonal ice-flow variability.” *The Cryosphere* 7: 1185-
15 1192. doi:10.5194/tc-7-1185-2013.

16 Joughin, I., B. E. Smith, D. E. Shean, and D. Floricioiu. 2014. “Brief Communication: Further
17 summer speedup of Jakobshavn Isbræ.” *The Cryosphere* 8: 209–214. doi:10.5194/tc-8-209-
18 2014.

19 Keegan, K. M., R.M. Albert, J. R. McConnell and I. Baker. 2014. “Climate change and forest
20 fires synergistically drive widespread melt events of the Greenland Ice Sheet.” *Proceedings of*
21 *the National Academy of Sciences* 111(22): 7964–7967. doi: 10.1073/pnas.1405397111.

22 Khan, S. A., L. Liu, J. Wahr, I. Howat, I. Joughin, T. van Dam, and K. Fleming. 2010. “GPS
23 measurements of crustal uplift near Jakobshavn Isbræ due to glacial ice mass loss.” *Journal of*
24 *Geophysical Research* 115: B09405. doi:10.1029/2010JB007490.

25 Khan, S. A., K. H. Kjær, M. Bevis, J. L. Bamber, J. Wahr, K. K. Kjeldsen, A. A. Bjørk, N. J.
26 Korsgaard, L. A. Stearns, M. R. van den Broeke, L. Liu, N. K. Larsen, and I. S. Muresan.
27 2014. “Sustained Mass Loss of the Northeast Greenland Ice Sheet Triggered by Regional
28 Warming.” *Nature Climate Change* 4: 292–299. doi:10.1038/nclimate2161.

29 Khan, S. A., A. Aschwanden, A. A. Bjørk, J. Wahr, K. K. Kjeldsen, and K. H. Kjær. 2015.
30 “Greenland ice sheet mass balance: a review.” *Reports on Progress in Physics* 78(4). doi:
31 10.1088/0034-4885/78/4/046801.

1 Kimura, S., P. R. Holland, A. Jenkins, and M. Piggott. 2014. "The effect of meltwater plumes
2 on the melting of a vertical glacier face." *Journal of Physical Oceanography* 44: 3099-3117.
3 doi: 10.1175/JPO-D-13-0219.1

4 Krabill, W., W. Abdalati, E. Frederick, S. Manizade, C. Martin, J. Sonntag, R. Swift, R.
5 Thomas, W. Wright, and J. Yungel. 2000. "Greenland Ice Sheet: High-Elevation Balance and
6 Peripheral Thinning." *Science* 289: 428–430. doi:10.1126/science.289.5478.428.

7 Krabill, W., E. Hanna, P. Huybrechts, W. Abdalati, J. Cappelen, B. Csatho, E. Frederick, S.
8 Manizade, C. Martin, J. Sonntag, R. Swift, R. Thomas, and J. Yungel. 2004. "Greenland Ice
9 Sheet: Increased coastal thinning", *Geophysical Research Letters* 31: L24402.
10 doi:10.1029/2004GL021533.

11 Krabill, W. B. 2014. "IceBridge ATM L2 Icessn Elevation, Slope, and Roughness, [1993-
12 2014]. Boulder, Colorado USA: NASA Distributed Active Archive Center at the National
13 Snow and Ice Data Center. Digital media. Updated 2014." <http://nsidc.org/data/ilatm2.html>.

14 Larour, E., H. Seroussi, M. Morlighem, and E. Rignot. 2012. "Continental scale, high order,
15 high spatial resolution, ice sheet modeling using the Ice Sheet System Model (ISSM)." *Journal of Geophysical Research: Earth Surface* (2003-2012) 117: F01022.
16 doi:10.1029/2011JF002140.

17 Levermann, A., T. Albrecht, R. Winkelmann, M. A. Martin, M. Haseloff, and I. Joughin.
18 2012. "Kinematic first-order calving law implies potential for abrupt ice-shelf retreat." *The Cryosphere* 6: 273–286. doi:10.5194/tc-6-273-2012.

19 Luckman, A., and T. Murray. 2005. "Seasonal variation in velocity before retreat of
20 Jakobshavn Isbræ, Greenland." *Journal of Geophysical Research Letters* 32: L08501.
21 doi:10.1029/2005GL022519.

22 MacAyeal, D. R., T. A. Scambos, C. L. Hulbe and M. A. Fahnestock. 2003. "Catastrophic
23 iceshelf break-up by an ice-shelf-fragment-capsize mechanism." *Journal of Glaciology*
24 49(164): 22-36.

25 Martin, M. A., R. Winkelmann, M. Haseloff, T. Albrecht, E. Bueler, C. Khroulev, and A.
26 Levermann. 2011. "The Potsdam Parallel Ice Sheet Model (PISM-PIK), Part II: Dynamical
27 equilibrium simulation of the Antarctic Ice Sheet." *The Cryosphere* 5: 727–740.
28 doi:10.5194/tc-5-727-2011.

1 Mengel, M., and A. Levermann. 2014. "Ice plug prevents irreversible discharge from East
2 Antarctica." *Nature Climate Change* 4: 451–455. doi:10.1038/nclimate2226.

3 Moon, T., I. Joughin, B. Smith, and I. Howat. 2012. "21st-Century evolution of Greenland
4 outlet glacier velocities." *Science* 336: 576–578. doi:10.1126/science.1219985.

5 Motyka, R. J., M. Truffer, M. Fahnestock, J. Mortensen, S. Rysgaard, and I. Howat. 2011.
6 "Submarine melting of the 1985 Jakobshavn Isbræ floating tongue and the triggering of the
7 current retreat." *Journal of Geophysical Research* 116: F01007. doi:10.1029/2009JF001632.

8 NSIDC. 2015. "2014 melt season in review." National Snow & Ice Data Center (NSIDC).
9 Accessed July 09, 2015. [http://nsidc.org/greenland-today/2015/01/2014-melt-season-in-](http://nsidc.org/greenland-today/2015/01/2014-melt-season-in-review/)
10 [review/](http://nsidc.org/greenland-today/2015/01/2014-melt-season-in-review/).

11 Nghiem, S. V., D. K. Hall, T. L. Mote, M. Tedesco, M. R. Albert, K. Keegan, C. A. Shuman,
12 N. E. DiGirolamo, and G. Neumann. 2012. "The extreme melt across the Greenland ice sheet
13 in 2012." *Geophysical Research Letters* 39: L20502. doi: 10.1029/2012GL053611.

14 Nick, F. M., A. Vieli, M. L. Andersen, I. Joughin, A. Payne, T. L. Edwards, F. Pattyn, and R.
15 S. van de Wal. 2013. "Future sea-level rise from Greenland's main outlet glaciers in a
16 warming climate." *Nature* 497: 235–238. doi:10.1038/nature12068.

17 Nick, F.M., A. Vieli, I. M. Howat, and I. Joughin. 2009. "Large-Scale Changes in Greenland
18 Outlet Glacier Dynamics Triggered at the Terminus." *Nature Geoscience* 2: 110–114.
19 doi:10.1038/ngeo394.

20 Nielsen, K., S. A. Khan, G. Spada, J. Wahr, M. Bevis, L. Liu, and T. van Dam. 2013.
21 "Vertical and horizontal surface displacements near Jakobshavn Isbræ driven by melt-induced
22 and dynamic ice loss." *Journal of Geophysical Research Solid Earth* 118: 1837–1844.
23 doi:10.1002/jgrb.50145.

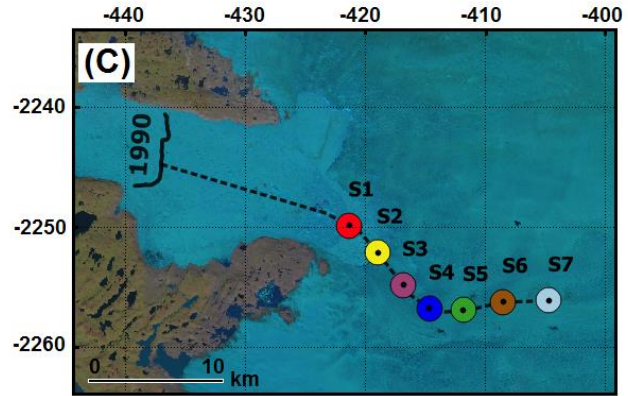
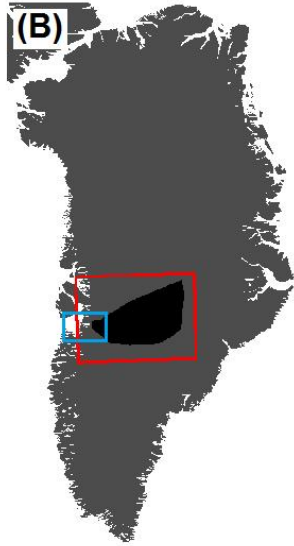
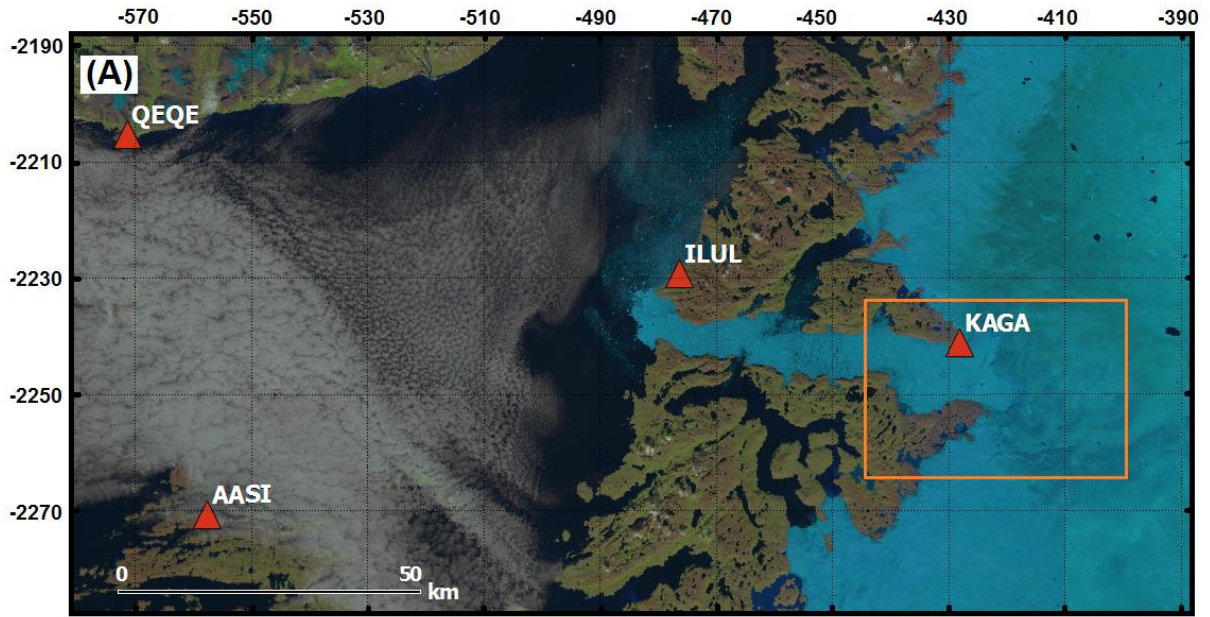
24 Noël, B., W. J. van de Berg, E. van Meijgaard, P. Kuipers Munneke, R. S. W. van de Wal,
25 and M. R. van den Broeke. 2015. "Summer snowfall on the Greenland Ice Sheet: a study with
26 the updated regional climate model RACMO2.3." *The Cryosphere Discussion* 9: 1177-1208.
27 doi: 10.5194/tcd-9-1177-2015.

28 Parizek, B.R., and R.T. Walker. 2010. "Implications of initial conditions and ice–ocean
29 coupling for grounding-line evolution." *Earth and Planetary Science Letters* 300: 351–358.
30 doi:10.1016/j.epsl.2010.10.016.

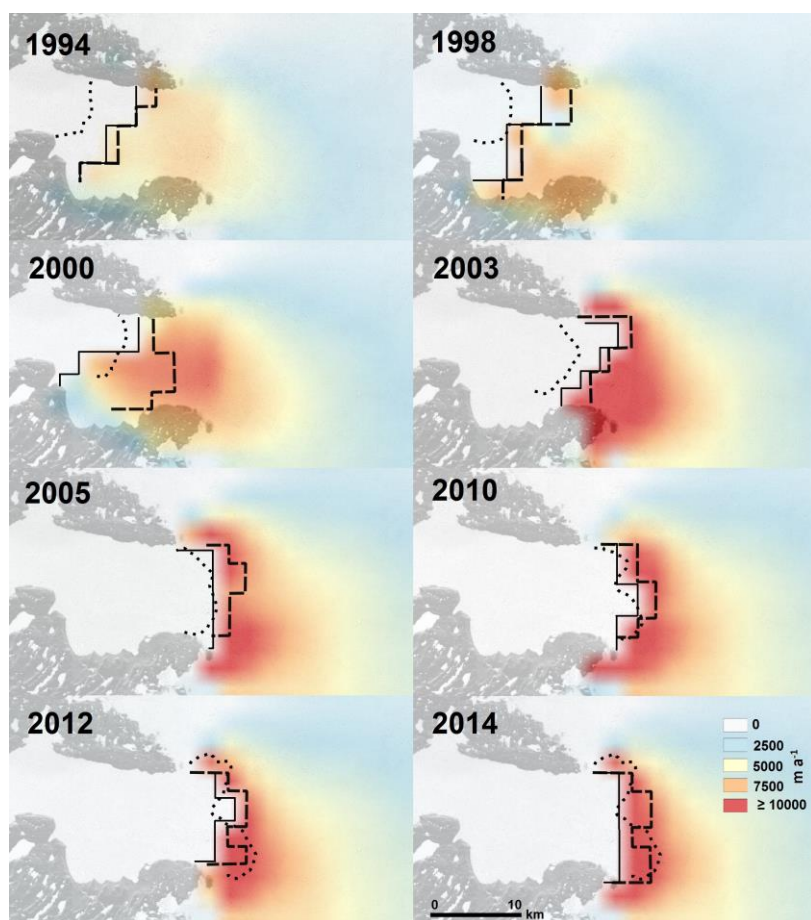
- 1 Pattyn, F., C. Schoof, L. Perichon, R. C. A. Hindmarsh, E. Bueler, B. de Fleurian, G. Durand,
2 et al. 2012. "Results of the Marine Ice Sheet Model Intercomparison Project, MISIMIP." *The*
3 *Cryosphere* 6: 573–588. doi:10.5194/tc-6-573-2012.
- 4 [Pattyn, F., Perichon, L., Durand, G., Favier, L., Gagliardini, O., Hindmarsh, R., Zwinger, T.,](#)
5 [Albrecht, T., Cornford, S., Docquier, D., Fust, J. J., Goldberg, D., Gudmundsson, G. H.,](#)
6 [Humbert, A., Hutter, M., Huybrechts, P., Jouvett, G., Kleiner, T., Larour, E. and Martin, D.,](#)
7 [Morlighem, M., Payne, A. J., Pollard, D., Ruckamp, M., Rybak, O., Seroussi, H.,](#)
8 [Thoma, M., and Wilkens, N. 2010. "Grounding-line migration in plan-view marine ice-sheet](#)
9 [models: results of the ice2sea MISIMIP3d intercomparison". *Journal of Glaciology* 59: 410–](#)
10 [422. doi:http://dx.doi.org/10.3189/2013JoG12J12910.3189/2013JoG12J129.](#)
- 11 Pollard, D., R. M. DeConto, and R. B. Alley. 2015. "Potential Antarctic Ice Sheet retreat
12 driven by hydrofracturing and ice cliff failure." *Earth and Planetary Science Letters* 412: 112–
13 121. doi: 10.1016/j.epsl.2014.12.035.
- 14 Price, S. F., A. J. Payne, I. M. Howat, and B. E. Smith. 2011. "Committed sea-level rise for
15 the next century from Greenland ice sheet dynamics during the past decade." *Proceedings of*
16 *the National Academy of Sciences of the United States of America* 108: 8978–8983.
17 doi:10.1073/pnas.1017313108.
- 18 Rignot, E., J. L. Bamber, M. R. van den Broeke, C. Davis, Y. Li, W. J. van de Berg, and E.
19 van Meijgaard. 2008. "Recent Antarctic ice mass loss from radar interferometry and regional
20 climate modeling." *Nature Geoscience* 1: 106–110. doi:10.1038/ngeo102.
- 21 Schoof, C. 2007. "Ice sheet grounding line dynamics: steady states, stability, and hysteresis."
22 *Journal of Geophysical Research* 112 (F03S28). doi:10.1029/2006JF000664.
- 23 Seroussi, H., H. B. Dhia, M. Morlighem, E. Larour, E. Rignot, and D. Aubry. 2012.
24 "Coupling ice flow models of varying orders of complexity with the Tiling method." *Journal*
25 *of Glaciology* 58: 776–786. doi:10.3189/2012JoG11J195.
- 26 Shapiro, N. M., and M. H. Ritzwoller. 2004. "Inferring surface heat flux distributions guided
27 by a global seismic model: particular application to Antarctica." *Earth and Planetary Science*
28 *Letters* 223: 213–224. doi: 10.1016/j.epsl.2004.04.011.
- 29 Shepherd, A., E. R. Ivins, A. Geruo, V. R. Barletta, M. J. Bentley, S. Bettadpur, K. H. Briggs,
30 D. H. Bromwich, et al. 2012. "A reconciled estimate of ice-sheet mass balance." *Science*
31 338(6111): 1183-1189. doi:10.1126/science.1228102.

- Slater, D. A., P. W. Nienow, T. R. Cowton, D. N. Goldberg, and A. J. Sole. 2015. "Effect of near-terminus subglacial hydrology on tidewater glacier submarine melt rates." *Geophysical Research Letters* 42: 2861-2868. doi: 10.1002/2014GL062494.
- Sohn, H. G., K. C. Jezek, and C. J. van der Veen. 1998. "Jakobshavn Glacier, west Greenland: 30 years of spaceborne observations." *Geophysical Research Letters* 25(14): 2699-2702. doi: 10.1029/98GL01973.
- Stanley, S. J., A. Jenkins, C. F. Giulivi and P. Dutrieux. 2011. "Stronger ocean circulation and increased melting under Pine Island Glacier ice shelf." *Nature Geoscience* 4: 519–523. doi: 10.1038/ngeo1188
- Tedesco, M., X. Fettweis, T. Mote, J. Wahr, P. Alexander, J. E. Box, and B. Wouters. 2013. "Evidence and analysis of 2012 Greenland records from spaceborne observations, a regional climate model and reanalysis data." *The Cryosphere* 7: 615-630. doi: 10.5194/tc-7-615-2013
- The PISM Authors. 2014. "PISM, a Parallel Ice Sheet Model. User's Manual." Accessed June 15, 2015. <http://www.pism-docs.org/wiki/lib/exe/fetch.php?media=manual.pdf>.
- Thomas, H. R., W. Abdalati, E. Frederick, W. B. Krabill, S. Manizade, and K. Steffen. 2003. "Investigation of surface melting and dynamic thinning on Jakobshavn Isbræ." *Journal of Glaciology* 49 (165): 231–239. doi:10.3189/172756503781830764.
- Thomas, R. H. 2004. "Force-perturbation analysis of recent thinning and acceleration of Jakobshavn Isbrae, Greenland." *Journal of Glaciology* 50(168): 57–66. doi: 10.3189/172756504781830321.
- Van der Veen, C. J., J. C. Plummer, and L. A. Stearns. 2011. "Controls on the recent speed-up of Jakobshavn Isbræ, West Greenland." *Journal of Glaciology* 57 (204): 770–782.
- Vieli, A., and F. M. Nick. 2011. "Understanding and Modeling Rapid Dynamic Changes of Tidewater Outlet Glaciers: Issues and Implications." *Surveys in Geophysics* 32: 437–458. doi: 10.1007/s10712-011-9132-4.
- Weis M., R. Greve, and K. Hutter. 1999. "Theory of shallow ice shelves". *Continuum Mechanics and Thermodynamics* 11(1): 15–50.
- Winkelmann, R., M. A. Martin, M. Haseloff, T. Albrecht, E. Bueler, C. Khroulev, and A. Levermann. 2011. "The Potsdam Parallel Ice Sheet Model (PISM-PIK) Part 1: Model description." *The Cryosphere* 5: 715–726. doi:10.5194/tc-5-715-2011.

- 1
- 2
- 3
- 4
- 5
- 6
- 7
- 8
- 9
- 10
- 11
- 12



1
2 Figure 1. (A) Landsat 8 image of Ilulissat fjord and part of Disko Bay acquired in August
3 2014. The dark orange triangles indicate the locations of the GPS stations (GPS data shown in
4 Fig. 5). The ~~polygon-rectangle~~ defined by light orange borders outlines the location of Fig.
5 1C. (B) Grey filled Greenland map. The black filled ~~polygon-rectangle~~ highlights the JI basin
6 used to compute the mass loss (Fig. 4) and is identical to Khan et al. (2014). The ~~polygon~~
7 ~~rectangle~~ defined by red borders indicates the computational domain. The light blue border
8 ~~polygon-rectangle~~ represents the location of Fig. 1A. (C) Coloured circles indicate the
9 locations plotted in Fig. 3. The thick black line denotes the JI terminus position in the 1990s.
10 The dotted black line represents the flow-line location plotted in Fig. 6. The coordinates
11 given in (A) and (C) are in polar-stereographic projection units (km).



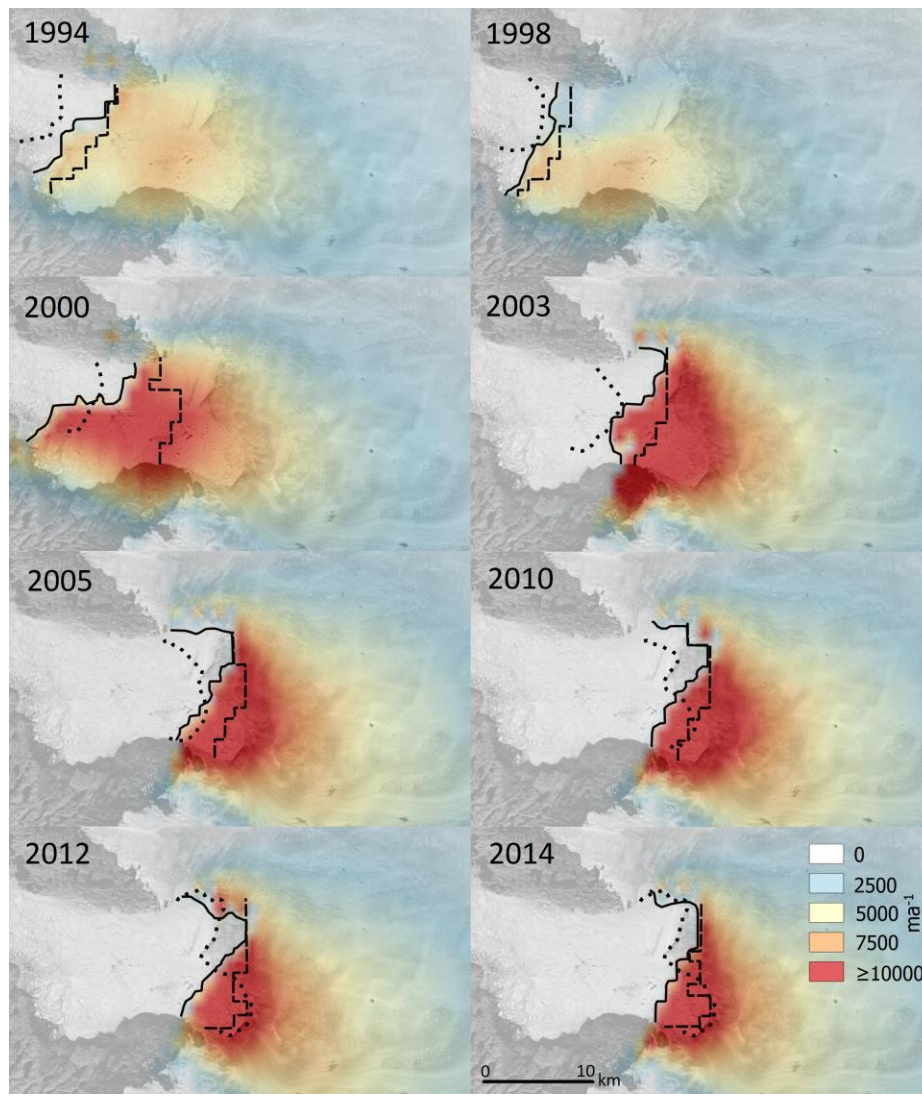


Figure 2. Modelled velocities at Jakobshavn Isbræ for December are shown for ~~seven~~eight different years. The black line represents the modelled front positions, the black dotted line denotes the observed front position and the thick black dashed line represents the modelled grounding line position. The velocities are superimposed over a Landsat 8 image acquired in August 2014.

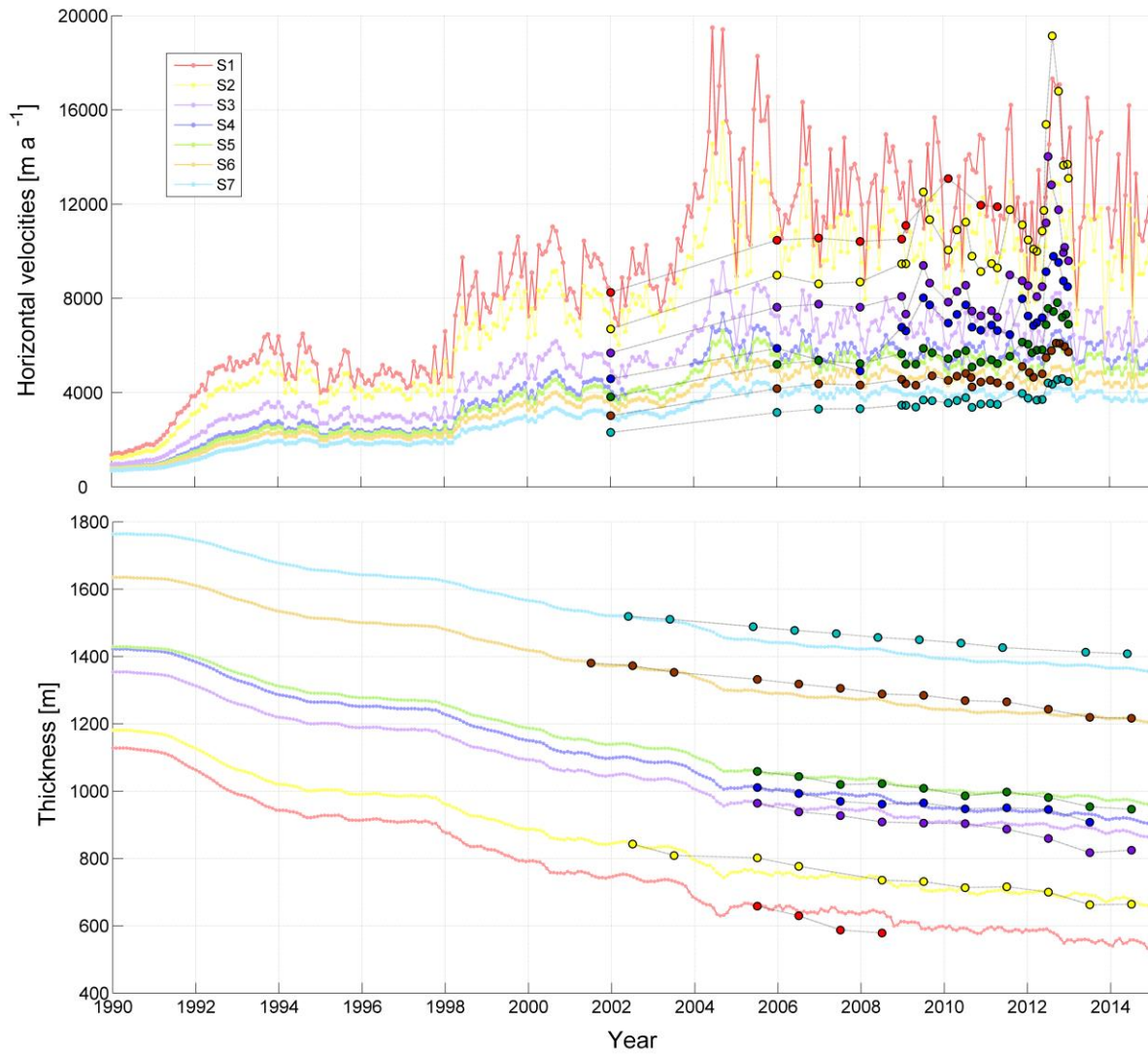


Figure 3. (A) Time series of modelled (filled circles) versus observed (filled circles with black edges) velocities (Joughin et al., 2010) (top figure) and ice thickness changes (Krabill, 2014) (bottom figure) for the period 1990-2014 at locations (S1 to S7) shown in Fig. 1C. The same colour scheme is used for the modelled and the observed data. The observed velocities prior to 2009 are mean winter velocities and are largely consistent with our modelled winter estimates for the same period. The observed thickness has been adjusted to match the model thickness at the first year at the first available observation (i.e., by summing the modelled ice thickness corresponding to the first available observation with the observed thickness changes).

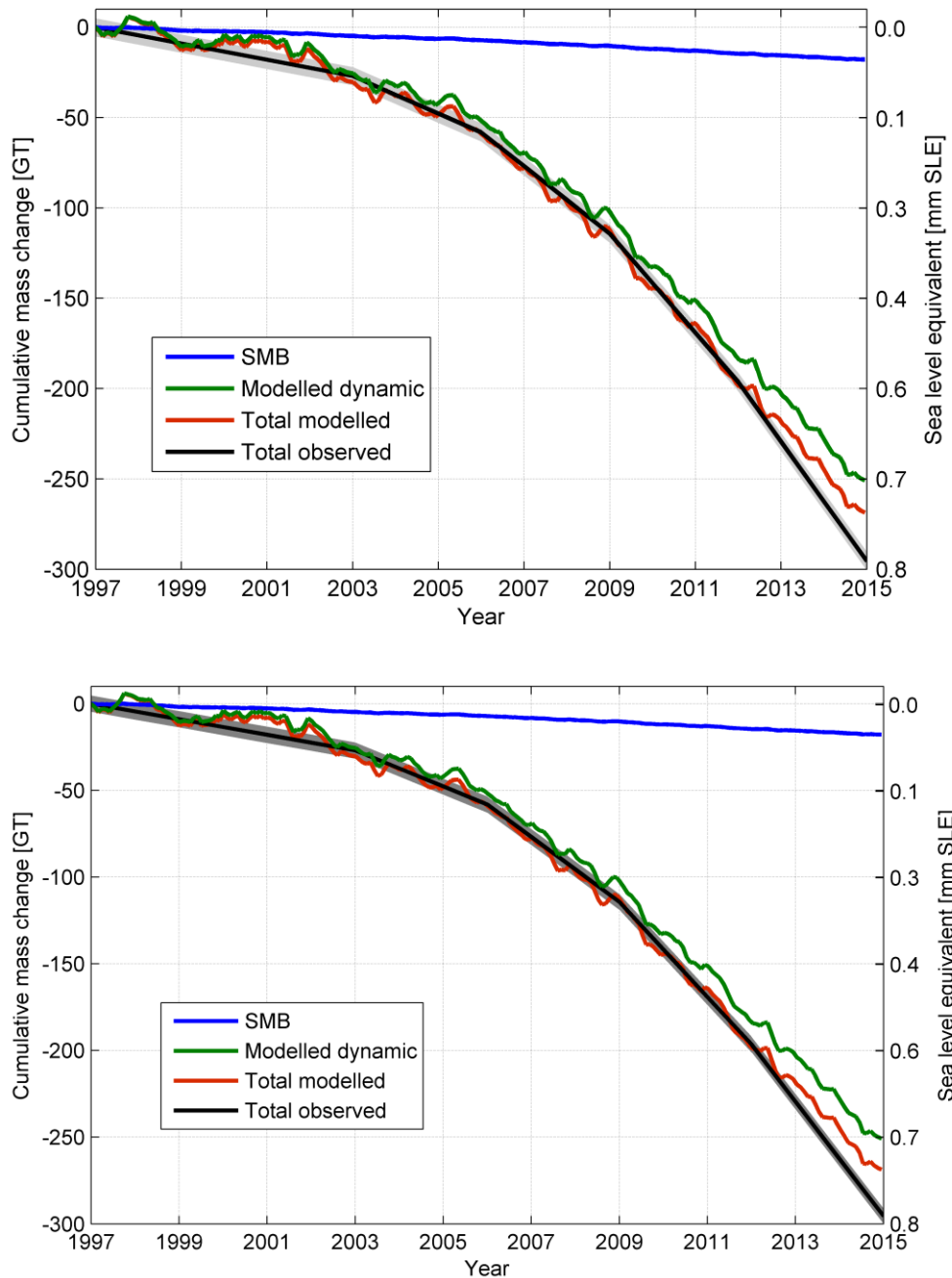


Figure 4. Modelled and observed cumulative mass change for Jakobshavn Isbræ. The blue curve represents the mass change due to SMB (Noël et al., 2015)– after the 1960-1990 baseline is removed. The green curve represents the modelled ice dynamics mass change (i.e., modelled mass change minus SMB change).– To estimate the mass change due to changes in

ice dynamics, we subtract the SMB mass change (as calculated based on RACMO 2.3 (Noël et al., 2015)) from the total modelled mass change. The red curve represents the total modelled mass change including both SMB and ice dynamic changes. The black curve with grey error limits represents the total observed mass change including both SMB and ice dynamic changes. The modelled mass change for the period 1997-2014 is ~269 Gt and the observed mass change is ~296 Gt.

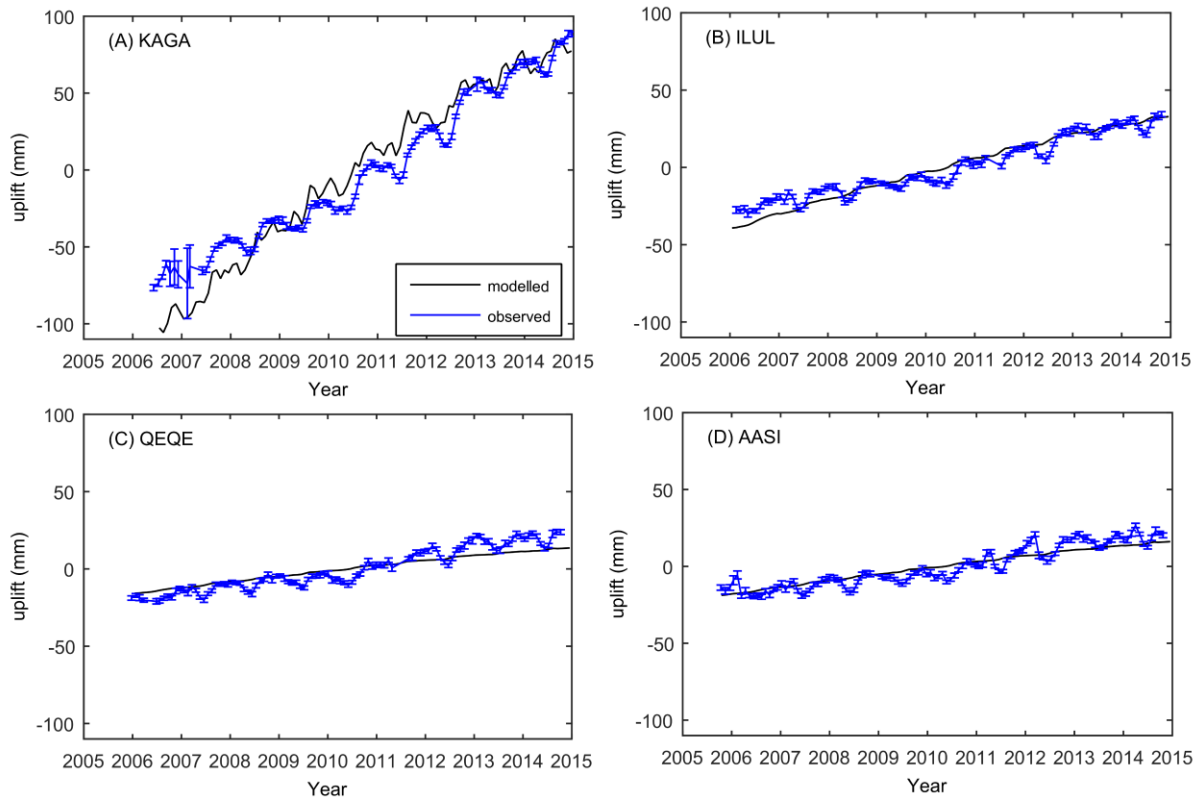


Figure 5. Observed versus modelled uplift in mm for the stations KAGA (A), ILUL (B), QEQE (C) and AASI (D). The positions of the four GPS stations are presented in Fig. 1A.

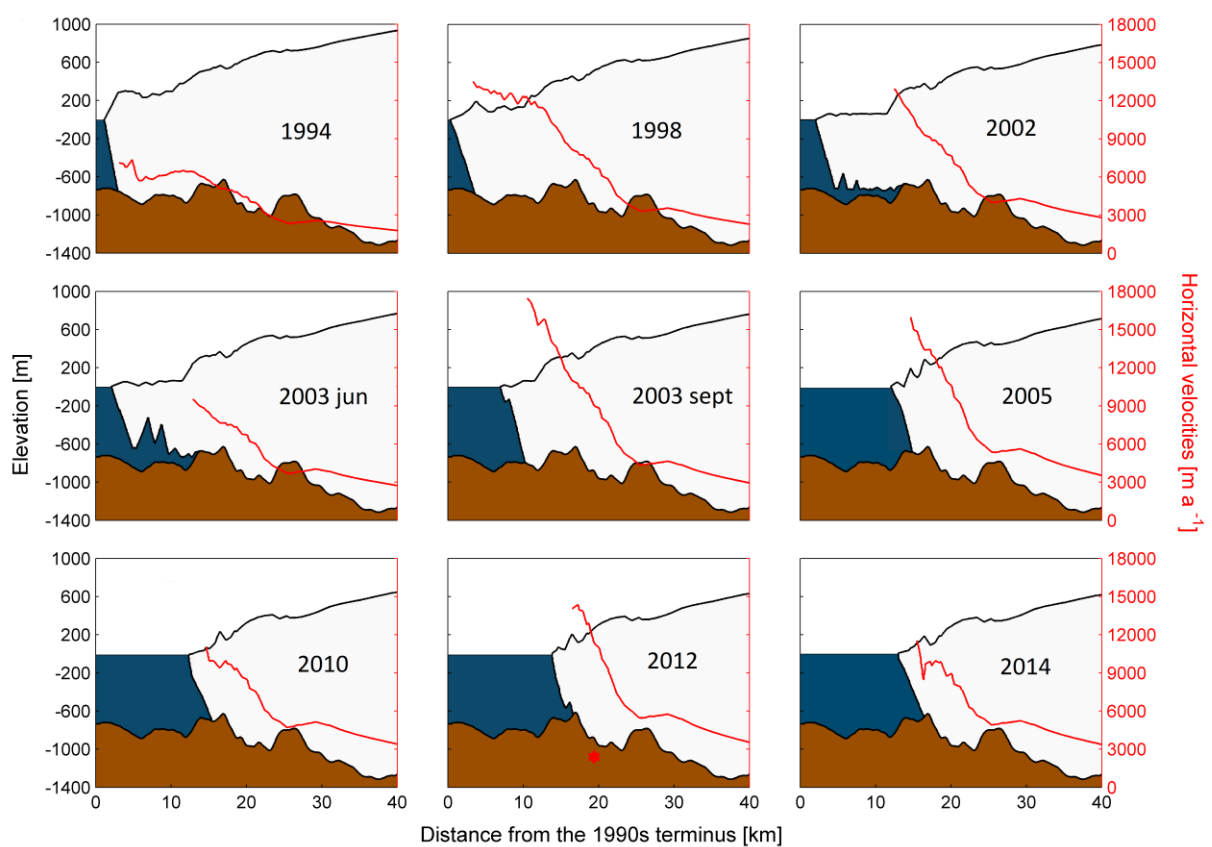
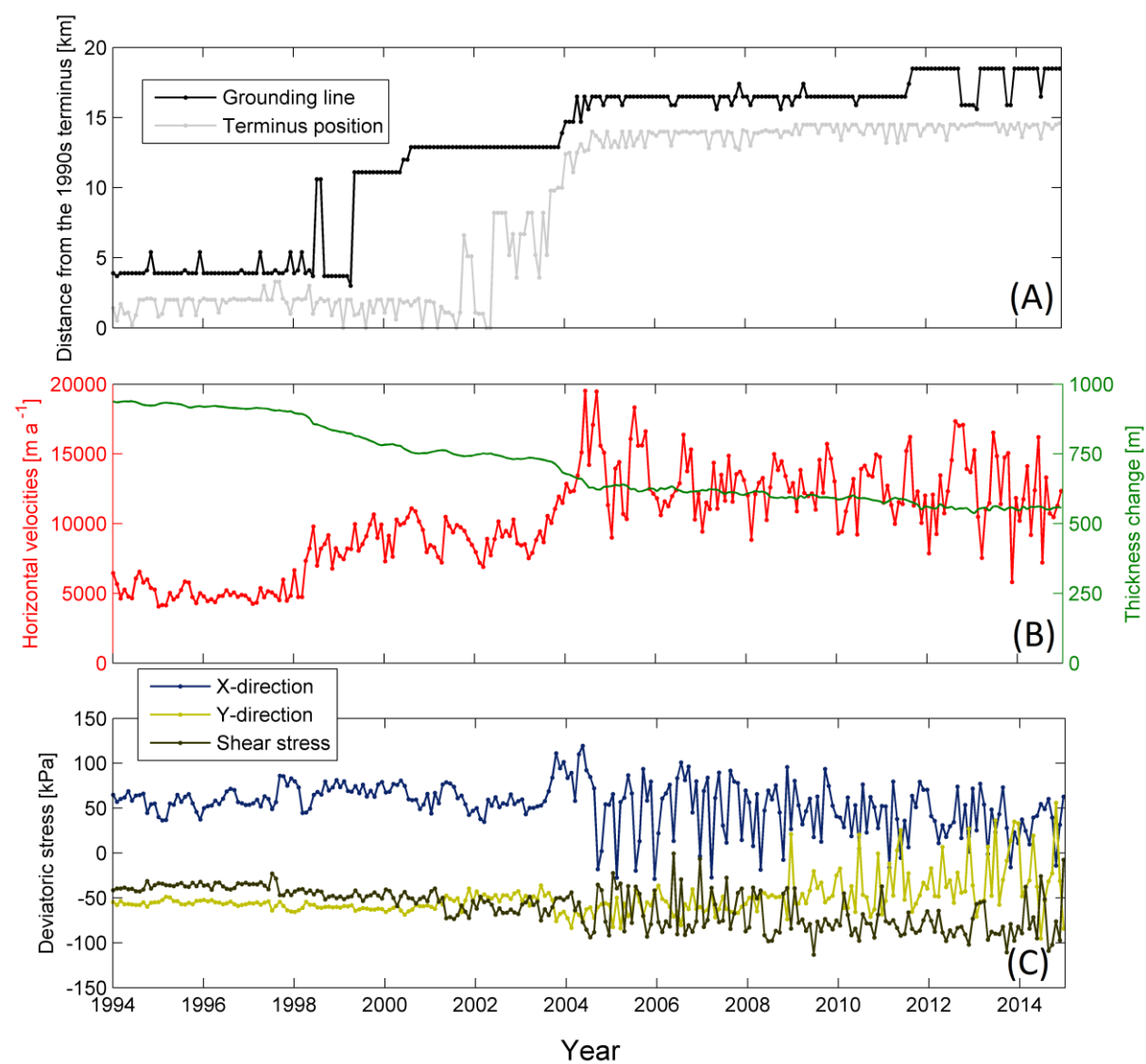


Figure 6. Modelled evolution of surface elevation (floating ice tongues thinner than 50 m are not shown~~ice shelves thinner than 50 m are not shown~~) and horizontal velocities of Jakobshavn Isbræ for December along the flow-line shown in Fig. 1C. Note the acceleration in speed between 1994-1998 and between June 2003 and September 2003 corresponding to

the final breakup of the floating tongue. The red star denotes the observed 2012 terminus position.



1
2
3
4
5
6
7

Figure 7. (A) Modelled grounding line and terminus position (floating ice tongues thinner than 50 m are not shown). (B) Modelled horizontal velocities and ice thickness changes at the point location S1 shown in Fig. 1C. (C) Modelled 2D deviatoric stresses (in the X direction, the Y direction, and the shear stress) at the point location S1 shown in Fig. 1C.

Editor #1

#Editor

#Page and Line numbers refer to the version of the manuscript which includes tracks the changes.#

for simulating slowly moving grounded ice in the interior part of the ice sheet

Authors: Changed to:

"The model uses the superposition of the non-sliding shallow ice approximation (SIA; Hutter, 1983) for simulating slowly moving grounded ice in the interior part of the ice sheet and the shallow shelf approximation (SSA; Weis et al., 1999) for simulating fast-flowing outlet glaciers and ice shelf systems. We solve the SIA with a non-sliding base and use the SSA as a basal sliding velocity for the grounded ice (Winkelmann et al., 2011)."

regarding the remark of referee #5 for the SSA enhancement factor, the reason might be the ice anisotropy, as explained in Ma et al., 2010, JoG.

Authors: True. We adjust for un-modeled anisotropy by using different enhancement factors for SIA and SSA. Normally with PISM this is done by using $SIA > 1$ and $SSA < 1$. See for example Winkelmann et al. 2011 which reads: "This difference in quality for the two enhancement factors is justified by the fact that under compression the fabric of ice becomes axisymmetric and easier to shear than isotropic ice, whereas under tension girdle-type fabrics evolve and make the ice stiffer (Ma et al., 2010)."

Which basal melt are you referencing to: below grounded or floating ice?

Authors: In this case is below grounded only.

This number is really not usual, other models using classically ~20 vertical layers. For which equations such refinement is needed (enthalpy)? This should be stated. Having 100 layers would change the results?

Authors: Yes, we agree ~20 vertical layers is good enough. However, PISM does not use sigma coordinates in the vertical. What it does is to divide the computational box (here 4000m) e.g. into 400 equidistant layers, resulting in a uniform layer thickness of 10m. To ensure that in areas where the ice is thin we are still able to accurately resolve the vertical gradients, we choose here to use a high number of layers. E.g. if the ice thickness is only a 100m, we can still resolve it by about 10 layers.

It was rewritten as: *"The enthalpy formulation models the mass and energy balance for the three-dimensional ice fluid field based on 200 regularly spaced ice layers within a domain extending 4000m above the bed elevation."*

Further, in PISM the vertical extent must be sufficient so that when the ice thickness grows large, especially before thermosoftening brings it back down, the vertical grid is tall enough to include all the ice (e.g. 4000 m).

Having 100 layers will probably slightly change the results.

Again, see previous remark. Why this need to be increased again when horizontal resolution is increased?

Authors: Our concurrent increase in the vertical and in the horizontal is just a coincidence. For an optimal computational time we choose to increase the vertical resolution only in the forward simulations. See also comment above.

What about melt over the ice front? See my remark below.

Authors: PISM does not apply any melt at a vertical ice front.

As the ice is confined in a fjord for such glacier (mostly compressive stress/strain rate), it should be mentioned that the proposed mechanism (fracture and rift intersection) is not governing process at JI. Therefore, it is not surprising that the eigen calving approach is not working solely here.

Authors: We added:

” In case of JI, whose terminus is confined in a narrow fjord, the strain rate pattern that defines the eigen calving parametrization is not the governing process, and therefore the need for the second calving parametrization.”

Why these two different values? Any physical reason on that?

Authors: No, for no particular physical reason. In the equilibrium simulation we are trying to keep the front as close as possible (still keeping the equilibrium) to the 1990 position (e.g no significant advance of the terminus). In the forward simulations, preparatory experiments showed that we need to decrease it in order to match observed terminus positions.

Do you mean : with the later calving parametrisation ?

Authors: True. We added:

” with the latter calving mechanism ”.

What is b ?

Authors: The bedrock elevation. The text has been changed accordingly.

this should be correct only if you have melting. In the case of accretion by refreezing, this condition should not be correct?

Authors: Yes, we would say so. We do not believe the model can take accretion into consideration.

Also, it should be specified that this BC is for the enthalpy solver.

Authors: Done. We added:

"necessary for the enthalpy solver (Aschwanden et al., 2012)"

I don't see how it can be smooth as the maximum of melt is reached at the GL and it is then zero for grounded ice. From my understanding, there is a discontinuity of the melt at the GL?

Authors: Rewritten as:

"At the grounding line PISM computes an extra flotation mask that accounts for the fraction of the cell that is grounded, by assigning 0 for cells with fully grounded ice, 1 for cells with ice-free or fully floating ice, and values between 0 and 1 for partially grounded grid cells. The basal melt rate in the cells containing the grounding line is then adjusted based on this flotation mask as following:

$$M_{b,adjusted} = \lambda M_{b,grounded} + (1 - \lambda)M_{b,shelf-base}$$

where M_b refers to the basal melt rate and λ is the value of the flotation mask. At the vertical ice front, we do not apply any melt."

this was a point made by reviewer #4, which is still not clear: do you distinguish between melt at the front and melt below the iceshelve. Melt rate occurring on the vertical ice front should be added to the calving rate. It should act whatever the configuration: presence or not of an ice-shelf. Such process has been shown to be very important for Greenland glaciers. It should be clearly stated if you are or not accounting for that process in your model.

Authors: PISM does not apply any melt at the vertical ice front. This is included in the main text now (page 9 L16-17):

"At the vertical ice front, we do not apply any melt."

Basal melt below the shelf should only exist if a shelf exist, so I don't understand the statement that the basal melt parametrization is only applied at the GL position (melt should only be applied over a surface, not at a point?).

Authors: True. The statement was removed.

Here is missing a presentation of what BC is applied at the interface between ice and bedrock, especially for sliding.

Authors: We added at page 5, L24-25:

"The boundary conditions for the enthalpy at the ice-bedrock interface follow Aschwanden et al (2012)."

grid

Authors: Done.

from Table S2, it is not clear why some of the parameter don't have range values (E_SSA, K, S_0, ...). Does it mean that only one value was tested? So that only 6 parameters were varied to realise the 50 simulations? This should be mentioned and the table S2 should be splitted in

two tables, one for the constant parameters and one for the varied parameters. Table S1 is not useful.

Authors: Yes that is true (we added 6 in the main text). Table S1 has been deleted and old table S2 has been splitted in 2 new tables, table S1 and table S2.

Also, Fig. S1 is very interesting but should show all results for all 6 varied parameters (put on the same figure Figs S5 and S6).

Authors: When we include all results on the same plot it becomes relatively hard to distinguish (note the magnitude of the simulation with $\delta=0.03$, orange line) between the different simulations (see Fig. 1 below). Therefore, we kept Fig. S1 as in the original version and we only merge Fig. S6 and Fig. S5.

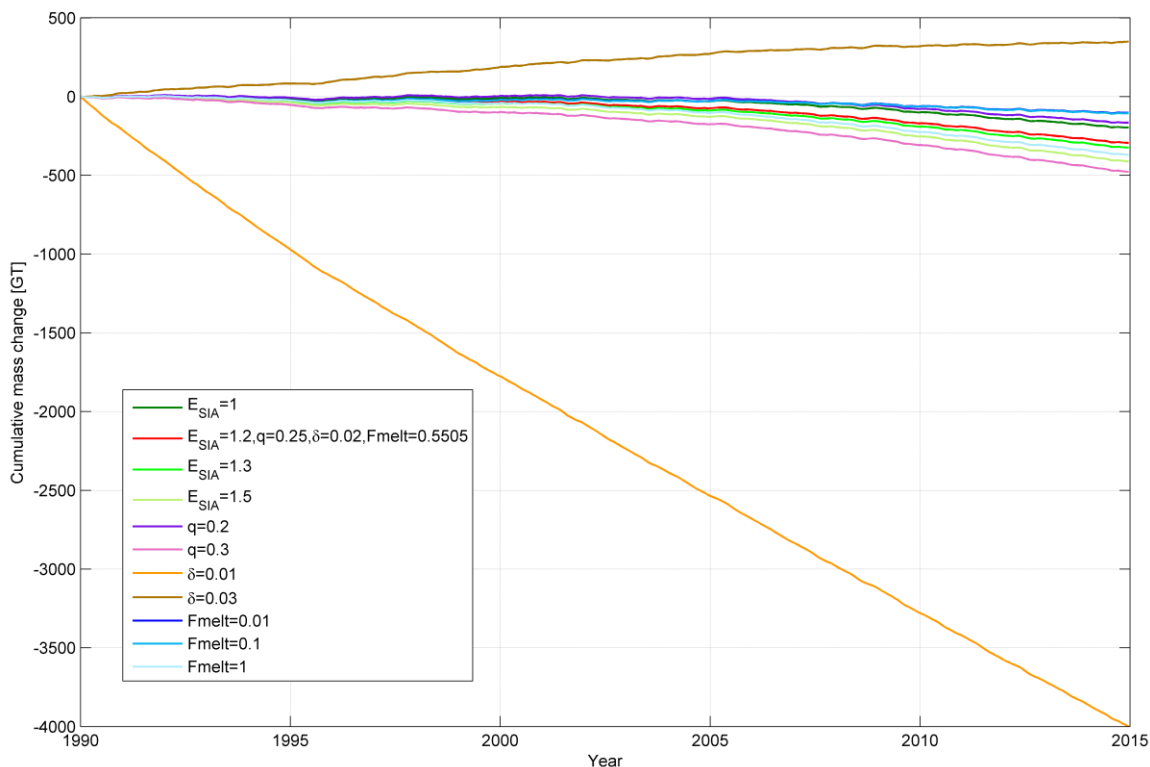


Figure 1.

Fig. 4 should be Fig.3, as it appear before Fig.3.

And Fig 3. should appear here also ? For thickness and velocity observations vs model?

Authors: Done.

How this is really done? Do you use error measurement between observation and model? Or this is just a visual choice from Figs.2 to 4? This should be specified.

Authors: We estimate the residual between modelled and observed mass loss (e.g. select the smallest residual signal). The text was changed accordingly.

In Fig. 2, it starts in 1994. you should add: (not shown in Fig. 2).

Authors: Done.

should be Fig. 5. Check in which order the different figure are cited in the text.

Authors: Statement has been deleted. The order of the figures cited in the text has been checked.

I cannot see from the model presentation in the SI how surface melt rate and flow acceleration in your model are linked. In the SI, the effective pressure is given by (4) which is a function of W_{till} , the effective thickness of water computed from the basal melt rate. How this basal melt rate is computed? Is it only the result of the friction heat? In that case, I don't see how an increase of surface runoff will influence the friction. This should really specified as it also certainly influence the seasonal modelled variations of velocity.

Authors: No, surface melt does not directly influence sliding in our model. What does happen is that a high melt year is most likely the consequence of high summer air temperatures. We do use the air temperatures as a boundary condition for the enthalpy equation. However, vertical advection/diffusion takes quite an while, and to get a significant impact on ice flow, the signal would have to propagate far down into the column to reach the high shearing layer at the base. Thus, for our relatively short runs it doesn't have a large impact on flow.

To avoid any misunderstandings we decided to delete these statements.

Moreover, the presentation of basal friction should be partly transferred from the SI to the main paper, similarly to what was done for calving and ice-shelf basal melting.

Authors: Done. The folowing text was added at page 4, Sect 2.1:

"In PISM, the basal shear stress is related to the sliding velocity by a nearly-plastic power law (Schoof and Hindmarsh, 2010). The Mohr-Coulomb criterion (Cuffey and Paterson, 2010) is used to connect a saturated and pressurized subglacial till with a modelled distribution of yield stress. The yield stress depends on the effective pressure and on a spatially varying till friction angle derived heuristically as a piecewise-linear function of the bed elevation (Martin et al., 2011; Winkelmann et al., 2011; Aschwanden et al., 2013). The effective pressure on the till is determined by the ice overburden pressure and the effective thickness of water in the till (Tulaczyk et al., 2000a; Tulaczyk et al., 2000b). In this subglacial hydrology model the water is not conserved and it is only stored locally in the till up to a maximum thickness of 2 m."

I don't see in the model presentation how this seasonal variability influence the ice flow model (only the surface evolution).

Authors: We added:

"In our model, the atmospheric forcing applied (Figs. S2 and S3) can influence JI's dynamics through changes in surface mass balance (SMB) (i.e., accumulation and ablation) which affect both the SIA and the SSA (Sect. 2.1), but also through changes in air temperature that can potentially influence sliding via the rate factor for the softness (SI, Eq. 1) which here is derived through an enthalpy formulation (Aschwanden et al., 2012)."

Furthermore, we added in the model description (Sect. 2.1.) : *"To determine driving stresses for the SIA and SSA stress balances, PISM computes surface gradients according to Mahaffy (1976)."*

parametrization or approach?

Authors: Parametrization.

Here you should tell for example that the eigen calving method accounted for xx% of the calving mass loss?

Authors: Done. The text has been changed accordingly (~ 96 % of the overall mass loss is driven by the basic calving mechanism).

I don't understand what you mean by "include melt rates modelled along the base of the shelf and in the proximity of the GL". The proximity of the GL is INCLUDED in the base of the ice-shelf? As I understood that from your melt parametrization the melt rate is not uniform at the base of the ice-shelf, you should specify in Tab. S3 if it is mean or max values of basal melt rate.

Authors: Done. The statement has been deleted and "Mean" was added to table S3.

As mentioned by Referee #5, it is very high values... You should discuss this and how realistic it is.

Authors: We added:

"The modelled melt rates for the period 1999-2003 are large and likely overestimated."

Why and again, is it a mean or a max value which is given in Tab. S3. This should be clearly specified.

Authors: The sentence was deleted (mean melt rates). See answer to comment above.

this should be specified much earlier, in the model presentation.

Authors: Done. Partly moved to page 13, line 9.

the ice overburden pressure. But, I suspect that, like the driving stress for the SIA, seasonal change in ice overburden pressure are very small?

Authors: Yes, we believe they would still be relatively small. But stronger than the effect via SIA.

Or there is something else that link basal melt to runoff? This must be clearly stated.

Authors: There is no direct link with runoff.

We added:

"In turn, this could have induced a retreat of the terminus that cannot be captured by our model (i.e., in its present configuration the model does not account directly for the influence of meltwater runoff and its role in the subglacial system during surface melt events). Nonetheless, a high melt year is generally the consequence of high summer air temperatures that in our model represent boundary conditions for the enthalpy equation (Aschwanden et al., 2012). Therefore, an increase in air temperatures could potentially soften the ice and enhance sliding. However, the time required for advection/diffusion to propagate down into the column and reach the high shearing layer at the base of the ice (Aschwanden et al., 2012) is generally much longer than our hindcasts and thus, we believe that in our simulations, this effect does not have a significant impact on the flow. "

Is it really observed here or do you refer to the simulation with the monthly variability in the atmospheric forcing depicted in Fig. 7B?

Authors: The statement was rewritten.

is this figure appropriate here?

Authors: No. It was deleted.

This must be mentioned much earlier in the paper, when the model is presented.

Authors: Included where we discuss the input for the atmospheric forcing (Sect. 2.1.1).

you have had 5 at the end...

Authors: Done.

Modelled glacier dynamics over the last quarter of a century at Jakobshavn Isbræ

Ioana S. Muresan¹, Shfaqat A. Khan¹, Andy Aschwanden², Constantine Khroulev², Tonie Van Dam³, Jonathan Bamber⁴, Michiel R. van den Broeke⁵, Bert Wouters^{4,5}, Peter Kuipers Munneke⁵, and Kurt H. Kjær⁶

[1]{Department of Geodesy, DTU Space, Technical University of Denmark, Kgs. Lyngby, Denmark}

[2]{Geophysical Institute, University of Alaska Fairbanks, Fairbanks, Alaska, USA}

[3]{University of Luxembourg, Faculty of Science, Technology and Communication (FSTC), Research Unit of Engineering Sciences, Luxembourg}

[4]{University of Bristol, School of Geographical Sciences, Bristol, England}

[5]{Institute for Marine and Atmospheric research Utrecht (IMAU), Utrecht University, The Netherlands}

[6]{Centre for GeoGenetics, Natural History Museum of Denmark, University of Copenhagen, Copenhagen, Denmark}

Correspondence to: I. S. Muresan (iomur@space.dtu.dk)

Abstract

Observations over the past two decades show substantial ice loss associated with the speedup of marine terminating glaciers in Greenland. Here we use a regional 3-D outlet glacier model to simulate the behaviour of Jakobshavn Isbræ (JI) located in west Greenland. Our approach is to model and understand the recent behaviour of JI with a physical process-based model. Using atmospheric forcing and an ocean parametrization we tune our model to reproduce observed frontal changes of JI during 1990–2014. In our simulations, most of the JI retreat during 1990–2014 is driven by the ocean parametrization used, and the glacier's subsequent

response, which is largely governed by bed geometry. In general, the study shows significant progress in modelling the temporal variability of the flow at JI. Our results suggest that the overall variability in modelled horizontal velocities is a response to variations in terminus position. The model simulates two major accelerations that are consistent with observations of changes in glacier terminus. The first event occurred in 1998, and was triggered by a retreat of the front and moderate thinning of JI prior to 1998. The second event, which started in 2003 and peaked in the summer 2004, was triggered by the final breakup of the floating tongue. This breakup reduced the buttressing at the JI terminus that resulted in further thinning. As the terminus retreated over a reverse bed slope into deeper water, sustained high velocities over the last decade have been observed at JI. Our model provides evidence that the 1998 and 2003 flow accelerations are most likely initiated by the ocean parametrization used but JIs subsequent dynamic response was governed by its own bed geometry. We are unable to reproduce the observed 2010-2012 terminus retreat in our simulations. We attribute this limitation to either inaccuracies in basal topography or to misrepresentations of the climatic forcings that were applied. Nevertheless, the model is able to simulate the previously observed increase in mass loss through 2014.

1 Introduction

The rate of net ice mass loss from Greenland's marine terminating glaciers has more than doubled over the past two decades (Rignot et al., 2008; Moon et al., 2012, Shepherd et al., 2012, Enderlin et al., 2014). Jakobshavn Isbræ, located mid-way up on the west side of Greenland, is one of the largest outlet glaciers in terms of drainage area as it drains ~6 % of the Greenland Ice Sheet (GrIS) (Krabill et al., 2000). Due to its consistently high ice flow rate and seasonally varying flow speed and front position, the glacier has received much attention over the last two decades (Thomas et al., 2003; Luckman and Murray, 2005; Holland et al., 2008; Amundson et al., 2010; Khan et al., 2010; Motyka et al., 2011; Joughin et al., 2012; Gladish et al., 2015a; Gladish et al., 2015b; de Juan et al., 2010). Measurements from synthetic aperture radar suggest that the ice flow speed of JI doubled between 1992 and 2003 (Joughin et al., 2004). More recent measurements show a steady increase in the flow rate over the glacier's faster-moving region of ~ 5% per year (Joughin et al., 2008). The speedup coincides with thinning of up to 15 m a⁻¹ between 2003 and 2012 near the glacier front (Krabill et al., 2004; Nielsen et al., 2013) as observed from airborne laser altimeter surveys.

The steady increase in the flow rate and glacier thinning suggest a continuous dynamic drawdown of mass, and they highlight JIs importance for the GrIS mass balance.

Over the past decade, we have seen significant improvements in the numerical modelling of glaciers and ice sheets (e.g. Price et al., 2011; Vieli and Nick, 2011; Winkelmann et al., 2011; Larour et al., 2012; Pattyn et al., 2012; Seroussi et al., 2012; Aschwanden et al., 2013; Nick et al., 2013; Mengel and Levermann, 2014; Aschwanden et al., 2016) and several processes have been identified as controlling the observed speedup of JI (Nick et al., 2009; Van der Veen et al., 2011; Joughin et al., 2012). One process is a reduction in resistance (buttressing) at the marine front through thinning and/or retreat of the glacier termini. But the details of the processes triggering and controlling thinning and retreat remain elusive. Accurately modelling complex interactions between thinning, retreat, and acceleration of flow speed as observed at JI, is challenging. Our knowledge of the mechanisms triggering these events is usually constrained to the period covered by observations. The initial speedup of JI occurred at a time when the satellite and airborne observations were infrequent and therefore insufficient to monitor the annual to seasonal evolution of glacier geometry and speed.

Here, we use a high-resolution, three-dimensional, time-dependent regional outlet glacier model that has been developed as part of the Parallel Ice Sheet Model (PISM; see Sect. 2.1 Ice sheet model) (The PISM Authors, 2014) to investigate the dynamic evolution of JI between 1990 and 2014. While previous 3-D modelling studies have mostly concentrated on modelling individual processes using stress perturbations (e.g. Van der Veen et al., 2011, Joughin et al. 2012), the present study aims to model the recent behaviour of JI with a process-based model. Our modelling approach is based on a regional equilibrium simulation and a time-integration over the period 1990 to 2014, in which the grounding lines and the calving fronts are free to evolve under the applied ocean parametrization and monthly atmospheric forcing.

2 Methods and forcing

2.1 Ice sheet model

The ice sheet model used in this study is the PISM (stable version 0.6). PISM is an open source, parallel, three-dimensional, thermodynamically coupled, and time dependent ice sheet model (Bueler and Brown, 2009; The PISM Authors, 2014). ~~The model uses the superposition of the non-sliding shallow ice approximation (SIA; Hutter, 1983) and the shallow shelf~~

approximation (SSA; Weis et al., 1999) for simulating slowly moving grounded ice in the interior part of the ice sheet, and the SSA for simulating fast-flowing outlet glaciers and ice shelf systems (Winkelmann et al., 2011). The model uses the superposition of the non-sliding shallow ice approximation (SIA; Hutter, 1983) for simulating slowly moving grounded ice in the interior part of the ice sheet and the shallow shelf approximation (SSA; Weis et al., 1999) for simulating fast-flowing outlet glaciers and ice shelf systems. We solve the SIA with a non-sliding base and use the SSA as a basal sliding velocity for the grounded ice regions (Winkelmann et al., 2011). This superposition of SIA and SSA (the “SIA+SSA” hybrid model) sustains a smooth transition between non-sliding, bedrock-frozen ice and sliding, fast-flowing ice and has been shown to reasonably simulate the flow of both grounded and floating ice (Winkelmann et al., 2011). To determine driving stresses for the SIA and SSA stress balances, PISM computes surface gradients according to Mahaffy (1976). For conservation of energy, PISM uses an enthalpy scheme (Aschwanden et al., 2012) that accounts for changes in temperature in cold ice (i.e., ice below the pressure melting point) and for changes in water content in temperate ice (i.e., ice at the pressure melting point).

In PISM, the basal shear stress is related to the sliding velocity through a nearly-plastic power law (Schoof and Hindmarsh, 2010). The Mohr-Coulomb criterion (Cuffey and Paterson, 2010) is used to connect a saturated and pressurized subglacial till with a modelled distribution of yield stress. The yield stress depends on the effective pressure and on a spatially varying till friction angle derived heuristically as a piecewise-linear function of the bed elevation (Martin et al., 2011; Winkelmann et al., 2011; Aschwanden et al., 2013). The effective pressure on the till is determined by the ice overburden pressure and the effective thickness of water in the till (Tulaczyk et al., 2000a; Tulaczyk et al., 2000b). In this subglacial hydrology model the water is not conserved and it is only stored locally in the till up to a maximum thickness of 2 m. The ice flow therefore develops in PISM as a consequence of plastic till failure, i.e. where the basal shear stress exceeds the yield stress, and is influenced by the thermal regime and the volume of water at the ice sheet bed. The underlying equations are further illustrated in the supplementary material (SI).

2.1.1 Input data

We use the bed topography from Bamber et al. (2013). This 1 km bed elevation dataset for all of Greenland was derived from a combination of multiple airborne ice thickness surveys and satellite-derived elevations during 1970–2012. The dataset has an increased resolution, along

the ice sheet margin. In the region close to the outlet of JI, data from an 125 m CReSIS DEM (that includes all the data collected in the region by CReSIS between 1997 and 2007) have been used to improve the accuracy of the dataset. Errors in bed elevation range from 10 m to 300 m, depending on the distance from an observation and the variability of the local topography (Bamber et al., 2013). The terminus position and surface elevation in the Jakobshavn region are based on 1985 aerial photographs (Csatho et al., 2008). Ice thickness in the JI basin is computed as the difference between surface and bedrock elevation. The model of the geothermal flux is adopted from Shapiro and Ritzwoller (2004). We use monthly input fields of near-surface air temperature and surface mass balance (SMB) from the regional climate model RACMO2.3 (Noël et al., 2015; Figs. S2 and S3). which -here represent the only seasonal input used in the model. The version used in this study is produced at a spatial resolution of ~ 11 km and covers the period from 1958 to 2014. Additional grid refinements are performed using bilinear interpolation for climatic datasets and a second order conservative remapping scheme (Jones, 1999) for bed topography data.

2.1.2 Initialization procedure, boundary conditions, calving and grounding line parametrization

In our model, the three-dimensional ice enthalpy field, basal melt for grounded ice, modelled amount of till-pore water, and lithospheric temperature are obtained from an ice-sheet-wide paleo-climatic spin-up. The paleo-climatic spin-up follows the initialization procedure described by Bindschadler et al. (2013) and Aschwanden et al. (2013). We start the spin-up on a 10 km grid, and then we further refine to 5 km at -5ka. It is important to note that during the paleo-climatic initialization the terminus is held fixed to the observed 1990 position in the JI region and to the position from Bamber et al. (2013) elsewhere.

In the regional outlet glacier model of PISM, the boundary conditions are handled in a 10 km strip positioned outside of the JI's drainage basin and around the edge of the computational domain (Fig. 1B). In this strip, the input values of the basal melt, the amount of till-pore water, ice enthalpy, and lithospheric temperature (Aschwanden et al., 2013) are held fixed and applied as Dirichlet boundary conditions in the conservation of energy model (The PISM Authors, 2014). The boundary conditions for the enthalpy at the ice-bedrock interface follow Aschwanden et al (2012). We start our regional JI runs with an equilibrium simulation on a horizontal grid with 5 km spacing. The enthalpy formulation models the mass and energy balance for the three-dimensional ice fluid field based on 200 regularly spaced ice layers

1 | within a domain extending 4000 m above the bed elevation~~within the ice~~. The temperature of
2 | the bedrock thermal layer is computed up to a depth of 1000 m with 50 regularly spaced
3 | layers. The first step is to obtain a 5 km regional equilibrium model for JI using constant
4 | mean climate (i.e. repeating the 1960-1990 mean air temperature and SMB; see Sect. 2.1.1).
5 | We consider that equilibrium has been established when the ice volume in the regional
6 | domain changes by less than 1% in the final 100 model years. Grid refinements are made
7 | from 5 km (125×86) to 2 km (310×213) after 3000 years. The 2 km simulation reaches
8 | equilibrium after 200 years with an ice volume of $0.25 \cdot 10^6 \text{ km}^3$ (or a 3.6% increase relative
9 | to the input dataset from Bamber et al. (2013)). Further, using our equilibrium simulations
10 | with a 2 km horizontal grid and 400 regularly spaced ice layers within a domain extending
11 | 4000 m above the bed elevation~~the ice~~, we simulate forward in time (hindcast) from 1990 to
12 | 2014 by imposing monthly fields of SMB and 2 m air temperatures through a one-way
13 | forcing scheme. For simulations performed on a 1 km horizontal grid, the exact same
14 | procedure is used with the additional constraint that in the regional equilibrium run a further
15 | grid refinement from 2 km to 1 km is made after 200 years. The length of the 1 km regional
16 | equilibrium simulation is 100 years.

17 | In our regional model, all boundaries (calving fronts, grounding lines, upper, and lower
18 | surfaces) are free to evolve in time both during the regional equilibrium and the forward
19 | simulations. Along the ice shelf calving front, we superimpose a physically based calving
20 | (eigen calving) parametrization (Winkelmann et al., 2011; Levermann et al., 2012) and a basic
21 | calving mechanism (Albrecht et al., 2011) that removes any floating ice at the calving front
22 | thinner than a given threshold at a maximum rate of one grid cell per time step. The average
23 | calving rate (c) is calculated as the product of the principal components of the horizontal
24 | strain rates ($\dot{\epsilon}_{\pm}$), derived from the SSA velocities, and a proportionality constant parameter
25 | (k) that captures the material properties relevant for calving:

$$c = k \dot{\epsilon}_{+} \dot{\epsilon}_{-} \quad \text{for } \dot{\epsilon}_{\pm} > 0. \quad (1)$$

27 | The strain rate pattern is strongly influenced by the geometry and the boundary conditions at
28 | the ice shelf front (Levermann et al. (2012)). The proportionality constant, k , is chosen such
29 | that the ice front variability is small (Leverman et. al., 2012). This physically based calving
30 | law appears to yield realistic calving front positions for various types of ice shelves having
31 | been successfully used for modelling calving front positions in entire Antarctica simulations
32 | (Martin et al., 2011) and regional east Antarctica simulations (Mengel and Levermann, 2014).

In contrast to Antarctica, known for its large shelves and shallow fjords, the GrIS is characterized by narrow and deep fjords, and JI is no exception. The strain rate pattern in the eigen calving parametrization performs well only if fractures in glacier ice can grow, and calving occurs only if these rifts intersect (i.e. possible only for relatively thin ~~ice shelves~~ and unconfined ice shelves). In the case of JI, whose terminus is confined in a narrow fjord, the strain rate pattern that defines the eigen calving parametrization is not the governing process, and therefore the need for the second calving parametrization. -In our model, the eigen calving law has priority over the basic calving mechanism. That is to say that the second calving law used (the basic calving mechanism) removes any ice at the calving front not calved by the eigen calving parametrization thinner than 500 m in the equilibrium simulations and 375 m in the forward runs. Therefore, the creation of the conditions under which calving can ~~finally~~ occur (e.g. a floating ice shelf) with the latter subsequent calving mechanism, relies solely on the parametrization for ice shelf melting (Sect. 2.1.3).

A partially-filled grid cell formulation (Albrecht et al., 2011), which allows for sub-grid scale retreat and advance of the ice shelf front, is used to connect the calving rate computed by the calving parametrizations with the mass transport scheme at the ice shelf terminus. This sub-grid scale retreat and advance of the shelf allows for realistic spreading rates that are important for the eigen calving parametrization. The sub-grid interpolation is performed only when a floating terminus exists. In both situations (i.e., floating ice or grounded terminus), the stress boundary conditions are applied at the calving front and in the discretization of the SSA equations (Winkelmann et al., 2011). The retreat and advance of the front through calving is restricted to at most one grid cell length per adaptive time step.

The parameterization of the grounding line position is based on a linear interpolation scheme (the “LI” parameterization; Gladstone et al., 2010) extended to two horizontal dimensions (x, y) and is not subject to any boundary conditions. This sub-grid treatment of the grounding line interpolates the basal shear stress in x, y based on the spatial gradient between cells below and above the grounding line and allows for a smooth transition of the basal friction from grounded to floating ice (Feldmann et al., 2014). At each time step the grounding line position is determined by a mask that distinguishes between grounded and floating ice using a flotation criterion based on the modelled ice thickness (Winkelmann et al., 2011):

$$b(x, y) = -\frac{\rho_i}{\rho_o} H(x, y) \quad (2)$$

~~Where~~where b represents the bedrock elevation, ρ_i is the density of the ice, ρ_o is the density of the ocean water and H represents the ice thickness. Therefore, the grounding line migration is influenced by the ice thickness evolution, which further depends on the velocities computed from the stress balance. The superposition of SIA and SSA, which implies that the SSA velocities are computed simultaneously for the shelf and for the sheet, ensures that the stress transmission across the grounding line is continuous and that buttressing effects are included. In the three-dimensional Marine Ice Sheet Model Intercomparison Project (Mismip3d), PISM was used to model reversible grounding line dynamics and produced results consistent with full-Stokes models (Pattyn et al. (2013); Feldmann et al., 2014; see parameters therein). We have not performed the Mismip3d experiments for our particular parameter settings and, therefore, the accuracy of the modelled grounding line migration is solely based on the results presented in Feldmann et al. (2014).

2.1.3 Parameterization for ice shelf melting

We use a simple parametrization for ice shelf melting where the melting effect of the ocean is based on both sub-shelf ocean temperature and salinity (Martin et al., 2011). To accommodate this parametrization, several changes have been made to PISM at the sub-shelf boundary (Winkelmann et al., 2011). First, the ice temperature at the base of the shelf ~~–~~(the pressure-melting temperature) necessary for the enthalpy solver (Aschwanden et al., 2012) is calculated from the Clausius-Clapeyron gradient and the elevation at the base of the shelf ~~;~~ ~~and then the~~ The ice temperature is then applied as a Dirichlet boundary condition in the conservation of energy equation.

Secondly, basal melting and refreezing is incorporated through a sub-shelf mass flux used as a sink/source term in the mass-continuity equation. This mass flux from shelf to ocean (Beckmann and Goosse, 2003) is computed as a heat flux between the ocean and ice and represents the melting effect of the ocean due to both temperature and salinity (Martin et al., 2011).

~~We start~~In our simulations ~~with~~ we use a constant ocean water temperature (T_o) of -1.7°C , which here represents the mean surface ocean temperature in the grid cells adjacent to the JI terminus. In the heat flux parametrization, the ocean temperature at the ice shelf base is computed as the difference between the input ocean temperature and a virtual temperature that represents the freezing point temperature of ocean water below the ice shelf (Fig. S4). The

freezing point temperature is calculated based on the elevation at the base of the shelf and the ocean water salinity. As a consequence of these constraints, as the glacier retreats and/or advances, both the pressure-melting temperature and the heat flux between the ocean and ice evolve alongside the modelled glacier ice shelf geometry. The ocean water salinity ($S_o = 35$ psu) is kept constant in time and space as the model does not capture the salinity gradient from the base of the ice shelf through layers of low and high salinity. A previous study conducted by Mengel and Levermann (2014) using the same model established that the sensitivity of the melt rate to salinity is negligible.

Following for this melting parametrization, the highest melt rates are modelled in the proximity of the glacier grounding lines and decrease with elevation such that the lowest melt rates are closer to the central to frontal area of the modelled ice shelf. ~~At the grounding line, the sub-grid scheme (Albrecht et al., 2011; Feldmann et al., 2014)~~ At the grounding line, PISM computes an extra flotation mask that accounts for the fraction of the cell that is grounded, by assigning 0 to~~for~~ cells with fully grounded ice, 1 for cells with ice-free or fully floating ice, and values between 0 and 1 for partially grounded grid cells. The basal melt rate in the cells containing the grounding line is then adjusted based on this flotation mask as following:

$$M_{b,adjusted} = \lambda M_{b,grounded} + (1 - \lambda) M_{b,shelf-base}$$

where M_b refers to the basal melt rate and λ is the value of the flotation mask. ~~interpolates the sub-shelf melt rate, allowing for a smooth transition between floating and grounded ice. For a completely grounded terminus (i.e. the case when no ice floating tongue exists), the melt parametrization is applied only at the grounding line position. At the vertical ice front, we do not apply any melt.~~

3 Results and discussion

This section is organized in two main subsections. Sect. 3.1 introduces the results obtained relative to observations, and Sect 3.2 focuses mainly on the limitations of the model that need to be considered before a final conclusion can be drawn. A short introduction to the different simulations and preparatory experiments performed is given below.

A total number of fifty simulations with different sets of parameters (excluding preparatory and additional experiments on the 1 km grid) are performed on a 2 km grid. We alter ~~the six~~ parameters controlling that control the ice dynamics (e.g. the flow enhancement factor, the

exponent of the pseudo-plastic basal resistance model, the till effective fraction overburden, etc.) ~~, but also parameters related with the~~ ice shelf melt, ~~the~~ ocean temperature, and ~~the~~ calving (i.e. the ice thickness threshold in the basic calving mechanism). These parameters are modified only during the regional JI runs such that the model reproduces the frontal positions and the ice mass change observations at JI during the period 1990-2014 (Fig. 2) and 1997-2014 (Figs. 3 and 44), respectively. From these results, we present the parameterization that best captures ~~(i.e., we estimate the residual between modelled and observed ice mass change and select the smallest residual signal)~~ the full observed evolution of JI during the period 1990–2014 (Figs. 2, 3, 4 and 5). The values of the ice sheet model parameters used ~~, together with their underlying equations~~ and the ice sheet model sensitivity to parameters controlling ice dynamics, basal processes, ice shelf melt, and ocean temperature, are further illustrated in the ~~supplementary material (SI)~~.

3.1 Observations vs. modelling results

3.1.1. Annual scale variations in velocities, terminus and grounding line positions

We investigate the processes driving the dynamic evolution of JI and its variation in velocity between 1990 and 2014 with a focus on the initial speedup of JI (1990) and the 2003 breakup of the ice tongue. The overall results from our simulations suggest a gradual increase in velocities that agree well with observations (Joughin et al., 2014) (Fig. 3). Three distinct stages of acceleration are identified in Fig. 3 (see also Movie 1 in the SI) and discussed in detail below.

- **1990–1997**

The first speedup produced by the simulation is caused by a retreat of the front position by approximately 2 to 4 km between 1990 and 1991. There is no observational evidence to confirm that this retreat actually occurred. The simulated retreat is probably a modelling artefact as the geometry obtained during the regional equilibrium simulation is forced with monthly atmospheric forcing and new oceanic conditions. This simulated acceleration (Fig. 3) is caused in our model by a reduction in buttressing due to a reduction in lateral resistance (Van der Veen et al., 2011), which is generated by the gradual retreat of the front and which triggers a dynamic response in the upstream region of JI.

Starting in 1992, the modelled and observed terminus positions agree (not shown in Fig. 2). Apart from the acceleration in 1991–1992, no significant seasonal fluctuations in flow rate are found in our simulations for this period, a result that is consistent with observations (Echelmeyer et al., 1994). From 1993 a stronger sub-annual velocity signal begins to emerge in our simulation that continues and intensifies in magnitude during 1994 and 1995. ~~The departure in 1995 from the normal seasonal invariance in velocity in our model seems to be influenced by the atmospheric forcing (Figs. 7 and S15). This result indicates that, as suggested by Luckman and Murray (2005), the 1995 anomalously high melt year (Figs. S2 and S10) may have potentially contributed to JI's retreat and flow acceleration during this period.~~ Modelled mean-annual velocities for 1992 and 1995 are consistent with observed velocities for the same period (Joughin et al., 2008; Vieli et al., 2011). In 1996 and 1997, the frontal extent and the grounding line position remain relatively stable (Figs. 2, 6 and 7), and no significant seasonal fluctuation in ice flow rate is observed in the simulation. These model results agree well with observations, which indicate that the glacier speed was relatively constant during this period (Luckman and Murray, 2005).

• 1998–2002

According to observations (Joughin et al., 2004; Luckman and Murray, 2005; Motyka et al., 2011; Bevan et al., 2012), the initial acceleration of JI occurred in May–August 1998, which coincides with our modelled results. In our simulation, the 1998 acceleration is generated by a retreat of the ice tongue's terminus in 1997–1998, which may be responsible for reducing buttressing (Fig. 7 and Movie 1 in the SI). Thinning, both near the terminus and inland (up to 10 km away from the 1990 front position), starts in our model in the summer of 1995 and continues to accelerate after 1998 (Figs. 3, 6 and 7). The modelled behaviour agrees well with the observed behaviour (Krabill et al., 2004). Although thinning appears to have increased in our model during three continuous years, it produced only minor additional speedup during the period prior to 1998 (Figs. 2, 6, and 7). In our simulation, JI's speed increased in the summer of 1998 by ~ 80% relative to the summer of 1992 (Fig. 3), at which time the grounding line position starts to retreat thereafter (Figs. 2, 6, and 7). Observations (Luckman and Murray, 2005) do not

show this level of speedup, and there are no observations of the grounding line position at this time with which to assess our model performance. Overall, modelling results suggest an advance of the terminus between 1999 and 2000 and a retreat of the southern tributary between 2000 and 2002 by ~4 km, which correlates with existing observations (Thomas, 2004). In our simulation, this retreat of the terminus triggers a decrease of resistive stresses at the terminus (Figs. 7 and [S9S8](#)). Concurrent with the 1998-2002 terminus retreat, the grounding line retreats in our model by ~6 km (Figs. 2, 6 and 7).

• 2003–2014

In the late summer of 2003, the simulated flow velocity increases (Fig. 3). This acceleration of JI is driven in our simulations by the final breakup of the ice tongue (see Figs. 2 and 6). The period 2002-2003 is characterized in our model by substantial retreat of the front (~4-6 km) and the grounding line (~4 km), which starts in June 2002 and continues throughout 2003. The simulated retreat that occurred in 2003 and the loss of large parts of the floating tongue (Figs. 2 and 6) caused a major decrease in resistive stresses near the terminus (Figs. 7 and [S9S8](#)). By 2004, the glacier had thinned significantly (Figs. 3 and 6) both near the front and further inland in response to a change in the near-terminus stress field (Fig. 7). During the final breakup of the ice tongue, the simulation produces speeds high as 20 km a⁻¹ (~ 120% increase relative to 1998). The modelled velocities decreased to 16 km a⁻¹ (~ 80% increase relative to 1998) in the subsequent months and remained substantially higher than the sparse observations from that time (e.g. Joughin et al., 2012). The high velocities modelled at JI after the loss of its floating tongue are further sustained in our simulation by the thinning that occurred after 2003 (Fig. 3), which continues to steepen the slopes near the terminus (Fig. 6), and is accompanied by a seasonal driven (sub-annual scale) retreat and advance of the front. This simulated thinning is combined in the following years with a reduction in surface mass balance due to increased melting and runoff (van den Broeke et al., 2009; Enderlin et al., 2014, Khan et al., 2014). The period 2004-2014 is characterized in our simulation by relatively uniform velocity peaks with strong sub-annual variations

(Fig. 3). During this period, only a small floating ice tongue is modelled and the terminus remained relatively stable, with no episodes of significant retreat.

In agreement with previous studies (e.g. Joughin et al. 2012), our results suggest that the overall variability in the modelled horizontal velocities is a response to variations in terminus position (Fig. 7). In our simulation, the retreat of the front reduced the buttressing at the terminus and generated a dynamic response in the upstream region of JI which finally led to flow acceleration. In contrast, when the front advanced the modelled flow slowed as the resistive stresses at the terminus were reinforced. This buttressing effect tends to govern JI's behaviour in our model. Regarding the overall terminus retreat, our simulations suggest that it is mostly driven by the sub-shelf melting parametrization applied (Figs. S5 and ~~S14~~S14). Although the heat flux supplied to the shelf evolves in time based on the modelled terminus geometry, the input ocean temperature is kept constant throughout the simulations. This constant ocean forcing at the terminus leads, in our simulation, to gradual thinning of JI and favours its retreat without any shift (e.g. increase) in ocean temperature. In terms of seasonality, ~~the only seasonal input into the model the only seasonal signal in the model~~ is introduced by the monthly atmospheric forcing ~~that is~~ applied (Sect. 2.1.1). In our model, the atmospheric forcing that is applied (Figs. S2 and S3) can influence JI's dynamics through changes in surface mass balance (SMB) (i.e., accumulation and ablation), which affects both the SIA and the SSA (Sect. 2.1), but also through changes in air temperature that can potentially influence sliding via the rate factor for the softness (SI, Eq. 1), which here is derived through an enthalpy formulation (Aschwanden et al., 2012). However, the modelled sub-annual variability in terms of terminus retreat and velocities does not always follow the seasonal signal (Fig. 3). We investigate this higher than seasonal variability in Sect. 3.2.

3.1.2 Ice mass change

Figure 4 shows observed and modelled mass change for the period 1997 to 2014. We estimate the observed rate of ice volume changes from airborne and satellite altimetry over the same period and convert these to rates of mass change (SI, Sect. 2). Overall we find good agreement between modelled and observed mass change (Fig. 4), and our results are in agreement with other similar studies (Howat et al., 2011; Nick et al., 2013). Dynamically driven discharge is known to control Jakobshavn's mass loss between 2000 and 2010 (Nick et al., 2013). The modelled cumulative mass loss is 269 Gt, of which 93% (~251 Gt) is dynamic in origin while the remaining 7% (~18 Gt) is attributed to a decrease in SMB (Fig. 4). Further,

the present-day unloading of ice causes the Earth to respond elastically. Thus, we can use modelled mass changes to predict elastic uplift. We compare modelled changes of the Earth's elastic response to changes in ice mass to uplift observed at four GPS sites (Fig. 5). Both model predictions and observations consistently suggest large uplift rates near the JI front (20 mm a⁻¹ for station KAGA) and somewhat minor uplift rates (~ 5 mm a⁻¹) at distances of >100 km from the ice margin.

Although the terminus has ceased to retreat in our simulations after 2009 (Figs. 6 and 7), the modelled mass loss, and more importantly the dynamic mass loss, continues to accelerate (Fig. 4). Our results show (Fig. 7) that during this period the mass change is mostly driven by the sub-annual terminus retreat and advance, which continues to generate dynamic changes at JI through seasonal (sub-annual scale) reductions in resistive stresses.

3.2 Feedback mechanisms, forcings and limitations

Representing the processes that act at the marine boundary (i.e. calving and ocean melt) are important for understanding and modelling the retreat/advance of marine terminating glaciers like JI. Determining terminus positions by using the superposition of a physically based calving (eigencalving) parametrization (Winkelmann et al., 2011; Levermann et al., 2012) and a basic calving mechanism (Albrecht et al., 2011) is motivated by the model's ability to maintain realistic calving front positions (Levermann et al., 2012). The eigen calving style parametrization cannot resolve individual calving events, and, thus, the introduction of the basic calving mechanism was necessary in order to accurately match observed front positions. Preparatory experiments have shown that overall calving is mostly driven in our model by the basic calving mechanism used (~ 96 % of the overall mass loss), and that the eigen calving parametrization is more important in modelling sub-annual to seasonal fluctuations of the terminus. Our simulations suggest that the superposition of these two calving mechanisms performs well for relatively narrow and deep fjords as those characterized by JI (Fig. 2). The benefit of using such a combination of calving laws is that it can evolve the terminus position with time and thus calving feedbacks are not ignored. As the terminus retreats, the feedback between calving and retreat generates dynamic changes due to a reduction in lateral shear and resistive stresses (Fig. 7). In a simulation in which the terminus position is kept fixed to the 1990s position, the velocity peaks are uniform (i.e. no acceleration is modelled except for some small seasonal related fluctuations generated by the atmospheric forcing applied), and

1 the mass loss remains relatively small (~ 70 Gt). Consistent with Vieli et al. (2011), we find
2 that the feedback between calving and retreat is highly important in modelling JI's dynamics.

3 As introduced in Sect. 2, our approach here is to adjust the terminus in the JI region to
4 simulate the 1990s observed front position and surface elevation based on 1985 aerial
5 photographs (Csatho et al., 2008). The glacier terminus in 1990s was floating (Csatho et al.,
6 2008; Motyka et al. 2011). Motyka et al. (2011) calculated the 1985 hydrostatic equilibrium
7 thickness of the south branch floating tongue from smoothed surface DEMs and obtained a
8 height of 600 m near the calving front and 940 m near the grounding zone. In this paper,
9 however, we compute the thickness as the difference between the surface elevation and the
10 bed topography, and allow the glacier to evolve its own terminus geometry during the
11 equilibrium simulation. Preparatory experiments have shown that in our model (disregarding
12 its initial geometry floating/ grounded terminus) JI attains equilibrium with a grounding line
13 position that stabilizes close to the 1990s observed terminus position. According to
14 observations, JI is characterized in 1990 by a large floating tongue (> 10 km; e.g. Motyka et
15 al., 2011) that we are not able to simulate during the equilibrium runs. In our model (Figs. 6
16 and 7), the glacier starts to develop a large floating tongue (~ 10 km) in 1999. Starting in
17 2000, the floating tongue is comparable in length and thickness with observations and the
18 model is able to simulate, with a high degree of accuracy, its breakup that occurred in late
19 summer 2003 and the subsequent glacier acceleration. Observations of terminus positions
20 (Sohn et al., 1998; Csatho et al., 2008) suggest that over more than 40 years, between 1946
21 and 1992, JI's terminus stabilized in the proximity of the 1990's observed terminus position.
22 Furthermore, during 1959 and 1985 the southern tributary was in balance (Csatho et al.,
23 2008). This suggests that, during the regional equilibrium and at the beginning of the forward
24 simulations, we are forcing our model with climatic conditions that favoured the glacier to
25 remain in balance. This may explain our unsuccessful attempts to simulate prior to 1998 a
26 floating tongue comparable in length and thickness with observations, and suggests that for
27 simulating the large floating tongue that characterized JI during this period, future studies
28 should consider to start modelling JI before the glacier begins to float in the late 1940s
29 (Csatho et al., 2008).

30 The geometry of the terminus plays an important role in parameterizing ice shelf melting, and
31 therefore our pre-1999 geometry will influence the magnitude of the basal melt rates (Sect.
32 | 2.1.3). The difference in geometry results in modelled mean basal melt rates that are larger

1 for the period 1999-2003 ([Table S3](#)), when JI begins to develop a large floating tongue and
2 when the calving front was already largely floating. [The modelled mean melt rates for the](#)
3 [period 1999-2003 are large and likely overestimated.](#) Relative to other studies, e.g. Motyka et
4 al. (2011), our [yearly mean](#) melt rate for 1998 is ~2 times larger (Table S3). While we choose
5 here to compare the two melt rates in order to offer a scale perspective, we acknowledge the
6 difference in geometry between the two studies. ~~Furthermore, our basal melt rates include~~
7 ~~both melting along the base of the shelf and in the proximity of the grounding line. In our~~
8 ~~model, the melt rates at the grounding line are higher than the melt rates modelled closer to~~
9 ~~the centre of the shelf (Sect. 2.1.3).~~

10 Starting in 2010, the retreat of the terminus modelled in our simulations did not correlate well
11 with observations (Fig. 2). The observed terminus and the grounding line retreats do not cease
12 after 2010. Further, observed front positions (Joughin et al., 2014) suggest that by the
13 summer 2010 JI was already retreating over the sill and on the over deepening indicated by
14 the red star in Fig. 6. The observed retreat is not reproduced in our simulations suggesting
15 that additional feedbacks and/or forcings most likely affect the glacier. Alternatively, the
16 mismatch between observations and simulation results may represent an incomplete
17 modelling of the physics, inaccuracies in atmospheric/oceanic conditions, or other various
18 limitations (e.g., bed topography model constraints and grid resolution issues). The particular
19 influence of these potential issues on our model is detailed below.

20 The basal topography of JIs channels represents a large source of uncertainty. JI is a marine
21 terminating glacier whose bedrock topography is characterized by a long and narrow channel
22 with deep troughs that contribute to its retreat and acceleration, e.g. once the grounding line
23 starts to retreat on a down-sloping bed, the flow increases, leading to further retreat and
24 acceleration (Vieli et al., 2011). The timing and the magnitude of these retreats depend on bed
25 topography and the glacier width changes (Jamieson et al., 2012; Enderlin et al., 2013).
26 Accurate modelling of the grounding line behaviour is, therefore, crucial for JIs dynamics as
27 its retreat removes areas of flow resistance at the base and may trigger unstable retreat if the
28 glacier is retreating into deeper waters. In our simulation, the grounding line position
29 stabilizes downstream of the sill after 2005 (Figs. 2 and 6), which is in accordance with
30 previous modelling studies (Vieli et al., 2001; Vieli et al., 2011). Vieli et al. (2011) found
31 that, by artificially lowering the same bed sill by 100 m, the grounding line eventually retreats
32 and triggers a catastrophic retreat of 80 km in just over 20 years. In an equivalent experiment

1 with Vieli et al. (2011) but performed with our model, lowering the bed sill by 100 m, did not
2 result in a retreat of the grounding line over the sill. Regarding the grid resolution, simulations
3 performed on a 1 km grid did not improve our simulations of ice thickness (Fig. ~~S11~~S10) or
4 surface speed (i.e. trend, overall magnitude, and shape of the flow; Fig. ~~S12~~S11).

5 From a climatic perspective, the summer of 2012 was characterized by exceptional surface
6 melt covering 98% of the entire ice sheet surface and including the high elevation Summit
7 region (Nghiem et al., 2012; Hanna et al., 2014). Overall, the 2012 melt-season was two
8 months longer than the 1979–2011 mean and the longest recorded in the satellite era (Tedesco
9 et al., 2013). Furthermore, the summer of 2012 was preceded by a series of warm summers
10 (2007, 2008, 2010 and 2011) (Hanna et al., 2014). Surface melt above average was already
11 recorded in May-June 2012 (see Fig. 3 from NSIDC (2015)) when most of the 2011-2012
12 winter accumulation melted and over 30% of the ice sheet surface experienced surface melt.
13 An intense and long melt year leads to extensive thinning of the ice and has the potential to
14 enhance hydrofracturing of the calving front due to melt water draining into surface crevasses
15 (MacAyeal et al., 2003; Joughin et al., 2013; Pollard et al., 2015) resulting in greater and/or
16 faster seasonal retreat and an increase in submarine melt at the terminus and the sub-shelf
17 cavity (Schoof, 2007; Stanley et al., 2011; Kimura et al., 2014; Slater et al., 2015).

18 The seasonal retreat of JIs terminus started relatively early in 2012, with a large calving event
19 having already occurred in June. While it seems difficult to attribute this particular calving
20 event solely to processes related to the 2012 melt season, it does seem probable that the series
21 of warm summers (2007-2011) together with the 2012 exceptional melt season could have
22 enhanced hydrofracturing of the calving front. In turn, this could have induced a retreat of the
23 terminus that cannot be captured by our model (i.e., in its present configuration the model
24 ~~does~~cannot account directly for the influence of meltwater runoff and its role in the
25 subglacial system during surface melt events). Nonetheless, a high melt year is generally the
26 consequence of high summer air temperatures that in our model represent boundary
27 conditions for the enthalpy equation (Aschwanden et al., 2012). Therefore, an increase in air
28 temperatures could potentially soften the ice and enhance sliding. However, the time required
29 for advection/diffusion to propagate down ~~into~~through the column and reach the high shearing
30 layer at the base of the ice (Aschwanden et al., 2012) is generally much longer than our
31 hindcasts and thus, we believe that in our simulations, this effect does not have a significant
32 impact on the flow. In our model, the atmospheric forcing applied (Sect. 2.1.1) can influence

~~It's dynamics only through changes in surface mass balance (SMB) (i.e., accumulation and ablation). While these changes~~ On the other hand, changes in ice thickness affect both the SIA and the SSA (Sect. 2.1). ~~While~~ the effect ~~on~~ the SIA is very weak as the driving stresses are not affected by a few meters of difference in thickness induced by SMB variability. ~~In~~ in the SSA, the coupling is achieved via the effective pressure term in the definition of the yield stress (see SI, Sect. 1.2 for detailed equations). The effective pressure is determined by the ice overburden pressure (i.e., ice thickness) and the effective thickness of water in the till, where the latter is computed by time-integrating the basal melt rate. Compared with SIA, ~~this effect is much stronger and favours the idea that in~~ may explain why in our model some seasonal velocity peaks could potentially be influenced by the ~~climatic-atmospheric~~ forcing applied (Figs. S10-S9 and S15S14).

We study the sensitivity of the model to atmospheric forcing by performing a simulation where we keep the atmospheric forcing constant (mean 1960-1990 temperature and SMB). By comparing this simulation with a simulation that includes full atmospheric variability (monthly temperature and SMB) ~~we see that in terms of terminus retreat and velocities the modelled sub-annual variability does not always correlate with the observed seasonal signal (Fig. S15). In particular, the simulations suggest we find~~ that to only a relatively small degree some of the variability appears to be influenced by the atmospheric forcing applied (Figs. S2, S10 and S15S14), which also represents the only seasonal input into the model. Some of the greater than seasonal frequency could be an issue with resolution in the model. We examined this sensitivity by performing additional runs at a higher spatial resolution. Simulations on a 1 km grid did show some improvement with respect to surface speed sub-annual variability (Fig. S13S12), suggesting that in our model the stress redistribution might be sensitive to the resolution of the calving event. However, given the short period spanned by the simulations, the stress redistribution does not change the overall modelled results, as seen in Figs. S11-S10 and S12S11. Although we acknowledge that some of the variability is due to the grid resolution, part of it may also be related to unmodeled physical processes acting at the terminus. We suggest that additional contributions to the seasonality, e.g. from ice mélange or seasonal ocean temperature variability, which are not included in our model could potentially influence the advance and retreat of the front at seasonal scales (Fig. S15S14). For example, the ice mélange can prevent the ice at the calving front from breaking off and could therefore reduce the calving rates. Consequently, the introduction of an ice mélange parametrization will probably help to minimize some of the sub-annual signal modelled in our simulations.

1 Similarly, seasonal ocean temperature variability can influence ice mélange formation and/or
2 clearance and the melt rates at the glacier front and can accentuate seasonal glacier terminus
3 and grounding line retreat and/or advance. However, at this point we find it difficult to
4 determine the relative importance of each process.

5 Finally, regarding the ocean conditions, warm water temperatures in the fjord were recorded
6 in 2012. Besides a cold anomaly in 2010, which was sustained until early 2011, the period
7 2008-2013 is characterized by high fjord waters temperatures - equal to or warmer than those
8 recorded in 1998-1999 (Gladish et al., 2015). In our model, the ice melt rates are determined
9 from the given conditions in temperature (-1.7°C , and salinity (35 psu) of the fjord waters,
10 and the given geometry (Sect. 2.1.3). The fact that we are able to model JIs retreat with a
11 constant ocean temperature suggests that the retreat and acceleration observed at JI are not
12 likely to be controlled by the year to year variability in ocean temperatures. This conclusion
13 agrees with the observational study of Gladish et al. (2015) who analysed ocean temperature
14 variability in the Ilulissat fjord with JI variability and who found that after 1999 there was no
15 clear correlation. Our results do not, however, imply that the ocean influence in JI's retreat is
16 negligible (Fig. S5), but rather that the glacier most likely responds to changes in ocean
17 temperature that are sustained for longer time periods, e.g. decadal time scales. Two
18 additional experiments, where the input ocean temperature (T_o) was increased to -1°C
19 indicate that higher melt rates beneath the grounding line could potentially explain the retreat
20 observed after 2010. In our first experiment, the input T_o was increased from -1.7°C to -1°C
21 starting 1997 ($\sim 0.7^{\circ}\text{C}$ relative to 1990). This temperature increase is consistent with observed
22 ocean temperatures at the mouth of the Ilulissat fjord (Gladish et al., 2015) and generated in
23 our simulation, for the period 1997-2014, an accelerated retreat of the front that does not
24 correlate with observations (Fig. S8S7). Similarly, mass loss estimates from the simulations
25 are significantly larger (by $\sim 50\%$; Fig. S7S6) than those calculated from airborne and
26 satellite altimetry observations (Sect. 3.1.2). Overall, the experiment shows that an increase in
27 ocean temperature that starts in 1997 and is sustained until 2014 generates modelled estimates
28 for the period 1998-2014 that do not agree with observations. In the second experiment, T_o
29 was increased to -1°C starting in 2010 ($\sim +0.7^{\circ}\text{C}$ at the base of the shelf in 2010). For the
30 period 2010-2014, our model predicted a faster retreat of the front that correlates well with
31 observations (Fig. S8S7), and an increase of mass loss by $\sim 7\text{ Gt}$ (Fig. S7S6). This experiment
32 shows that an increase in ocean temperature beginning in 2010 could potentially explain the
33 retreat observed thereafter.

4 Conclusions

In this study, a three-dimensional, time-dependent regional outlet glacier model is used to investigate the processes driving the dynamic evolution of JI and its seasonal variation in ice velocity between 1990 and 2014. Here, we attempted to simulate the recent behaviour of JI with a process-based model. The model parameters were calibrated such that the model reproduced observed front positions (Fig. 2) and ice mass change observations (Fig. 4) at JI over the periods 1990-2014 and 1997-2014, respectively. We obtain a good agreement of our model output with time series of measured horizontal velocities, observed thickness changes, and GPS derived elastic uplift of the crust (Figs. 3 and 5). Overall, the study shows progress in modelling the temporal variability of the flow at JI.

Our results suggest that most of the JI retreat during 1990-2014 is driven by the ocean parametrization, and the glacier's subsequent response, which is largely governed by its own bed geometry (Figs. 6, 7 and S5). In agreement with previous studies (e.g. Joughin et al. 2012), our simulations suggest that the overall variability in the modelled horizontal velocities is a response to variations in terminus position (Fig. 7). In our model, the seasonal variability is likely driven by processes related to the atmospheric forcing applied (e.g. temperature and SMB variability), which in fact represents the only seasonal input used in the model. The greater than seasonal frequency seen in our simulations is attributed to grid resolution and missing seasonal scale processes (e.g., ice mélange variability or seasonal ocean temperature variability) in the model. Sensitivity experiments performed on a 1 km grid did not show significant improvement with respect to ice thickness (Fig. S4+S10) or surface speed (i.e. shape of the flow and overall magnitude; Fig. S4+S11).

In 1990, JI had a large floating tongue (> 10 km; e.g. Motyka et al., 2011) that we are not able to simulate during the equilibrium runs. In our model (Fig. 6), the glacier starts to develop a floating tongue comparable with observations in 1999. Starting in 2000, the floating tongue is consistent in length and thickness with observations and the model is able to simulate its breakup (that occurred in late summer 2003) and the subsequent glacier acceleration. The difference between observed and modelled pre-1999 geometry results in relatively large basal melt rates for the period 1997-2003 (Fig. S4+S9). Nevertheless, the model is able to capture the overall retreat of the terminus and the trends in the observed velocities (Figs. 2 and 3) for the period 1990-2010. Finally, the 2010-2012 observed terminus retreat (Joughin et al., 2014) is not reproduced in our simulations, likely due to inaccuracies in basal topography, or

misrepresentations of the atmospheric forcing and the ocean parametrization that we used. Additional sensitivity experiments showed that an increase in ocean temperature of $\sim 0.7^{\circ}\text{C}$ for the period 2010-2014 may trigger a retreat of the terminus that agrees better with observations (Figs. [S7-S6](#) and [S8S7](#)).

Our model reproduces two distinct flow accelerations in 1998 and 2003 that are consistent with observations. The first was generated by a retreat of the terminus and moderate thinning prior to 1998; the latter was triggered by the final breakup of the floating tongue. During this period, JI attained in our simulation unprecedented velocities as high as 20 km a^{-1} . Additionally, the final breakup of the floating tongue generated a reduction in buttressing that resulted in further thinning. Similar to previous studies (Nick et al., 2009; Vieli et al., 2011; Joughin et al. 2012), our results show that the dynamic changes observed at JI are triggered at the terminus (Figs. 7, S5, [S15-S14](#) and [S17S16](#)).

In accordance with previous studies (Thomas, 2004; Joughin et al., 2012), our findings suggest that the speeds observed today at JI are a result of thinning induced changes due to reduction in resistive stress (buttressing) near the terminus correlated with inland steepening slopes (Figs. 6 and 7). Both model and observations suggest that JI has been losing mass at an accelerating rate and that the glacier has continued to accelerate through 2014 (Fig. 4).

Author Contributions

I.S.M. was responsible for the numerical modelling part. J.B. provided the bed model. M.R.V.D.B, and P.K.M. provided climate data. S.A.K and B.W. provided observational data. I.S.M. and S.A.K created the figures and wrote the manuscript with contributions from A. A, J.B., T.V.D., M.R.V.D.B, B.W., P.K.M, K.K., and C.K.

Acknowledgements

Ioana S. Muresan is funded by the Forskningsraadet for Natur og Univers (grant no. 12-155118). Shfaqat A. Khan is supported by Carlsbergfondet (grant no. CF14-0145). Jonathan Bamber was part funded by UK NERC grant NE/M000869/1. Bert Wouters is funded by a Marie Curie International Outgoing Fellowship within the 7th European Community Framework Programme (FP7-PEOPLE-2011-IOF-301260). The development of PISM is supported by NASA grants NNX13AM16G and NNX13AK27G. We thank the editor, ~~three~~ five anonymous reviewers for their valuable comments and suggestions to improve and clarify the manuscript, and Veit Helm for providing cryosat-2 data.

1 **References**

- 2 Albrecht, T., M. Martin, M. Haseloff, R. Winkelmann, and A. Levermann. 2011.
3 “Parameterization for subgrid-scale motion of ice-shelf calving fronts.” *The Cryosphere* 5:
4 35–44. doi:10.5194/tc-5-35-2011.
- 5 Amundson, J. M., M. Fahnestock, M. Truffer, J. Brown, M. P. Lüthi, and R. J. Motyka. 2010.
6 “Ice mélange dynamics and implications for terminus stability, Jakobshavn Isbræ,
7 Greenland.” *J. Geophys. Res.* 115: F01005. doi:10.1029/2009JF001405.
- 8 Aschwanden, A., E. Bueler, C. Khroulev, and H. Blatter. 2012. “An enthalpy formulation for
9 glaciers and ice sheets.” *J. Glaciol.* 58(209): 441–457. doi:10.5194/tcd-6-5069-2012.
10 doi:10.3189/2012JoG11J088.
- 11 Aschwanden, A., G. Aðalgeirsdóttir, and C. Khroulev. 2013. “Hindcast to measure ice sheet
12 model sensitivity to initial states.” *The Cryosphere* 7: 1083–1093. doi:10.5194/tcd-6-5069-
13 2012.
- 14 Aschwanden, A., M. A. Fahnestock and M. Truffer. 2016. “Complex Greenland outlet glacier
15 flow captured”. *Nat. Commun.* 7 (10524). doi: 10.1038/ncomms10524.
- 16 Bamber, J. L., J. A. Griggs, R. T. W. L. Hurkmans, J. A. Dowdeswell, S. P. Gogineni, I.
17 Howat, J. Mouginot, J. Paden, S. Palmer, E. Rignot, and D. Steinhage. 2013. “A new bed
18 elevation dataset for Greenland.” *The Cryosphere* 7: 499–510. doi:10.5194/tc-7-499-2013.
- 19 Beckmann, A., and H. Goosse. 2003. “A parameterization of ice shelf–ocean interaction for
20 climate models.” *Ocean Model.* 5 (2): 157–170. doi:10.1016/S1463-5003(02)00019-7.
- 21 Bevan, S. L., A. J. Luckman, and T. Murray. 2012. “Glacier dynamics over the last quarter of
22 a century at Helheim, Kangerdlugssuaq and other major Greenland outlet glaciers.” *The*
23 *Cryosphere* 6: 923–937. doi:10.5194/tc-6-923-2012.
- 24 Bindschadler, R. A., S. Nowicki, A. Abe-Ouchi, A. Aschwanden, H. Choi, J. Fastook, G.
25 Granzow, et al. 2013. “Ice-Sheet Model Sensitivities to Environmental Forcing and Their Use
26 in Projecting Future Sea Level (the SeaRISE Project).” *J. Glaciol.* 59 (214): 195–224.
27 doi:10.3189/2013JoG12J125.
- 28 Broeke, M. van den, J. Bamber, J. Ettema, Eric Rignot, E. Schrama, W. J. van de Berg, E. van
29 Meijgaard, I. Velicogna, and B. Wouters. 2009. “Partitioning recent Greenland mass loss.”
30 *Science* 326 (5955): 984–986. doi:10.1126/science.1178176.

Bueler, E., and J. Brown. 2009. "Shallow shelf approximation as a 'sliding law' in a thermodynamically coupled ice sheet model." *J. Geophys. Res.* 114: F03008. doi:10.1029/2008JF001179.

Csatho, B., T. Schenk, C. J. Van Der Veen and W. B. Krabill. 2008. "Intermittent thinning of Jakobshavn Isbræ, West Greenland, since the Little Ice Age." *J. Glaciol.* 54 (184): 131–144. doi: 10.3189/002214308784409035.

Cuffey, K. M., and W. S. B. Paterson. 2010. "The Physics of Glaciers". Elsevier, 4th edition. ISBN 9780123694614.

de Juan, J., P. Elósegui, M. Nettles, T.B. Larsen, J.L. Davis, G.S. Hamilt, L.A. Stearns, M. L. Anderson, G. Ekström, L. Stenseng, S. A. Khan, R. Forsberg. 2010. "Sudden increase in tidal response linked to calving and acceleration at a large Greenland outlet glacier". *Geophys. Res. Lett.* 37: L12501. doi:10.1029/2010GL043289.

Echelmeyer, K.A., W.D. Harrison, C. Larson, and J.E. Mitchell. 1994. The role of the margins in the dynamics of an active ice stream. *J. Glaciol.* 40(136): 527–538.

Enderlin, E. M., I. M. Howat, and A. Vieli. 2013. "High sensitivity of tidewater outlet glacier dynamics to shape." *The Cryosphere* 7: 1007–1015. doi: 10.5194/tc-7-1007-2013.

Enderlin, E. M., I. M. Howat, S. Jeong, M. J. Noh, J. H. van Angelen, and M. R. van den Broeke. 2014. "An improved mass budget for the Greenland ice sheet." *Geophys. Res. Lett.* 41: 866–872. doi:10.1002/2013GL059010.

Feldmann, J., T. Albrecht, C. Khroulev, F. Pattyn, and A. Levermann. 2014. "Resolution-dependent performance of grounding line motion in a shallow model compared with a full-Stokes model according to the MISMIP3d intercomparison." *J. Glaciol.* 60 (220): 353–360. doi:10.3189/2014JoG13J093.

Feldmann, J., Albrecht, T., Khroulev, C., Pattyn, F., and Levermann, A.: Resolution-dependent performance of grounding line motion in a shallow model compared with a full-Stokes model according to the MISMIP3d intercomparison, *J. Glaciol.*, 60, 353–360, doi:10.3189/2014JoG13J093, 2014.

Gladish, C. V., D. M. Holland, and C. M. Lee. 2015a. "Oceanic boundary conditions for Jakobshavn Glacier. Part II: Provenance and sources of variability of Disko Bay and Ilulissat icefjord waters, 1990–2011." *J. Phys. Oceanogr.* 45: 33–63. doi:dx.doi.org/10.1175/JPO-D-14-0045.1.

1 Gladish, C. V., D. M. Holland, A. Rosing-Asvid, J. W. Behrens, and J. Boje. 2015b. "Oceanic
2 boundary conditions for Jakobshavn Glacier. Part I: Variability and renewal of Ilulissat
3 icefjord waters, 2001–2014." *J. Phys. Oceanogr.* 45: 3–32. doi:dx.doi.org/10.1175/JPO-D-14-
4 0044.1.

5 Gladstone, R. M., A. J. Payne, and S. L. Cornford. 2010. "Parameterising the grounding line
6 in flow-line ice sheet models." *The Cryosphere* 4: 605–19. doi:10.5194/tc-4-605-2010.

7 Hanna, E., X. Fettweis, S. Mernild, J. Cappelen, M. Ribergaard, C. Shuman, K. Steffen, L.
8 Wood, and T. Mote. 2014. "Atmospheric and oceanic climate forcing of the exceptional
9 Greenland ice sheet surface melt in summer 2012." *Int. J. Climatol.* 34 (4): 1022–1037.
10 doi:10.1002/joc.3743.

11 Holland, D. M., R. H. Thomas, B. de Young, M. H. Ribergaard, and B. Lyberth. 2008.
12 "Acceleration of Jakobshavn Isbræ Triggered by Warm Subsurface Ocean Waters." *Nat.*
13 *Geosci.* 1: 659–664. doi:10.1038/ngeo316.

14 Howat I. M., Y. Ahn, I. Joughin, M. R. van den Broeke, J. T. M. Lenaerts, and B. Smith.
15 2011. "Mass balance of Greenland's three largest outlet glaciers, 2000–2010." *Geophys. Res.*
16 *Lett.* 38(12): L12501. doi: 10.1029/2011GL047565.

17 Hutter K. 1983. "Theoretical Glaciology: Material Science of Ice and the Mechanics of
18 Glaciers and Ice Sheets." D. Reidel Publishing Co. Tokyo, Terra Scientific Publishing Co.
19 xxxii, 510 p.

20 IPCC. 2013. "Climate Change 2013: The Physical Science Basis. Contribution of Working
21 Group I to the Fifth Assessment Report of the Intergovernmental Panel on Climate Change."
22 Cambridge University Press, Cambridge, United Kingdom and New York, NY, USA: 1535
23 pp. doi:10.1017/CBO9781107415324.

24 Jamieson, S. S. R., A. Vieli, S. J. Livingstone, C. Ó Cofaigh, C. Stokes, C.-D. Hillenbrand,
25 and J. A. Dowdeswell. 2012. "Icestream stability on a reverse bed slope". *Nat. Geosci.* 5
26 :799–802. doi:10.1038/NCEO1600.

27 Jones, P. W. 1999. "First- and Second-Order Conservative Remapping Schemes for Grids in
28 Spherical Coordinates". *Mon. Weather Rev.* 127 (9): 2204–2210. doi:
29 [http://dx.doi.org/10.1175/1520-0493\(1999\)127<2204:FASOCR>2.0.CO;2](http://dx.doi.org/10.1175/1520-0493(1999)127<2204:FASOCR>2.0.CO;2).

1 Joughin, I., W. Abdalati, and M. Fahnestock. 2004. "Large fluctuations in speed on
2 Greenland's Jakobshavn Isbræ glacier." *Nature* 432: 608–610. doi:10.1038/nature03130.

3 Joughin, I., I. M. Howat, M. Fahnestock, B. Smith, W. Krabill, R. B. Alley, H. Stern, and M.
4 Truffer. 2008. "Continued evolution of Jakobshavn Isbrae Following Its Rapid Speedup." *J.*
5 *Geophys. Res.* 113: F04006. doi:10.1029/2008JF001023.

6 Joughin, I., B. E. Smith, I. M. Howat, T. Scambos, and T. Moon. 2010. "Greenland Flow
7 Variability from Ice-Sheet-Wide Velocity Mapping". *J. Glaciol.* 56 (197): 415-430.
8 doi:10.3189/002214310792447734.

9 Joughin, I., I. Howat, B. Smith, and T. Scambos. 2011. "MEaSURES Greenland Ice Velocity:
10 Selected Glacier Site Velocity Maps from InSAR". Boulder, Colorado, USA: NASA DAAC
11 at the National Snow and Ice Data Center. doi:10.5067/MEASURES/CRYOSPHERE/nsidc-
12 0481.001.

13 Joughin, I., B. E. Smith, I. M. Howat, D. Floricioiu, R. B. Alley, M. Truffer, and M.
14 Fahnestock. 2012. "Seasonal to decadal scale variations in the surface velocity of Jakobshavn
15 Isbræ, Greenland: Observation and model-based analysis." *J. Geophys. Res.* 117: F02030.
16 doi:10.1029/2011JF002110.

17 Joughin, I., S. B. Das, G. E. Flowers, M. D. Behn, R. B. Alley, M. A. King, B. E. Smith, J. L.
18 Bamber, M. R. van den Broeke, and J. H. van Angelen. 2013. "Influence of ice-sheet
19 geometry and supraglacial lakes on seasonal ice-flow variability." *The Cryosphere* 7: 1185-
20 1192. doi:10.5194/tc-7-1185-2013.

21 Joughin, I., B. E. Smith, D. E. Shean, and D. Floricioiu. 2014. "Brief Communication: Further
22 summer speedup of Jakobshavn Isbræ." *The Cryosphere* 8: 209–214. doi:10.5194/tc-8-209-
23 2014.

24 Keegan, K. M., R.M. Albert, J. R. McConnell and I. Baker. 2014. "Climate change and forest
25 fires synergistically drive widespread melt events of the Greenland Ice Sheet." *P. Natl. Acad.*
26 *Sci.* 111(22): 7964–7967. doi: 10.1073/pnas.1405397111.

27 Khan, S. A., L. Liu, J. Wahr, I. Howat, I. Joughin, T. van Dam, and K. Fleming. 2010. "GPS
28 measurements of crustal uplift near Jakobshavn Isbræ due to glacial ice mass loss." *J.*
29 *Geophys. Res.* 115: B09405. doi:10.1029/2010JB007490.

1 Khan, S. A., K. H. Kjær, M. Bevis, J. L. Bamber, J. Wahr, K. K. Kjeldsen, A. A. Bjørk, N. J.
2 Korsgaard, L. A. Stearns, M. R. van den Broeke, L. Liu, N. K. Larsen, and I. S. Muresan.
3 2014. “Sustained Mass Loss of the Northeast Greenland Ice Sheet Triggered by Regional
4 Warming.” *Nat. Clim. Change* 4: 292–299. doi:10.1038/nclimate2161.

5 Khan, S. A., A. Aschwanden, A. A. Bjørk, J. Wahr, K. K. Kjeldsen, and K. H. Kjær. 2015.
6 “Greenland ice sheet mass balance: a review.” *Rep. Prog. Phys.* 78(4). doi: 10.1088/0034-
7 4885/78/4/046801.

8 Kimura, S., P. R. Holland, A. Jenkins, and M. Piggott. 2014. “The effect of meltwater plumes
9 on the melting of a vertical glacier face.” *J. Phys. Oceanogr.* 44: 3099-3117. doi:
10 10.1175/JPO-D-13-0219.1

11 Krabill, W., W. Abdalati, E. Frederick, S. Manizade, C. Martin, J. Sonntag, R. Swift, R.
12 Thomas, W. Wright, and J. Yungel. 2000. “Greenland Ice Sheet: High-Elevation Balance and
13 Peripheral Thinning.” *Science* 289: 428–430. doi:10.1126/science.289.5478.428.

14 Krabill, W., E. Hanna, P. Huybrechts, W. Abdalati, J. Cappelen, B. Csatho, E. Frederick, S.
15 Manizade, C. Martin, J. Sonntag, R. Swift, R. Thomas, and J. Yungel. 2004. “Greenland Ice
16 Sheet: Increased coastal thinning”, *Geophys. Res. Lett.* 31: L24402.
17 doi:10.1029/2004GL021533.

18 Krabill, W. B. 2014. “IceBridge ATM L2 Icessn Elevation, Slope, and Roughness, [1993-
19 2014]. Boulder, Colorado USA: NASA Distributed Active Archive Center at the National
20 Snow and Ice Data Center. Digital media. Updated 2014.” <http://nsidc.org/data/ilatm2.html>.

21 Larour, E., H. Seroussi, M. Morlighem, and E. Rignot. 2012. “Continental scale, high order,
22 high spatial resolution, ice sheet modeling using the Ice Sheet System Model (ISSM).” *J.*
23 *Geophys. Res.-Earth* (2003-2012) 117: F01022. doi:10.1029/2011JF002140.

24 Levermann, A., T. Albrecht, R. Winkelmann, M. A. Martin, M. Haseloff, and I. Joughin.
25 2012. “Kinematic first-order calving law implies potential for abrupt ice-shelf retreat.” *The*
26 *Cryosphere* 6: 273–286. doi:10.5194/tc-6-273-2012.

27 Luckman, A., and T. Murray. 2005. “Seasonal variation in velocity before retreat of
28 Jakobshavn Isbræ, Greenland.” *J. Geophys. Res. Letters* 32: L08501.
29 doi:10.1029/2005GL022519.

- 1 MacAyeal, D. R., T. A. Scambos, C. L. Hulbe and M. A. Fahnestock. 2003. "Catastrophic
- 2 iceshelf break-up by an ice-shelf-fragment-capsize mechanism." *J. Glaciol.* 49(164): 22-36.
- 3 Mahaffy, M. W. 1976. "A three-dimensional numerical model of ice sheets: tests on the
- 4 Barnes Ice Cap, Northwest Territories". *J. Geophys. Res.*, 81(6):1059–1066.
- 5 Martin, M. A., R. Winkelmann, M. Haseloff, T. Albrecht, E. Bueler, C. Khroulev, and A.
- 6 Levermann. 2011. "The Potsdam Parallel Ice Sheet Model (PISM-PIK), Part II: Dynamical
- 7 equilibrium simulation of the Antarctic Ice Sheet." *The Cryosphere* 5: 727–740.
- 8 doi:10.5194/tc-5-727-2011.
- 9 Mengel, M., and A. Levermann. 2014. "Ice plug prevents irreversible discharge from East
- 10 Antarctica." *Nat. Clim. Change* 4: 451–455. doi:10.1038/nclimate2226.
- 11 Moon, T., I. Joughin, B. Smith, and I. Howat. 2012. "21st-Century evolution of Greenland
- 12 outlet glacier velocities." *Science* 336: 576–578. doi:10.1126/science.1219985.
- 13 Motyka, R. J., M. Truffer, M. Fahnestock, J. Mortensen, S. Rysgaard, and I. Howat. 2011.
- 14 "Submarine melting of the 1985 Jakobshavn Isbræ floating tongue and the triggering of the
- 15 current retreat." *J. Geophys. Res.* 116: F01007. doi:10.1029/2009JF001632.
- 16 NSIDC. 2015. "2014 melt season in review." National Snow & Ice Data Center (NSIDC).
- 17 Accessed July 09, 2015. [http://nsidc.org/greenland-today/2015/01/2014-melt-season-in-](http://nsidc.org/greenland-today/2015/01/2014-melt-season-in-review/)
- 18 [review/](http://nsidc.org/greenland-today/2015/01/2014-melt-season-in-review/).
- 19 Nghiem, S. V., D. K. Hall, T. L. Mote, M. Tedesco, M. R. Albert, K. Keegan, C. A. Shuman,
- 20 N. E. DiGirolamo, and G. Neumann. 2012. "The extreme melt across the Greenland ice sheet
- 21 in 2012." *Geophys. Res. Lett.* 39: L20502. doi: 10.1029/2012GL053611.
- 22 Nick, F. M., A. Vieli, M. L. Andersen, I. Joughin, A. Payne, T. L. Edwards, F. Pattyn, and R.
- 23 S. van de Wal. 2013. "Future sea-level rise from Greenland's main outlet glaciers in a
- 24 warming climate." *Nature* 497: 235–238. doi:10.1038/nature12068.
- 25 Nick, F.M., A. Vieli, I. M. Howat, and I. Joughin. 2009. "Large-Scale Changes in Greenland
- 26 Outlet Glacier Dynamics Triggered at the Terminus." *Nat. Geosci.* 2: 110–114.
- 27 doi:10.1038/ngeo394.
- 28 Nielsen, K., S. A. Khan, G. Spada, J. Wahr, M. Bevis, L. Liu, and T. van Dam. 2013.
- 29 "Vertical and horizontal surface displacements near Jakobshavn Isbræ driven by melt-induced
- 30 and dynamic ice loss." *J. Geophys. Res.-Sol. Ea.* 118: 1837–1844. doi:10.1002/jgrb.50145.

- Noël, B., W. J. van de Berg, E. van Meijgaard, P. Kuipers Munneke, R. S. W. van de Wal, and M. R. van den Broeke. 2015. "Summer snowfall on the Greenland Ice Sheet: a study with the updated regional climate model RACMO2.3." *The Cryosphere Discussion* 9: 1177-1208. doi: 10.5194/tcd-9-1177-2015.
- Parizek, B.R., and R.T. Walker. 2010. "Implications of initial conditions and ice–ocean coupling for grounding-line evolution." *Earth Planet. Sci. Lett.* 300: 351–358. doi:10.1016/j.epsl.2010.10.016.
- Pattyn, F., C. Schoof, L. Perichon, R. C. A. Hindmarsh, E. Bueler, B. de Fleurian, G. Durand, et al. 2012. "Results of the Marine Ice Sheet Model Intercomparison Project, MISMIP." *The Cryosphere* 6: 573–588. doi:10.5194/tc-6-573-2012.
- Pattyn, F., Perichon, L., Durand, G., Favier, L., Gagliardini, O., Hindmarsh, R., Zwinger, T., Albrecht, T., Cornford, S., Docquier, D., Fust, J. J., Goldberg, D., Gudmundsson, G. H., Humbert, A., Hutten, M., Huybrechts, P., Jouvett, G., Kleiner, T., Larour, E. and Martin, D., Morlighem, M., Payne, A. J., Pollard, D., Ruckamp, M., Rybak, O., Seroussi, H., Thoma, M., and Wilkens, N. 2010. "Grounding-line migration in plan-view marine ice-sheet models: results of the ice2sea MISMIP3d intercomparison". *J. Glaciol.* 59: 410–422. doi:http://dx.doi.org/10.3189/2013JoG12J12910.3189/2013JoG12J129.
- Pollard, D., R. M. DeConto, and R. B. Alley. 2015. "Potential Antarctic Ice Sheet retreat driven by hydrofracturing and ice cliff failure." *Earth Planet. Sci. Lett.* 412: 112–121. doi: 10.1016/j.epsl.2014.12.035.
- Price, S. F., A. J. Payne, I. M. Howat, and B. E. Smith. 2011. "Committed sea-level rise for the next century from Greenland ice sheet dynamics during the past decade." *P. Natl. Acad. Sci. USA* 108: 8978–8983. doi:10.1073/pnas.1017313108.
- Rignot, E., J. L. Bamber, M. R. van den Broeke, C. Davis, Y. Li, W. J. van de Berg, and E. van Meijgaard. 2008. "Recent Antarctic ice mass loss from radar interferometry and regional climate modeling." *Nat. Geosci.* 1: 106–110. doi:10.1038/ngeo102.
- Schoof, C. 2007. "Ice sheet grounding line dynamics: steady states, stability, and hysteresis." *J. Geophys. Res.* 112 (F03S28). doi:10.1029/2006JF000664.
- Schoof, C. and R. Hindmarsh. 2010. "Thin-film flows with wall slip: an asymptotic analysis of higher order glacier flow models". *Quart. J. Mech. Appl. Math.* 63(1): 73–114. doi: 10.1093/qjmam/hbp025.

1 Seroussi, H., H. B. Dhia, M. Morlighem, E. Larour, E. Rignot, and D. Aubry. 2012.
2 “Coupling ice flow models of varying orders of complexity with the Tiling method.” *J.*
3 *Glaciol.* 58: 776–786. doi:10.3189/2012JoG11J195.

4 Shapiro, N. M., and M. H. Ritzwoller. 2004. “Inferring surface heat flux distributions guided
5 by a global seismic model: particular application to Antarctica.” *Earth Planet. Sci. Lett.* 223:
6 213–224. doi: 10.1016/j.epsl.2004.04.011.

7 Shepherd, A., E. R. Ivins, A. Geruo, V. R. Barletta, M. J. Bentley, S. Bettadpur, K. H. Briggs,
8 D. H. Bromwich, et al. 2012. “A reconciled estimate of ice-sheet mass balance.” *Science*
9 338(6111): 1183-1189. doi:10.1126/science.1228102.

10 Slater, D. A., P. W. Nienow, T. R. Cowton, D. N. Goldberg, and A. J. Sole. 2015. “Effect of
11 near-terminus subglacial hydrology on tidewater glacier submarine melt rates.” *Geophys. Res.*
12 *Lett.* 42: 2861-2868. doi: 10.1002/2014GL062494.

13 Sohn, H. G., K. C. Jezek, and C. J. van der Veen. 1998. “Jakobshavn Glacier, west Greenland:
14 30 years of spaceborne observations.” *Geophys. Res. Lett.* 25(14): 2699-2702. doi:
15 10.1029/98GL01973.

16 Stanley, S. J., A. Jenkins, C. F. Giulivi and P. Dutrieux. 2011. “Stronger ocean circulation and
17 increased melting under Pine Island Glacier ice shelf.” *Nat. Geosci.* 4: 519–523. doi:
18 10.1038/ngeo1188

19 Tedesco, M., X. Fettweis, T. Mote, J. Wahr, P. Alexander, J. E. Box, and B. Wouters. 2013.
20 “Evidence and analysis of 2012 Greenland records from spaceborne observations, a regional
21 climate model and reanalysis data.” *The Cryosphere* 7: 615-630. doi: 10.5194/tc-7-615-2013

22 The PISM Authors. 2014. “PISM, a Parallel Ice Sheet Model. User’s Manual.” Accessed
23 June 15, 2015. <http://www.pism-docs.org/wiki/lib/exe/fetch.php?media=manual.pdf>.

24 Thomas, H. R., W. Abdalati, E. Frederick, W. B. Krabill, S. Manizade, and K. Steffen. 2003.
25 “Investigation of surface melting and dynamic thinning on Jakobshavn Isbræ.” *J. Glaciol.* 49
26 (165): 231–239. doi:10.3189/172756503781830764.

27 Thomas, R. H. 2004. “Force-perturbation analysis of recent thinning and acceleration of
28 Jakobshavn Isbrae, Greenland.” *J. Glaciol.* 50(168): 57–66. doi:
29 10.3189/172756504781830321.

- 1 [Tulaczyk, S., W. B. Kamb, and H. F. Engelhardt. 2000a. "Basal mechanics of Ice Stream B,](#)
- 2 [West Antarctica 1. Till mechanics". J. Geophys. Res. 105\(B1\):463–481. doi:](#)
- 3 [10.1029/1999JB900329.](#)
- 4 [Tulaczyk, S., W. B. Kamb, and H. F. Engelhardt. 2000b. "Basal mechanics of Ice Stream B,](#)
- 5 [West Antarctica 2. Undrained plastic bed model". J. Geophys. Res. 105\(B1\): 483–494. doi:](#)
- 6 [10.1029/1999JB900328.](#)
- 7 Van der Veen, C. J., J. C. Plummer, and L. A. Stearns. 2011. "Controls on the recent speed-up
- 8 of Jakobshavn Isbræ, West Greenland." J. Glaciol. 57 (204): 770–782.
- 9 Vieli, A., and F. M. Nick. 2011. "Understanding and Modeling Rapid Dynamic Changes of
- 10 Tidewater Outlet Glaciers: Issues and Implications." Surv. Geophys. 32: 437–458. doi:
- 11 10.1007/s10712-011-9132-4.
- 12 Weis M., R. Greve, and K. Hutter. 1999. "Theory of shallow ice shelves". Continuum
- 13 Mechanics and Thermodynamics 11(1): 15–50.
- 14 Winkelmann, R., M. A. Martin, M. Haseloff, T. Albrecht, E. Bueler, C. Khroulev, and A.
- 15 Levermann. 2011. "The Potsdam Parallel Ice Sheet Model (PISM-PIK) Part 1: Model
- 16 description." The Cryosphere 5: 715–726. doi:10.5194/tc-5-715-2011.

Editor #2

#Editor

"I have still one issue with the manuscript, regarding the link between high melt rate and potential increase in sliding. In the real world, this link might happen through enhanced runoff reaching the base, which is not a process included in your model. At two time, you suggest that it might happen because of warmer surface temperature that propagate in the ice and modify the viscosity. There is no way that such process acts at a seasonal scale (even at a decade scale). Changes in surface temperature to affect bottom temperature might take centuries. So this "potential" process by being evoked is confusing and deserve the credibility of the work. I would suggest to remove these explanations (page 13, lines 19-21 and page 17, lines 25-31)."

Authors: We agree. At page 17, lines 25-31 we imply that for such short hindcasts this effect does not have a significant impact on the flow. Both statements have been removed.

Modelled glacier dynamics over the last quarter of a century at Jakobshavn Isbræ

Ioana S. Muresan¹, Shfaqat A. Khan¹, Andy Aschwanden², Constantine Khroulev², Tonie Van Dam³, Jonathan Bamber⁴, Michiel R. van den Broeke⁵, Bert Wouters^{4,5}, Peter Kuipers Munneke⁵, and Kurt H. Kjær⁶

[1]{Department of Geodesy, DTU Space, Technical University of Denmark, Kgs. Lyngby, Denmark}

[2]{Geophysical Institute, University of Alaska Fairbanks, Fairbanks, Alaska, USA}

[3]{University of Luxembourg, Faculty of Science, Technology and Communication (FSTC), Research Unit of Engineering Sciences, Luxembourg}

[4]{University of Bristol, School of Geographical Sciences, Bristol, England}

[5]{Institute for Marine and Atmospheric research Utrecht (IMAU), Utrecht University, The Netherlands}

[6]{Centre for GeoGenetics, Natural History Museum of Denmark, University of Copenhagen, Copenhagen, Denmark}

Correspondence to: I. S. Muresan (iomur@space.dtu.dk)

Abstract

Observations over the past two decades show substantial ice loss associated with the speedup of marine terminating glaciers in Greenland. Here we use a regional 3-D outlet glacier model to simulate the behaviour of Jakobshavn Isbræ (JI) located in west Greenland. Our approach is to model and understand the recent behaviour of JI with a physical process-based model. Using atmospheric forcing and an ocean parametrization we tune our model to reproduce observed frontal changes of JI during 1990–2014. In our simulations, most of the JI retreat during 1990–2014 is driven by the ocean parametrization used, and the glacier's subsequent

response, which is largely governed by bed geometry. In general, the study shows significant progress in modelling the temporal variability of the flow at JI. Our results suggest that the overall variability in modelled horizontal velocities is a response to variations in terminus position. The model simulates two major accelerations that are consistent with observations of changes in glacier terminus. The first event occurred in 1998, and was triggered by a retreat of the front and moderate thinning of JI prior to 1998. The second event, which started in 2003 and peaked in the summer 2004, was triggered by the final breakup of the floating tongue. This breakup reduced the buttressing at the JI terminus that resulted in further thinning. As the terminus retreated over a reverse bed slope into deeper water, sustained high velocities over the last decade have been observed at JI. Our model provides evidence that the 1998 and 2003 flow accelerations are most likely initiated by the ocean parametrization used but JIs subsequent dynamic response was governed by its own bed geometry. We are unable to reproduce the observed 2010-2012 terminus retreat in our simulations. We attribute this limitation to either inaccuracies in basal topography or to misrepresentations of the climatic forcings that were applied. Nevertheless, the model is able to simulate the previously observed increase in mass loss through 2014.

1 Introduction

The rate of net ice mass loss from Greenland's marine terminating glaciers has more than doubled over the past two decades (Rignot et al., 2008; Moon et al., 2012, Shepherd et al., 2012, Enderlin et al., 2014). Jakobshavn Isbræ, located mid-way up on the west side of Greenland, is one of the largest outlet glaciers in terms of drainage area as it drains ~6 % of the Greenland Ice Sheet (GrIS) (Krabill et al., 2000). Due to its consistently high ice flow rate and seasonally varying flow speed and front position, the glacier has received much attention over the last two decades (Thomas et al., 2003; Luckman and Murray, 2005; Holland et al., 2008; Amundson et al., 2010; Khan et al., 2010; Motyka et al., 2011; Joughin et al., 2012; Gladish et al., 2015a; Gladish et al., 2015b; de Juan et al., 2010). Measurements from synthetic aperture radar suggest that the ice flow speed of JI doubled between 1992 and 2003 (Joughin et al., 2004). More recent measurements show a steady increase in the flow rate over the glacier's faster-moving region of ~ 5% per year (Joughin et al., 2008). The speedup coincides with thinning of up to 15 m a⁻¹ between 2003 and 2012 near the glacier front (Krabill et al., 2004; Nielsen et al., 2013) as observed from airborne laser altimeter surveys.

1 The steady increase in the flow rate and glacier thinning suggest a continuous dynamic
2 drawdown of mass, and they highlight JIs importance for the GrIS mass balance.

3 Over the past decade, we have seen significant improvements in the numerical modelling of
4 glaciers and ice sheets (e.g. Price et al., 2011; Vieli and Nick, 2011; Winkelmann et al., 2011;
5 Larour et al., 2012; Pattyn et al., 2012; Seroussi et al., 2012; Aschwanden et al., 2013; Nick et
6 al., 2013; Mengel and Levermann, 2014; Aschwanden et al., 2016) and several processes have
7 been identified as controlling the observed speedup of JI (Nick et al., 2009; Van der Veen et
8 al., 2011; Joughin et al., 2012). One process is a reduction in resistance (buttressing) at the
9 marine front through thinning and/or retreat of the glacier termini. But the details of the
10 processes triggering and controlling thinning and retreat remain elusive. Accurately modelling
11 complex interactions between thinning, retreat, and acceleration of flow speed as observed at
12 JI, is challenging. Our knowledge of the mechanisms triggering these events is usually
13 constrained to the period covered by observations. The initial speedup of JI occurred at a time
14 when the satellite and airborne observations were infrequent and therefore insufficient to
15 monitor the annual to seasonal evolution of glacier geometry and speed.

16 Here, we use a high-resolution, three-dimensional, time-dependent regional outlet glacier
17 model that has been developed as part of the Parallel Ice Sheet Model (PISM; see Sect. 2.1
18 Ice sheet model) (The PISM Authors, 2014) to investigate the dynamic evolution of JI
19 between 1990 and 2014. While previous 3-D modelling studies have mostly concentrated on
20 modelling individual processes using stress perturbations (e.g. Van der Veen et al., 2011,
21 Joughin et al. 2012), the present study aims to model the recent behaviour of JI with a
22 process-based model. Our modelling approach is based on a regional equilibrium simulation
23 and a time-integration over the period 1990 to 2014, in which the grounding lines and the
24 calving fronts are free to evolve under the applied ocean parametrization and monthly
25 atmospheric forcing.

26 **2 Methods and forcing**

27 **2.1 Ice sheet model**

28 The ice sheet model used in this study is the PISM (stable version 0.6). PISM is an open
29 source, parallel, three-dimensional, thermodynamically coupled, and time dependent ice sheet
30 model (Bueler and Brown, 2009; The PISM Authors, 2014). The model uses the superposition
31 of the non-sliding shallow ice approximation (SIA; Hutter, 1983) for simulating slowly

moving grounded ice in the interior part of the ice sheet and the shallow shelf approximation (SSA; Weis et al., 1999) for simulating fast-flowing outlet glaciers and ice shelf systems. We solve the SIA with a non-sliding base and use the SSA as a basal sliding velocity for the ice grounded regions (Winkelmann et al., 2011). This superposition of SIA and SSA (the “SIA+SSA” hybrid model) sustains a smooth transition between non-sliding, bedrock-frozen ice and sliding, fast-flowing ice and has been shown to reasonably simulate the flow of both grounded and floating ice (Winkelmann et al., 2011). To determine driving stresses for the SIA and SSA stress balances, PISM computes surface gradients according to Mahaffy (1976). For conservation of energy, we use an enthalpy scheme (Aschwanden et al., 2012) that accounts for changes in temperature in cold ice (i.e., ice below the pressure melting point) and for changes in water content in temperate ice (i.e., ice at the pressure melting point).

In PISM, the basal shear stress is related to the sliding velocity through a nearly-plastic power law (Schoof and Hindmarsh, 2010). The Mohr-Coulomb criterion (Cuffey and Paterson, 2010) is used to connect a saturated and pressurized subglacial till with a modelled distribution of yield stress. The yield stress depends on the effective pressure and on a spatially varying till friction angle derived heuristically as a piecewise-linear function of the bed elevation (Martin et al., 2011; Winkelmann et al., 2011; Aschwanden et al., 2013). The effective pressure on the till is determined by the ice overburden pressure and the effective thickness of water in the till (Tulaczyk et al., 2000a; Tulaczyk et al., 2000b). In this subglacial hydrology model the water is not conserved and it is only stored locally in the till up to a maximum thickness of 2 m. The ice flow therefore develops in PISM as a consequence of plastic till failure, i.e. where the basal shear stress exceeds the yield stress, and is influenced by the thermal regime and the volume of water at the ice sheet bed.

The underlying equations are further illustrated in the supplementary material (SI).

2.1.1 Input data

We use the bed topography from Bamber et al. (2013). This 1 km bed elevation dataset for all of Greenland was derived from a combination of multiple airborne ice thickness surveys and satellite-derived elevations during 1970–2012. The dataset has an increased resolution, along the ice sheet margin. In the region close to the outlet of JI, data from an 125 m CReSIS DEM (that includes all the data collected in the region by CReSIS between 1997 and 2007) have been used to improve the accuracy of the dataset. Errors in bed elevation range from 10 m to

300 m, depending on the distance from an observation and the variability of the local topography (Bamber et al., 2013). The terminus position and surface elevation in the Jakobshavn region are based on 1985 aerial photographs (Csatho et al., 2008). Ice thickness in the JI basin is computed as the difference between surface and bedrock elevation. The model of the geothermal flux is adopted from Shapiro and Ritzwoller (2004). We use monthly input fields of near-surface air temperature and surface mass balance (SMB) from the regional climate model RACMO2.3 (Noël et al., 2015; Figs. S2 and S3), which here represent the only seasonal input used in the model. The version used in this study is produced at a spatial resolution of ~ 11 km and covers the period from 1958 to 2014. Additional grid refinements are performed using bilinear interpolation for climatic datasets and a second order conservative remapping scheme (Jones, 1999) for bed topography data.

2.1.2 Initialization procedure, boundary conditions, calving and grounding line parametrization

In our model, the three-dimensional ice enthalpy field, basal melt for grounded ice, modelled amount of till-pore water, and lithospheric temperature are obtained from an ice-sheet-wide paleo-climatic spin-up. The paleo-climatic spin-up follows the initialization procedure described by Bindschadler et al. (2013) and Aschwanden et al. (2013). We start the spin-up on a 10 km grid, and then we further refine to 5 km at -5ka. It is important to note that during the paleo-climatic initialization the terminus is held fixed to the observed 1990 position in the JI region and to the position from Bamber et al. (2013) elsewhere.

In the regional outlet glacier model of PISM, the boundary conditions are handled in a 10 km strip positioned outside of the JI's drainage basin and around the edge of the computational domain (Fig. 1B). In this strip, the input values of the basal melt, the amount of till-pore water, ice enthalpy, and lithospheric temperature (Aschwanden et al., 2013) are held fixed and applied as Dirichlet boundary conditions in the conservation of energy model (The PISM Authors, 2014). The boundary conditions for the enthalpy at the ice-bedrock interface follow Aschwanden et al (2012). We start our regional JI runs with an equilibrium simulation on a horizontal grid with 5 km spacing. The enthalpy formulation models the mass and energy balance for the three-dimensional ice fluid field based on 200 regularly spaced ice layers within a domain extending 4000 m above the bed elevation. The temperature of the bedrock thermal layer is computed up to a depth of 1000 m with 50 regularly spaced layers. The first step is to obtain a 5 km regional equilibrium model for JI using constant mean climate (i.e.

repeating the 1960-1990 mean air temperature and SMB; see Sect. 2.1.1). We consider that equilibrium has been established when the ice volume in the regional domain changes by less than 1% in the final 100 model years. Grid refinements are made from 5 km (125×86) to 2 km (310×213) after 3000 years. The 2 km simulation reaches equilibrium after 200 years with an ice volume of $0.25 \cdot 10^6 \text{ km}^3$ (or a 3.6% increase relative to the input dataset from Bamber et al. (2013)). Further, using our equilibrium simulations with a 2 km horizontal grid and 400 regularly spaced ice layers within a domain extending 4000 m above the bed elevation, we simulate forward in time (hindcast) from 1990 to 2014 by imposing monthly fields of SMB and 2 m air temperatures through a one-way forcing scheme. For simulations performed on a 1 km horizontal grid, the exact same procedure is used with the additional constraint that in the regional equilibrium run a further grid refinement from 2 km to 1 km is made after 200 years. The length of the 1 km regional equilibrium simulation is 100 years.

In our regional model, all boundaries (calving fronts, grounding lines, upper, and lower surfaces) are free to evolve in time both during the regional equilibrium and the forward simulations. Along the ice shelf calving front, we superimpose a physically based calving (eigen calving) parametrization (Winkelmann et al., 2011; Levermann et al., 2012) and a basic calving mechanism (Albrecht et al., 2011) that removes any floating ice at the calving front thinner than a given threshold at a maximum rate of one grid cell per time step. The average calving rate (c) is calculated as the product of the principal components of the horizontal strain rates ($\dot{\epsilon}_{\pm}$), derived from the SSA velocities, and a proportionality constant parameter (k) that captures the material properties relevant for calving:

$$c = k \dot{\epsilon}_{+} \dot{\epsilon}_{-} \quad \text{for } \dot{\epsilon}_{\pm} > 0. \quad (1)$$

The strain rate pattern is strongly influenced by the geometry and the boundary conditions at the ice shelf front (Levermann et al. (2012)). The proportionality constant, k , is chosen such that the ice front variability is small (Leverman et. al., 2012). This physically based calving law appears to yield realistic calving front positions for various types of ice shelves having been successfully used for modelling calving front positions in entire Antarctica simulations (Martin et al., 2011) and regional east Antarctica simulations (Mengel and Levermann, 2014). In contrast to Antarctica, known for its large shelves and shallow fjords, the GrIS is characterized by narrow and deep fjords, and JI is no exception. The strain rate pattern in the eigen calving parametrization performs well only if fractures in glacier ice can grow, and calving occurs only if these rifts intersect (i.e. possible only for relatively thin and unconfined

ice shelves). In the case of JI, whose terminus is confined in a narrow fjord, the strain rate pattern that defines the eigen calving parametrization is not the governing process and therefore the need for the second calving parametrization. In our model, the eigen calving law has priority over the basic calving mechanism. That is to say that the second calving law used (the basic calving mechanism) removes any ice at the calving front not calved by the eigen calving parametrization thinner than 500 m in the equilibrium simulations and 375 m in the forward runs. Therefore, the creation of the conditions under which calving can occur (e.g. a floating ice shelf) with the subsequent calving mechanism, relies solely on the parametrization for ice shelf melting (Sect. 2.1.3).

A partially-filled grid cell formulation (Albrecht et al., 2011), which allows for sub-grid scale retreat and advance of the ice shelf front, is used to connect the calving rate computed by the calving parametrizations with the mass transport scheme at the ice shelf terminus. This sub-grid scale retreat and advance of the shelf allows for realistic spreading rates that are important for the eigen calving parametrization. The sub-grid interpolation is performed only when a floating terminus exists. In both situations (i.e., floating ice or grounded terminus), the stress boundary conditions are applied at the calving front and in the discretization of the SSA equations (Winkelmann et al., 2011). The retreat and advance of the front through calving is restricted to at most one grid cell length per adaptive time step.

The parameterization of the grounding line position is based on a linear interpolation scheme (the “LI” parameterization; Gladstone et al., 2010) extended to two horizontal dimensions (x, y) and is not subject to any boundary conditions. This sub-grid treatment of the grounding line interpolates the basal shear stress in x, y based on the spatial gradient between cells below and above the grounding line and allows for a smooth transition of the basal friction from grounded to floating ice (Feldmann et al., 2014). At each time step the grounding line position is determined by a mask that distinguishes between grounded and floating ice using a flotation criterion based on the modelled ice thickness (Winkelmann et al., 2011):

$$b(x, y) = -\frac{\rho_i}{\rho_o} H(x, y) \quad (2)$$

where b represents the bedrock elevation, ρ_i is the density of the ice, ρ_o is the density of the ocean water and H represents the ice thickness. Therefore, the grounding line migration is influenced by the ice thickness evolution, which further depends on the velocities computed from the stress balance. The superposition of SIA and SSA, which implies that the SSA

1 velocities are computed simultaneously for the shelf and for the sheet, ensures that the stress
2 transmission across the grounding line is continuous and that buttressing effects are included.
3 In the three-dimensional Marine Ice Sheet Model Intercomparison Project (Mismip3d), PISM
4 was used to model reversible grounding line dynamics and produced results consistent with
5 full-Stokes models (Pattyn et al. (2013); Feldmann et al., 2014; see parameters therein). We
6 have not performed the Mismip3d experiments for our particular parameter settings and,
7 therefore, the accuracy of the modelled grounding line migration is solely based on the results
8 presented in Feldmann et al. (2014).

9 **2.1.3 Parameterization for ice shelf melting**

10 We use a simple parametrization for ice shelf melting where the melting effect of the ocean is
11 based on both sub-shelf ocean temperature and salinity (Martin et al., 2011). To accommodate
12 this parametrization, several changes have been made to PISM at the sub-shelf boundary
13 (Winkelmann et al., 2011). First, the ice temperature at the base of the shelf (the pressure-
14 melting temperature) necessary for the enthalpy solver (Aschwandten et al., 2012) is
15 calculated from the Clausius-Clapeyron gradient and the elevation at the base of the shelf.
16 The ice temperature is then applied as a Dirichlet boundary condition in the conservation of
17 energy equation.

18 Secondly, basal melting and refreezing is incorporated through a sub-shelf mass flux used as a
19 sink/source term in the mass-continuity equation. This mass flux from shelf to ocean
20 (Beckmann and Goosse, 2003) is computed as a heat flux between the ocean and ice and
21 represents the melting effect of the ocean due to both temperature and salinity (Martin et al.,
22 2011).

23 In our simulations we use a constant ocean water temperature (T_o) of -1.7 °C, which here
24 represents the mean surface ocean temperature in the grid cells adjacent to the JI terminus. In
25 the heat flux parametrization, the ocean temperature at the ice shelf base is computed as the
26 difference between the input ocean temperature and a virtual temperature that represents the
27 freezing point temperature of ocean water below the ice shelf (Fig. S4). The freezing point
28 temperature is calculated based on the elevation at the base of the shelf and the ocean water
29 salinity. As a consequence of these constraints, as the glacier retreats and/or advances, both
30 the pressure-melting temperature and the heat flux between the ocean and ice evolve
31 alongside the modelled glacier ice shelf geometry. The ocean water salinity ($S_o = 35$ psu) is

kept constant in time and space as the model does not capture the salinity gradient from the base of the ice shelf through layers of low and high salinity. A previous study conducted by Mengel and Levermann (2014) using the same model established that the sensitivity of the melt rate to salinity is negligible.

Following for this melting parametrization, the highest melt rates are modelled in the proximity of the glacier grounding lines and decrease with elevation such that the lowest melt rates are closer to the central to frontal area of the modelled ice shelf. At the grounding line, PISM computes an extra flotation mask that accounts for the fraction of the cell that is grounded, by assigning 0 to cells with fully grounded ice, 1 for cells with ice-free or fully floating ice, and values between 0 and 1 for partially grounded grid cells. The basal melt rate in the cells containing the grounding line is then adjusted based on this flotation mask as following (The PISM Authors, 2014):

$$M_{b,adjusted} = \lambda M_{b,grounded} + (1 - \lambda)M_{b,shelf-base} \quad (3)$$

where M_b refers to the basal melt rate and λ is the value of the flotation mask. At the vertical ice front, we do not apply any melt.

3 Results and discussion

This section is organized in two main subsections. Sect. 3.1 introduces the results obtained relative to observations, and Sect 3.2 focuses mainly on the limitations of the model that need to be considered before a final conclusion can be drawn. A short introduction to the different simulations and preparatory experiments performed is given below.

A total number of fifty simulations with different sets of parameters (excluding preparatory and additional experiments on the 1 km grid) are performed on a 2 km grid. We alter six parameters that control the ice dynamics (e.g. the flow enhancement factor, the exponent of the pseudo-plastic basal resistance model, the till effective fraction overburden, etc.) , the ice shelf melt, the ocean temperature, and the calving (i.e. the ice thickness threshold in the basic calving mechanism). These parameters are modified only during the regional JI runs such that the model reproduces the frontal positions and the ice mass change observations at JI during the period 1990-2014 (Fig. 2) and 1997-2014 (Figs. 3 and 4), respectively. From these results, we present the parameterization that best captures (i.e., we estimate the residual between modelled and observed ice mass change and select the smallest residual signal) the full observed evolution of JI during the period 1990–2014 (Figs. 2, 3, 4 and 5). The values of the

ice sheet model parameters used and the ice sheet model sensitivity to parameters controlling ice dynamics, basal processes, ice shelf melt, and ocean temperature, are further illustrated in the SI.

3.1 Observations vs. modelling results

3.1.1. Annual scale variations in velocities, terminus and grounding line positions

We investigate the processes driving the dynamic evolution of JI and its variation in velocity between 1990 and 2014 with a focus on the initial speedup of JI (1990) and the 2003 breakup of the ice tongue. The overall results from our simulations suggest a gradual increase in velocities that agree well with observations (Joughin et al., 2014) (Fig. 3). Three distinct stages of acceleration are identified in Fig. 3 (see also Movie 1 in the SI) and discussed in detail below.

- **1990–1997**

The first speedup produced by the simulation is caused by a retreat of the front position by approximately 2 to 4 km between 1990 and 1991. There is no observational evidence to confirm that this retreat actually occurred. The simulated retreat is probably a modelling artefact as the geometry obtained during the regional equilibrium simulation is forced with monthly atmospheric forcing and new oceanic conditions. This simulated acceleration (Fig. 3) is caused in our model by a reduction in buttressing due to a reduction in lateral resistance (Van der Veen et al., 2011), which is generated by the gradual retreat of the front and which triggers a dynamic response in the upstream region of JI.

Starting in 1992, the modelled and observed terminus positions agree (not shown in Fig. 2). Apart from the acceleration in 1991–1992, no significant seasonal fluctuations in flow rate are found in our simulations for this period, a result that is consistent with observations (Echelmeyer et al., 1994). From 1993 a stronger sub-annual velocity signal begins to emerge in our simulation that continues and intensifies in magnitude during 1994 and 1995. Modelled mean-annual velocities for 1992 and 1995 are consistent with observed velocities for the same period (Joughin et al., 2008; Vieli et al., 2011). In 1996 and 1997, the frontal extent and the grounding line position remain relatively stable (Figs. 2, 6 and 7), and no

significant seasonal fluctuation in ice flow rate is observed in the simulation. These model results agree well with observations, which indicate that the glacier speed was relatively constant during this period (Luckman and Murray, 2005).

- **1998–2002**

According to observations (Joughin et al., 2004; Luckman and Murray, 2005; Motyka et al., 2011; Bevan et al., 2012), the initial acceleration of JI occurred in May-August 1998, which coincides with our modelled results. In our simulation, the 1998 acceleration is generated by a retreat of the ice tongue's terminus in 1997-1998, which may be responsible for reducing buttressing (Fig. 7 and Movie 1 in the SI). Thinning, both near the terminus and inland (up to 10 km away from the 1990 front position), starts in our model in the summer of 1995 and continues to accelerate after 1998 (Figs. 3, 6 and 7). The modelled behaviour agrees well with the observed behaviour (Krabill et al., 2004). Although thinning appears to have increased in our model during three continuous years, it produced only minor additional speedup during the period prior to 1998 (Figs. 2, 6, and 7). In our simulation, JI's speed increased in the summer of 1998 by ~ 80% relative to the summer of 1992 (Fig. 3), at which time the grounding line position starts to retreat thereafter (Figs. 2, 6, and 7). Observations (Luckman and Murray, 2005) do not show this level of speedup, and there are no observations of the grounding line position at this time with which to assess our model performance. Overall, modelling results suggest an advance of the terminus between 1999 and 2000 and a retreat of the southern tributary between 2000 and 2002 by ~4 km, which correlates with existing observations (Thomas, 2004). In our simulation, this retreat of the terminus triggers a decrease of resistive stresses at the terminus (Figs. 7 and S8). Concurrent with the 1998-2002 terminus retreat, the grounding line retreats in our model by ~6 km (Figs. 2, 6 and 7).

- **2003–2014**

In the late summer of 2003, the simulated flow velocity increases (Fig. 3). This acceleration of JI is driven in our simulations by the final breakup of the ice tongue (see Figs. 2 and 6). The period 2002-2003 is characterized in our model by

substantial retreat of the front ($\sim 4\text{--}6$ km) and the grounding line (~ 4 km), which starts in June 2002 and continues throughout 2003. The simulated retreat that occurred in 2003 and the loss of large parts of the floating tongue (Figs. 2 and 6) caused a major decrease in resistive stresses near the terminus (Figs. 7 and S8). By 2004, the glacier had thinned significantly (Figs. 3 and 6) both near the front and further inland in response to a change in the near-terminus stress field (Fig. 7). During the final breakup of the ice tongue, the simulation produces speeds high as 20 km a^{-1} ($\sim 120\%$ increase relative to 1998). The modelled velocities decreased to 16 km a^{-1} ($\sim 80\%$ increase relative to 1998) in the subsequent months and remained substantially higher than the sparse observations from that time (e.g. Joughin et al., 2012). The high velocities modelled at JI after the loss of its floating tongue are further sustained in our simulation by the thinning that occurred after 2003 (Fig. 3), which continues to steepen the slopes near the terminus (Fig. 6), and is accompanied by a seasonal driven (sub-annual scale) retreat and advance of the front. This simulated thinning is combined in the following years with a reduction in surface mass balance due to increased melting and runoff (van den Broeke et al., 2009; Enderlin et al., 2014, Khan et al., 2014). The period 2004–2014 is characterized in our simulation by relatively uniform velocity peaks with strong sub-annual variations (Fig. 3). During this period, only a small floating ice tongue is modelled and the terminus remained relatively stable, with no episodes of significant retreat.

In agreement with previous studies (e.g. Joughin et al. 2012), our results suggest that the overall variability in the modelled horizontal velocities is a response to variations in terminus position (Fig. 7). In our simulation, the retreat of the front reduced the buttressing at the terminus and generated a dynamic response in the upstream region of JI which finally led to flow acceleration. In contrast, when the front advanced the modelled flow slowed as the resistive stresses at the terminus were reinforced. This buttressing effect tends to govern JI's behaviour in our model. Regarding the overall terminus retreat, our simulations suggest that it is mostly driven by the sub-shelf melting parametrization applied (Figs. S5 and S14). Although the heat flux supplied to the shelf evolves in time based on the modelled terminus geometry, the input ocean temperature is kept constant throughout the simulations. This constant ocean forcing at the terminus leads, in our simulation, to gradual thinning of JI and favours its retreat without any shift (e.g. increase) in ocean temperature. In terms of seasonality, the only seasonal input into the model is introduced by the monthly atmospheric

forcing that is applied (Sect. 2.1.1). In our model, the atmospheric forcing that is applied (Figs. S2 and S3) can influence JI's dynamics through changes in surface mass balance (SMB) (i.e., accumulation and ablation), which affects both the SIA and the SSA (Sect. 2.1), ~~but also through changes in air temperature that can potentially influence sliding via the rate factor for the softness (SI, Eq. 1), which here is derived through an enthalpy formulation (Sect. 2.1).~~ However, the modelled sub-annual variability in terms of terminus retreat and velocities does not always follow the seasonal signal (Fig. 3). We investigate this higher than seasonal variability in Sect. 3.2.

3.1.2 Ice mass change

Figure 4 shows observed and modelled mass change for the period 1997 to 2014. We estimate the observed rate of ice volume changes from airborne and satellite altimetry over the same period and convert these to rates of mass change (SI, Sect. 2). Overall we find good agreement between modelled and observed mass change (Fig. 4), and our results are in agreement with other similar studies (Howat et al., 2011; Nick et al., 2013). Dynamically driven discharge is known to control Jakobshavn's mass loss between 2000 and 2010 (Nick et al., 2013). The modelled cumulative mass loss is 269 Gt, of which 93% (~251 Gt) is dynamic in origin while the remaining 7% (~18 Gt) is attributed to a decrease in SMB (Fig. 4). Further, the present-day unloading of ice causes the Earth to respond elastically. Thus, we can use modelled mass changes to predict elastic uplift. We compare modelled changes of the Earth's elastic response to changes in ice mass to uplift observed at four GPS sites (Fig. 5). Both model predictions and observations consistently suggest large uplift rates near the JI front (20 mm a⁻¹ for station KAGA) and somewhat minor uplift rates (~ 5 mm a⁻¹) at distances of >100 km from the ice margin.

Although the terminus has ceased to retreat in our simulations after 2009 (Figs. 6 and 7), the modelled mass loss, and more importantly the dynamic mass loss, continues to accelerate (Fig. 4). Our results show (Fig. 7) that during this period the mass change is mostly driven by the sub-annual terminus retreat and advance, which continues to generate dynamic changes at JI through seasonal (sub-annual scale) reductions in resistive stresses.

3.2 Feedback mechanisms, forcings and limitations

Representing the processes that act at the marine boundary (i.e. calving and ocean melt) are important for understanding and modelling the retreat/advance of marine terminating glaciers

like JI. Determining terminus positions by using the superposition of a physically based calving (eigencalving) parametrization (Winkelmann et al., 2011; Levermann et al., 2012) and a basic calving mechanism (Albrecht et al., 2011) is motivated by the model's ability to maintain realistic calving front positions (Levermann et al., 2012). The eigen calving parametrization cannot resolve individual calving events, and, thus, the introduction of the basic calving mechanism was necessary in order to accurately match observed front positions. Preparatory experiments have shown that calving is mostly driven in our model by the basic calving mechanism used ($\sim 96\%$ of the overall mass loss), and that the eigen calving parametrization is more important in modelling sub-annual to seasonal fluctuations of the terminus. Our simulations suggest that the superposition of these two calving mechanisms performs well for relatively narrow and deep fjords as those characterized by JI (Fig. 2). The benefit of using such a combination of calving laws is that it can evolve the terminus position with time and thus calving feedbacks are not ignored. As the terminus retreats, the feedback between calving and retreat generates dynamic changes due to a reduction in lateral shear and resistive stresses (Fig. 7). In a simulation in which the terminus position is kept fixed to the 1990s position, the velocity peaks are uniform (i.e. no acceleration is modelled except for some small seasonal related fluctuations generated by the atmospheric forcing applied), and the mass loss remains relatively small (~ 70 Gt). Consistent with Vieli et al. (2011), we find that the feedback between calving and retreat is highly important in modelling JI's dynamics.

As introduced in Sect. 2, our approach here is to adjust the terminus in the JI region to simulate the 1990s observed front position and surface elevation based on 1985 aerial photographs (Csatho et al., 2008). The glacier terminus in 1990s was floating (Csatho et al., 2008; Motyka et al. 2011). Motyka et al. (2011) calculated the 1985 hydrostatic equilibrium thickness of the south branch floating tongue from smoothed surface DEMs and obtained a height of 600 m near the calving front and 940 m near the grounding zone. In this paper, however, we compute the thickness as the difference between the surface elevation and the bed topography, and allow the glacier to evolve its own terminus geometry during the equilibrium simulation. Preparatory experiments have shown that in our model (disregarding its initial geometry floating/ grounded terminus) JI attains equilibrium with a grounding line position that stabilizes close to the 1990s observed terminus position. According to observations, JI is characterized in 1990 by a large floating tongue (> 10 km; e.g. Motyka et al., 2011) that we are not able to simulate during the equilibrium runs. In our model (Figs. 6 and 7), the glacier starts to develop a large floating tongue (~ 10 km) in 1999. Starting in

2000, the floating tongue is comparable in length and thickness with observations and the model is able to simulate, with a high degree of accuracy, its breakup that occurred in late summer 2003 and the subsequent glacier acceleration. Observations of terminus positions (Sohn et al., 1998; Csatho et al., 2008) suggest that over more than 40 years, between 1946 and 1992, JIs terminus stabilized in the proximity of the 1990's observed terminus position. Furthermore, during 1959 and 1985 the southern tributary was in balance (Csatho et al., 2008). This suggests that, during the regional equilibrium and at the beginning of the forward simulations, we are forcing our model with climatic conditions that favoured the glacier to remain in balance. This may explain our unsuccessful attempts to simulate prior to 1998 a floating tongue comparable in length and thickness with observations, and suggests that for simulating the large floating tongue that characterized JI during this period, future studies should consider to start modelling JI before the glacier begins to float in the late 1940s (Csatho et al., 2008).

The geometry of the terminus plays an important role in parameterizing ice shelf melting, and therefore our pre-1999 geometry will influence the magnitude of the basal melt rates (Sect. 2.1.3). The difference in geometry results in modelled mean basal melt rates that are larger for the period 1999-2003 (Table S3), when JI begins to develop a large floating tongue and when the calving front was already largely floating. The modelled mean melt rates for the period 1999-2003 are large and likely overestimated. Relative to other studies, e.g. Motyka et al. (2011), our yearly mean melt rate for 1998 is ~2 times larger (Table S3). While we choose here to compare the two melt rates in order to offer a scale perspective, we acknowledge the difference in geometry between the two studies.

Starting in 2010, the retreat of the terminus modelled in our simulations did not correlate well with observations (Fig. 2). The observed terminus and the grounding line retreats do not cease after 2010. Further, observed front positions (Joughin et al., 2014) suggest that by the summer 2010 JI was already retreating over the sill and on the over deepening indicated by the red star in Fig. 6. The observed retreat is not reproduced in our simulations suggesting that additional feedbacks and/or forcings most likely affect the glacier. Alternatively, the mismatch between observations and simulation results may represent an incomplete modelling of the physics, inaccuracies in atmospheric/oceanic conditions, or other various limitations (e.g., bed topography model constraints and grid resolution issues). The particular influence of these potential issues on our model is detailed below.

1 The basal topography of JIs channels represents a large source of uncertainty. JI is a marine
2 terminating glacier whose bedrock topography is characterized by a long and narrow channel
3 with deep troughs that contribute to its retreat and acceleration, e.g. once the grounding line
4 starts to retreat on a down-sloping bed, the flow increases, leading to further retreat and
5 acceleration (Vieli et al., 2011). The timing and the magnitude of these retreats depend on bed
6 topography and the glacier width changes (Jamieson et al., 2012; Enderlin et al., 2013).
7 Accurate modelling of the grounding line behaviour is, therefore, crucial for JIs dynamics as
8 its retreat removes areas of flow resistance at the base and may trigger unstable retreat if the
9 glacier is retreating into deeper waters. In our simulation, the grounding line position
10 stabilizes downstream of the sill after 2005 (Figs. 2 and 6), which is in accordance with
11 previous modelling studies (Vieli et al., 2001; Vieli et al., 2011). Vieli et al. (2011) found
12 that, by artificially lowering the same bed sill by 100 m, the grounding line eventually retreats
13 and triggers a catastrophic retreat of 80 km in just over 20 years. In an equivalent experiment
14 with Vieli et al. (2011) but performed with our model, lowering the bed sill by 100 m, did not
15 result in a retreat of the grounding line over the sill. Regarding the grid resolution, simulations
16 performed on a 1 km grid did not improve our simulations of ice thickness (Fig. S10) or
17 surface speed (i.e. trend, overall magnitude, and shape of the flow; Fig. S11).

18 From a climatic perspective, the summer of 2012 was characterized by exceptional surface
19 melt covering 98% of the entire ice sheet surface and including the high elevation Summit
20 region (Nghiem et al., 2012; Hanna et al., 2014). Overall, the 2012 melt-season was two
21 months longer than the 1979–2011 mean and the longest recorded in the satellite era (Tedesco
22 et al., 2013). Furthermore, the summer of 2012 was preceded by a series of warm summers
23 (2007, 2008, 2010 and 2011) (Hanna et al., 2014). Surface melt above average was already
24 recorded in May-June 2012 (see Fig. 3 from NSIDC (2015)) when most of the 2011-2012
25 winter accumulation melted and over 30% of the ice sheet surface experienced surface melt.
26 An intense and long melt year leads to extensive thinning of the ice and has the potential to
27 enhance hydrofracturing of the calving front due to melt water draining into surface crevasses
28 (MacAyeal et al., 2003; Joughin et al., 2013; Pollard et al., 2015) resulting in greater and/or
29 faster seasonal retreat and an increase in submarine melt at the terminus and the sub-shelf
30 cavity (Schoof, 2007; Stanley et al., 2011; Kimura et al., 2014; Slater et al., 2015).

31 The seasonal retreat of JIs terminus started relatively early in 2012, with a large calving event
32 having already occurred in June. While it seems difficult to attribute this particular calving

1 event solely to processes related to the 2012 melt season, it does seem probable that the series
2 of warm summers (2007-2011) together with the 2012 exceptional melt season could have
3 enhanced hydrofracturing of the calving front. In turn, this could have induced a retreat of the
4 terminus that cannot be captured by our model (i.e., in its present configuration the model
5 cannot account directly for the influence of meltwater runoff and its role in the subglacial
6 system during surface melt events). ~~Nonetheless, a high melt year is generally the~~
7 ~~consequence of high summer air temperatures that in our model represent boundary~~
8 ~~conditions for the enthalpy equation (Aschwanden et al., 2012). Therefore, an increase in air~~
9 ~~temperatures could potentially soften the ice and enhance sliding. However, the time required~~
10 ~~for advection/diffusion to propagate down through the column and reach the high shearing~~
11 ~~layer at the base of the ice (Aschwanden et al., 2012) is generally much longer than our~~
12 ~~hindcasts and thus, we believe that in our simulations, this effect does not have a significant~~
13 ~~impact on the flow.~~ On the other hand, changes in ice thickness affect both the SIA and the
14 SSA (Sect. 2.1). While the effect on the SIA is very weak as the driving stresses are not
15 affected by a few meters of difference in thickness induced by SMB variability, in the SSA,
16 the coupling is achieved via the effective pressure term in the definition of the yield stress
17 (see SI, Sect. 1.2 for detailed equations). The effective pressure is determined by the ice
18 overburden pressure (i.e., ice thickness) and the effective thickness of water in the till, where
19 the latter is computed by time-integrating the basal melt rate. Compared with SIA, this effect
20 is stronger and may explain why in our model some seasonal velocity peaks could potentially
21 be influenced by the atmospheric forcing applied (Figs. S9 and S14).

22 We study the sensitivity of the model to atmospheric forcing by performing a simulation
23 where we keep the atmospheric forcing constant (mean 1960-1990 temperature and SMB). By
24 comparing this simulation with a simulation that includes full atmospheric variability
25 (monthly temperature and SMB) we find that to only a relatively small degree some of the
26 variability appears to be influenced by the atmospheric forcing applied (Figs. S2 and S14),
27 which also represents the only seasonal input into the model. Some of the greater than
28 seasonal frequency could be an issue with resolution in the model. We examined this
29 sensitivity by performing additional runs at a higher spatial resolution. Simulations on a 1 km
30 grid did show some improvement with respect to surface speed sub-annual variability (Fig.
31 S12), suggesting that in our model the stress redistribution might be sensitive to the resolution
32 of the calving event. However, given the short period spanned by the simulations, the stress
33 redistribution does not change the overall modelled results, as seen in Figs. S10 and S11.

1 Although we acknowledge that some of the variability is due to the grid resolution, part of it
2 may also be related to unmodeled physical processes acting at the terminus. We suggest that
3 additional contributions to the seasonality, e.g. from ice mélange or seasonal ocean
4 temperature variability, which are not included in our model could potentially influence the
5 advance and retreat of the front at seasonal scales (Fig. S14). For example, the ice mélange
6 can prevent the ice at the calving front from breaking off and could therefore reduce the
7 calving rates. Consequently, the introduction of an ice mélange parametrization will probably
8 help to minimize some of the sub-annual signal modelled in our simulations. Similarly,
9 seasonal ocean temperature variability can influence ice mélange formation and/or clearance
10 and the melt rates at the glacier front and can accentuate seasonal glacier terminus and
11 grounding line retreat and/or advance. However, at this point we find it difficult to determine
12 the relative importance of each process.

13 Finally, regarding the ocean conditions, warm water temperatures in the fjord were recorded
14 in 2012. Besides a cold anomaly in 2010, which was sustained until early 2011, the period
15 2008-2013 is characterized by high fjord waters temperatures - equal to or warmer than those
16 recorded in 1998-1999 (Gladish et al., 2015). In our model, the ice melt rates are determined
17 from the given conditions in temperature (-1.7°C , and salinity (35 psu) of the fjord waters),
18 and the given geometry (Sect. 2.1.3). The fact that we are able to model JIs retreat with a
19 constant ocean temperature suggests that the retreat and acceleration observed at JI are not
20 likely to be controlled by the year to year variability in ocean temperatures. This conclusion
21 agrees with the observational study of Gladish et al. (2015) who analysed ocean temperature
22 variability in the Ilulissat fjord with JI variability and who found that after 1999 there was no
23 clear correlation. Our results do not, however, imply that the ocean influence in JI's retreat is
24 negligible (Fig. S5), but rather that the glacier most likely responds to changes in ocean
25 temperature that are sustained for longer time periods, e.g. decadal time scales. Two
26 additional experiments, where the input ocean temperature (T_o) was increased to -1°C
27 indicate that higher melt rates beneath the grounding line could potentially explain the retreat
28 observed after 2010. In our first experiment, the input T_o was increased from -1.7°C to -1°C
29 starting 1997 ($\sim 0.7^{\circ}\text{C}$ relative to 1990). This temperature increase is consistent with observed
30 ocean temperatures at the mouth of the Ilulissat fjord (Gladish et al., 2015) and generated in
31 our simulation, for the period 1997-2014, an accelerated retreat of the front that does not
32 correlate with observations (Fig. S7). Similarly, mass loss estimates from the simulations are
33 significantly larger (by $\sim 50\%$; Fig. S6) than those calculated from airborne and satellite

altimetry observations (Sect. 3.1.2). Overall, the experiment shows that an increase in ocean temperature that starts in 1997 and is sustained until 2014 generates modelled estimates for the period 1998-2014 that do not agree with observations. In the second experiment, T_o was increased to $-1\text{ }^{\circ}\text{C}$ starting in 2010 ($\sim +0.7^{\circ}\text{C}$ at the base of the shelf in 2010). For the period 2010-2014, our model predicted a faster retreat of the front that correlates well with observations (Fig. S7), and an increase of mass loss by $\sim 7\text{ Gt}$ (Fig. S6). This experiment shows that an increase in ocean temperature beginning in 2010 could potentially explain the retreat observed thereafter.

4 Conclusions

In this study, a three-dimensional, time-dependent regional outlet glacier model is used to investigate the processes driving the dynamic evolution of JI and its seasonal variation in ice velocity between 1990 and 2014. Here, we attempted to simulate the recent behaviour of JI with a process-based model. The model parameters were calibrated such that the model reproduced observed front positions (Fig. 2) and ice mass change observations (Fig. 4) at JI over the periods 1990-2014 and 1997-2014, respectively. We obtain a good agreement of our model output with time series of measured horizontal velocities, observed thickness changes, and GPS derived elastic uplift of the crust (Figs. 3 and 5). Overall, the study shows progress in modelling the temporal variability of the flow at JI.

Our results suggest that most of the JI retreat during 1990-2014 is driven by the ocean parametrization, and the glacier's subsequent response, which is largely governed by its own bed geometry (Figs. 6, 7 and S5). In agreement with previous studies (e.g. Joughin et al. 2012), our simulations suggest that the overall variability in the modelled horizontal velocities is a response to variations in terminus position (Fig. 7). In our model, the seasonal variability is likely driven by processes related to the atmospheric forcing applied (e.g. temperature and SMB variability), which in fact represents the only seasonal input used in the model. The greater than seasonal frequency seen in our simulations is attributed to grid resolution and missing seasonal scale processes (e.g., ice mélange variability or seasonal ocean temperature variability) in the model. Sensitivity experiments performed on a 1 km grid did not show significant improvement with respect to ice thickness (Fig. S10) or surface speed (i.e. shape of the flow and overall magnitude; Fig. S11).

In 1990, JI had a large floating tongue ($> 10\text{ km}$; e.g. Motyka et al., 2011) that we are not able to simulate during the equilibrium runs. In our model (Fig. 6), the glacier starts to develop a

1 floating tongue comparable with observations in 1999. Starting in 2000, the floating tongue is
2 consistent in length and thickness with observations and the model is able to simulate its
3 breakup (that occurred in late summer 2003) and the subsequent glacier acceleration. The
4 difference between observed and modelled pre-1999 geometry results in relatively large basal
5 melt rates for the period 1997-2003 (Fig. S9). Nevertheless, the model is able to capture the
6 overall retreat of the terminus and the trends in the observed velocities (Figs. 2 and 3) for the
7 period 1990-2010. Finally, the 2010-2012 observed terminus retreat (Joughin et al., 2014) is
8 not reproduced in our simulations, likely due to inaccuracies in basal topography, or
9 misrepresentations of the atmospheric forcing and the ocean parametrization that we used.
10 Additional sensitivity experiments showed that an increase in ocean temperature of ~ 0.7 °C
11 for the period 2010-2014 may trigger a retreat of the terminus that agrees better with
12 observations (Figs. S6 and S7).

13 Our model reproduces two distinct flow accelerations in 1998 and 2003 that are consistent
14 with observations. The first was generated by a retreat of the terminus and moderate thinning
15 prior to 1998; the latter was triggered by the final breakup of the floating tongue. During this
16 period, JI attained in our simulation unprecedented velocities as high as 20 km a^{-1} .
17 Additionally, the final breakup of the floating tongue generated a reduction in buttressing that
18 resulted in further thinning. Similar to previous studies (Nick et al., 2009; Vieli et al., 2011;
19 Joughin et al. 2012), our results show that the dynamic changes observed at JI are triggered at
20 the terminus (Figs. 7, S5, S14 and S16).

21 In accordance with previous studies (Thomas, 2004; Joughin et al., 2012), our findings
22 suggest that the speeds observed today at JI are a result of thinning induced changes due to
23 reduction in resistive stress (buttressing) near the terminus correlated with inland steepening
24 slopes (Figs. 6 and 7). Both model and observations suggest that JI has been losing mass at an
25 accelerating rate and that the glacier has continued to accelerate through 2014 (Fig. 4).

Author Contributions

I.S.M. was responsible for the numerical modelling part. J.B. provided the bed model. M.R.V.D.B, and P.K.M. provided climate data. S.A.K and B.W. provided observational data. I.S.M. and S.A.K created the figures and wrote the manuscript with contributions from A. A, J.B., T.V.D., M.R.V.D.B, B.W., P.K.M, K.K., and C.K.

Acknowledgements

Ioana S. Muresan is funded by the Forskningsraadet for Natur og Univers (grant no. 12-155118). Shfaqat A. Khan is supported by Carlsbergfondet (grant no. CF14-0145). Jonathan Bamber was part funded by UK NERC grant NE/M000869/1. Bert Wouters is funded by a Marie Curie International Outgoing Fellowship within the 7th European Community Framework Programme (FP7-PEOPLE-2011-IOF-301260). The development of PISM is supported by NASA grants NNX13AM16G and NNX13AK27G. We thank the editor, five anonymous reviewers for their valuable comments and suggestions to improve and clarify the manuscript, and Veit Helm for providing cryosat-2 data.

References

- Albrecht, T., M. Martin, M. Haseloff, R. Winkelmann, and A. Levermann. 2011. "Parameterization for subgrid-scale motion of ice-shelf calving fronts." *The Cryosphere* 5: 35–44. doi:10.5194/tc-5-35-2011.
- Amundson, J. M., M. Fahnestock, M. Truffer, J. Brown, M. P. Lüthi, and R. J. Motyka. 2010. "Ice mélange dynamics and implications for terminus stability, Jakobshavn Isbræ, Greenland." *J. Geophys. Res.* 115: F01005. doi:10.1029/2009JF001405.
- Aschwanden, A., E. Bueler, C. Khroulev, and H. Blatter. 2012. "An enthalpy formulation for glaciers and ice sheets." *J. Glaciol.* 58(209): 441–457. doi:10.5194/tcd-6-5069-2012. doi:10.3189/2012JoG11J088.
- Aschwanden, A., G. Aðalgeirsdóttir, and C. Khroulev. 2013. "Hindcast to measure ice sheet model sensitivity to initial states." *The Cryosphere* 7: 1083–1093. doi:10.5194/tcd-6-5069-2012.

1 Aschwanden, A., M. A. Fahnestock and M. Truffer. 2016. "Complex Greenland outlet glacier
2 flow captured". *Nat. Commun.* 7 (10524). doi: 10.1038/ncomms10524.

3 Bamber, J. L., J. A. Griggs, R. T. W. L. Hurkmans, J. A. Dowdeswell, S. P. Gogineni, I.
4 Howat, J. Mouginot, J. Paden, S. Palmer, E. Rignot, and D. Steinhage. 2013. "A new bed
5 elevation dataset for Greenland." *The Cryosphere* 7: 499–510. doi:10.5194/tc-7-499-2013.

6 Beckmann, A., and H. Goosse. 2003. "A parameterization of ice shelf–ocean interaction for
7 climate models." *Ocean Model.* 5 (2): 157–170. doi:10.1016/S1463-5003(02)00019-7.

8 Bevan, S. L., A. J. Luckman, and T. Murray. 2012. "Glacier dynamics over the last quarter of
9 a century at Helheim, Kangerdlugssuaq and other major Greenland outlet glaciers." *The*
10 *Cryosphere* 6: 923–937. doi:10.5194/tc-6-923-2012.

11 Bindshadler, R. A., S. Nowicki, A. Abe-Ouchi, A. Aschwanden, H. Choi, J. Fastook, G.
12 Granzow, et al. 2013. "Ice-Sheet Model Sensitivities to Environmental Forcing and Their Use
13 in Projecting Future Sea Level (the SeaRISE Project)." *J. Glaciol.* 59 (214): 195–224.
14 doi:10.3189/2013JoG12J125.

15 Broeke, M. van den, J. Bamber, J. Ettema, Eric Rignot, E. Schrama, W. J. van de Berg, E. van
16 Meijgaard, I. Velicogna, and B. Wouters. 2009. "Partitioning recent Greenland mass loss."
17 *Science* 326 (5955): 984–986. doi:10.1126/science.1178176.

18 Bueler, E., and J. Brown. 2009. "Shallow shelf approximation as a 'sliding law' in a
19 thermodynamically coupled ice sheet model." *J. Geophys. Res.* 114: F03008.
20 doi:10.1029/2008JF001179.

21 Csatho, B., T. Schenk, C. J. Van Der Veen and W. B. Krabill. 2008. "Intermittent thinning of
22 Jakobshavn Isbræ, West Greenland, since the Little Ice Age." *J. Glaciol.* 54 (184): 131–144.
23 doi: 10.3189/002214308784409035.

24 Cuffey, K. M., and W. S. B. Paterson. 2010. "The Physics of Glaciers". Elsevier, 4th edition.
25 ISBN 9780123694614.

26 de Juan, J., P. Elósegui, M. Nettles, T.B. Larsen, J.L. Davis, G.S. Hamilt, L.A. Stearns, M.
27 L. Anderson, G. Ekström, L. Stenseng, S. A. Khan, R. Forsberg. 2010. "Sudden increase in
28 tidal response linked to calving and acceleration at a large Greenland outlet glacier".
29 *Geophys. Res. Lett.* 37: L12501. doi:10.1029/2010GL043289.

1 Echelmeyer, K.A., W.D. Harrison, C. Larson, and J.E. Mitchell. 1994. The role of the
2 margins in the dynamics of an active ice stream. *J. Glaciol.* 40(136): 527–538.

3 Enderlin, E. M., I. M. Howat, and A. Vieli. 2013. “High sensitivity of tidewater outlet glacier
4 dynamics to shape.” *The Cryosphere* 7: 1007–1015. doi: 10.5194/tc-7-1007-2013.

5 Enderlin, E. M., I. M. Howat, S. Jeong, M. J. Noh, J. H. van Angelen, and M. R. van den
6 Broeke. 2014. “An improved mass budget for the Greenland ice sheet.” *Geophys. Res. Lett.*
7 41: 866–872. doi:10.1002/2013GL059010.

8 Feldmann, J., T. Albrecht, C. Khroulev, F. Pattyn, and A. Levermann. 2014. “Resolution-dependent performance of grounding line motion in a
9 shallow model compared with a full-Stokes model according to the MISMIP3d
10 intercomparison.” *J. Glaciol.* 60 (220): 353–360. doi:10.3189/2014JoG13J093.

11 Feldmann, J., Albrecht, T., Khroulev, C., Pattyn, F., and Levermann, A.: Resolution-
12 dependent performance of grounding line motion in a shallow model compared with a full-
13 Stokes model according to the MISMIP3d intercomparison, *J. Glaciol.*, 60, 353–360,
14 doi:10.3189/2014JoG13J093, 2014.

15 Gladish, C. V., D. M. Holland, and C. M. Lee. 2015a. “Oceanic boundary conditions for
16 Jakobshavn Glacier. Part II: Provenance and sources of variability of Disko Bay and Ilulissat
17 icefjord waters, 1990–2011.” *J. Phys. Oceanogr.* 45: 33–63. doi:dx.doi.org/10.1175/JPO-D-
18 14-0045.1.

19 Gladish, C. V., D. M. Holland, A. Rosing-Asvid, J. W. Behrens, and J. Boje. 2015b. “Oceanic
20 boundary conditions for Jakobshavn Glacier. Part I: Variability and renewal of Ilulissat
21 icefjord waters, 2001–2014.” *J. Phys. Oceanogr.* 45: 3–32. doi:dx.doi.org/10.1175/JPO-D-14-
22 0044.1.

23 Gladstone, R. M., A. J. Payne, and S. L. Cornford. 2010. “Parameterising the grounding line
24 in flow-line ice sheet models.” *The Cryosphere* 4: 605–19. doi:10.5194/tc-4-605-2010.

25 Hanna, E., X. Fettweis, S. Mernild, J. Cappelen, M. Ribergaard, C. Shuman, K. Steffen, L.
26 Wood, and T. Mote. 2014. “Atmospheric and oceanic climate forcing of the exceptional
27 Greenland ice sheet surface melt in summer 2012.” *Int. J. Climatol.* 34 (4): 1022–1037.
28 doi:10.1002/joc.3743.

29 Holland, D. M., R. H. Thomas, B. de Young, M. H. Ribergaard, and B. Lyberth. 2008.
30 “Acceleration of Jakobshavn Isbræ Triggered by Warm Subsurface Ocean Waters.” *Nat.*
31 *Geosci.* 1: 659–664. doi:10.1038/ngeo316.

1 Howat I. M., Y. Ahn, I. Joughin, M. R. van den Broeke, J. T. M. Lenaerts, and B. Smith.
2 2011. "Mass balance of Greenland's three largest outlet glaciers, 2000–2010." *Geophys. Res.*
3 *Lett.* 38(12): L12501. doi: 10.1029/2011GL047565.

4 Hutter K. 1983. "Theoretical Glaciology: Material Science of Ice and the Mechanics of
5 Glaciers and Ice Sheets." D. Reidel Publishing Co. Tokyo, Terra Scientific Publishing Co.
6 xxxii, 510 p.

7 IPCC. 2013. "Climate Change 2013: The Physical Science Basis. Contribution of Working
8 Group I to the Fifth Assessment Report of the Intergovernmental Panel on Climate Change."
9 Cambridge University Press, Cambridge, United Kingdom and New York, NY, USA: 1535
10 pp. doi:10.1017/CBO9781107415324.

11 Jamieson, S. S. R., A. Vieli, S. J. Livingstone, C. Ó Cofaigh, C. Stokes, C.-D. Hillenbrand,
12 and J. A. Dowdeswell. 2012. "Icestream stability on a reverse bed slope". *Nat. Geosci.* 5
13 :799–802. doi:10.1038/N GEO1600.

14 Jones, P. W. 1999. "First- and Second-Order Conservative Remapping Schemes for Grids in
15 Spherical Coordinates". *Mon. Weather Rev.* 127 (9): 2204–2210. doi:
16 [http://dx.doi.org/10.1175/1520-0493\(1999\)127<2204:FASOCR>2.0.CO;2](http://dx.doi.org/10.1175/1520-0493(1999)127<2204:FASOCR>2.0.CO;2).

17 Joughin, I., W. Abdalati, and M. Fahnestock. 2004. "Large fluctuations in speed on
18 Greenland's Jakobshavn Isbræ glacier." *Nature* 432: 608–610. doi:10.1038/nature03130.

19 Joughin, I., I. M. Howat, M. Fahnestock, B. Smith, W. Krabill, R. B. Alley, H. Stern, and M.
20 Truffer. 2008. "Continued evolution of Jakobshavn Isbrae Following Its Rapid Speedup." *J.*
21 *Geophys. Res.* 113: F04006. doi:10.1029/2008JF001023.

22 Joughin, I., B. E. Smith, I. M. Howat, T. Scambos, and T. Moon. 2010. "Greenland Flow
23 Variability from Ice-Sheet-Wide Velocity Mapping". *J. Glaciol.* 56 (197): 415-430.
24 doi:10.3189/002214310792447734.

25 Joughin, I., I. Howat, B. Smith, and T. Scambos. 2011. "MEaSURES Greenland Ice Velocity:
26 Selected Glacier Site Velocity Maps from InSAR". Boulder, Colorado, USA: NASA DAAC
27 at the National Snow and Ice Data Center. doi:10.5067/MEASURES/CRYOSPHERE/nsidc-
28 0481.001.

29 Joughin, I., B. E. Smith, I. M. Howat, D. Floricioiu, R. B. Alley, M. Truffer, and M.
30 Fahnestock. 2012. "Seasonal to decadal scale variations in the surface velocity of Jakobshavn

1 Isbræ, Greenland: Observation and model-based analysis.” *J. Geophys. Res.* 117: F02030.
2 doi:10.1029/2011JF002110.

3 Joughin, I., S. B. Das, G. E. Flowers, M. D. Behn, R. B. Alley, M. A. King, B. E. Smith, J. L.
4 Bamber, M. R. van den Broeke, and J. H. van Angelen. 2013. “Influence of ice-sheet
5 geometry and supraglacial lakes on seasonal ice-flow variability.” *The Cryosphere* 7: 1185-
6 1192. doi:10.5194/tc-7-1185-2013.

7 Joughin, I., B. E. Smith, D. E. Shean, and D. Floricioiu. 2014. “Brief Communication: Further
8 summer speedup of Jakobshavn Isbræ.” *The Cryosphere* 8: 209–214. doi:10.5194/tc-8-209-
9 2014.

10 Keegan, K. M., R.M. Albert, J. R. McConnell and I. Baker. 2014. “Climate change and forest
11 fires synergistically drive widespread melt events of the Greenland Ice Sheet.” *P. Natl. Acad.*
12 *Sci.* 111(22): 7964–7967. doi: 10.1073/pnas.1405397111.

13 Khan, S. A., L. Liu, J. Wahr, I. Howat, I. Joughin, T. van Dam, and K. Fleming. 2010. “GPS
14 measurements of crustal uplift near Jakobshavn Isbræ due to glacial ice mass loss.” *J.*
15 *Geophys. Res.* 115: B09405. doi:10.1029/2010JB007490.

16 Khan, S. A., K. H. Kjær, M. Bevis, J. L. Bamber, J. Wahr, K. K. Kjeldsen, A. A. Bjørk, N. J.
17 Korsgaard, L. A. Stearns, M. R. van den Broeke, L. Liu, N. K. Larsen, and I. S. Muresan.
18 2014. “Sustained Mass Loss of the Northeast Greenland Ice Sheet Triggered by Regional
19 Warming.” *Nat. Clim. Change* 4: 292–299. doi:10.1038/nclimate2161.

20 Khan, S. A., A. Aschwanden, A. A. Bjørk, J. Wahr, K. K. Kjeldsen, and K. H. Kjær. 2015.
21 “Greenland ice sheet mass balance: a review.” *Rep. Prog. Phys.* 78(4). doi: 10.1088/0034-
22 4885/78/4/046801.

23 Kimura, S., P. R. Holland, A. Jenkins, and M. Piggott. 2014. “The effect of meltwater plumes
24 on the melting of a vertical glacier face.” *J. Phys. Oceanogr.* 44: 3099-3117. doi:
25 10.1175/JPO-D-13-0219.1

26 Krabill, W., W. Abdalati, E. Frederick, S. Manizade, C. Martin, J. Sonntag, R. Swift, R.
27 Thomas, W. Wright, and J. Yungel. 2000. “Greenland Ice Sheet: High-Elevation Balance and
28 Peripheral Thinning.” *Science* 289: 428–430. doi:10.1126/science.289.5478.428.

29 Krabill, W., E. Hanna, P. Huybrechts, W. Abdalati, J. Cappelen, B. Csatho, E. Frederick, S.
30 Manizade, C. Martin, J. Sonntag, R. Swift, R. Thomas, and J. Yungel. 2004. “Greenland Ice

1 Sheet: Increased coastal thinning”, *Geophys. Res. Lett.* 31: L24402.
2 doi:10.1029/2004GL021533.

3 Krabill, W. B. 2014. “IceBridge ATM L2 Icessn Elevation, Slope, and Roughness, [1993-
4 2014]. Boulder, Colorado USA: NASA Distributed Active Archive Center at the National
5 Snow and Ice Data Center. Digital media.Updated 2014.” <http://nsidc.org/data/ilatm2.html>.

6 Larour, E., H. Seroussi, M. Morlighem, and E. Rignot. 2012. “Continental scale, high order,
7 high spatial resolution, ice sheet modeling using the Ice Sheet System Model (ISSM).” *J.*
8 *Geophys. Res.-Earth* (2003-2012) 117: F01022. doi:10.1029/2011JF002140.

9 Levermann, A., T. Albrecht, R. Winkelmann, M. A. Martin, M. Haseloff, and I. Joughin.
10 2012. “Kinematic first-order calving law implies potential for abrupt ice-shelf retreat.” *The*
11 *Cryosphere* 6: 273–286. doi:10.5194/tc-6-273-2012.

12 Luckman, A., and T. Murray. 2005. “Seasonal variation in velocity before retreat of
13 Jakobshavn Isbræ, Greenland.” *J. Geophys. Res. Letters* 32: L08501.
14 doi:10.1029/2005GL022519.

15 MacAyeal, D. R., T. A. Scambos, C. L. Hulbe and M. A. Fahnestock. 2003. “Catastrophic
16 iceshelf break-up by an ice-shelf-fragment-capsize mechanism.” *J. Glaciol.* 49(164): 22-36.

17 Mahaffy, M. W. 1976. “A three-dimensional numerical model of ice sheets: tests on the
18 Barnes Ice Cap, Northwest Territories”. *J. Geophys. Res.*, 81(6):1059–1066.

19 Martin, M. A., R. Winkelmann, M. Haseloff, T. Albrecht, E. Bueler, C. Khroulev, and A.
20 Levermann. 2011. “The Potsdam Parallel Ice Sheet Model (PISM-PIK), Part II: Dynamical
21 equilibrium simulation of the Antarctic Ice Sheet.” *The Cryosphere* 5: 727–740.
22 doi:10.5194/tc-5-727-2011.

23 Mengel, M., and A. Levermann. 2014. “Ice plug prevents irreversible discharge from East
24 Antarctica.” *Nat. Clim. Change* 4: 451–455. doi:10.1038/nclimate2226.

25 Moon, T., I. Joughin, B. Smith, and I. Howat. 2012. “21st-Century evolution of Greenland
26 outlet glacier velocities.” *Science* 336: 576–578. doi:10.1126/science.1219985.

27 Motyka, R. J., M. Truffer, M. Fahnestock, J. Mortensen, S. Rysgaard, and I. Howat. 2011.
28 “Submarine melting of the 1985 Jakobshavn Isbræ floating tongue and the triggering of the
29 current retreat.” *J. Geophys. Res.* 116: F01007. doi:10.1029/2009JF001632.

1 NSIDC. 2015. "2014 melt season in review." National Snow & Ice Data Center (NSIDC).
2 Accessed July 09, 2015. [http://nsidc.org/greenland-today/2015/01/2014-melt-season-in-](http://nsidc.org/greenland-today/2015/01/2014-melt-season-in-review/)
3 [review/](http://nsidc.org/greenland-today/2015/01/2014-melt-season-in-review/).

4 Nghiem, S. V., D. K. Hall, T. L. Mote, M. Tedesco, M. R. Albert, K. Keegan, C. A. Shuman,
5 N. E. DiGirolamo, and G. Neumann. 2012. "The extreme melt across the Greenland ice sheet
6 in 2012." *Geophys. Res. Lett.* 39: L20502. doi: 10.1029/2012GL053611.

7 Nick, F. M., A. Vieli, M. L. Andersen, I. Joughin, A. Payne, T. L. Edwards, F. Pattyn, and R.
8 S. van de Wal. 2013. "Future sea-level rise from Greenland's main outlet glaciers in a
9 warming climate." *Nature* 497: 235–238. doi:10.1038/nature12068.

10 Nick, F.M., A. Vieli, I. M. Howat, and I. Joughin. 2009. "Large-Scale Changes in Greenland
11 Outlet Glacier Dynamics Triggered at the Terminus." *Nat. Geosci.* 2: 110–114.
12 doi:10.1038/ngeo394.

13 Nielsen, K., S. A. Khan, G. Spada, J. Wahr, M. Bevis, L. Liu, and T. van Dam. 2013.
14 "Vertical and horizontal surface displacements near Jakobshavn Isbræ driven by melt-induced
15 and dynamic ice loss." *J. Geophys. Res.-Sol. Ea.* 118: 1837–1844. doi:10.1002/jgrb.50145.

16 Noël, B., W. J. van de Berg, E. van Meijgaard, P. Kuipers Munneke, R. S. W. van de Wal,
17 and M. R. van den Broeke. 2015. "Summer snowfall on the Greenland Ice Sheet: a study with
18 the updated regional climate model RACMO2.3." *The Cryosphere Discussion* 9: 1177-1208.
19 doi: 10.5194/tcd-9-1177-2015.

20 Parizek, B.R., and R.T. Walker. 2010. "Implications of initial conditions and ice–ocean
21 coupling for grounding-line evolution." *Earth Planet. Sci. Lett.* 300: 351–358.
22 doi:10.1016/j.epsl.2010.10.016.

23 Pattyn, F., C. Schoof, L. Perichon, R. C. A. Hindmarsh, E. Bueler, B. de Fleurian, G. Durand,
24 et al. 2012. "Results of the Marine Ice Sheet Model Intercomparison Project, MISMP." *The*
25 *Cryosphere* 6: 573–588. doi:10.5194/tc-6-573-2012.

26 Pattyn, F., Perichon, L., Durand, G., Favier, L., Gagliardini, O., Hindmarsh, R., Zwinger, T.,
27 Albrecht, T., Cornford, S., Docquier, D., Fust, J. J., Goldberg, D., Gudmundsson, G. H.,
28 Humbert, A., Hutten, M., Huybrechts, P., Jouvett, G., Kleiner, T., Larour, E. and Martin, D.,
29 Morlighem, M., Payne, A. J., Pollard, D., Ruckamp, M., Rybak, O., Seroussi, H.,
30 Thoma, M., and Wilkens, N. 2010. "Grounding-line migration in plan-view marine ice-sheet

1 models: results of the ice2sea MISMIP3d intercomparison“. J. Glaciol. 59: 410–422.
2 doi:<http://dx.doi.org/10.3189/2013JoG12J12910.3189/2013JoG12J129>.

3 Pollard, D., R. M. DeConto, and R. B. Alley. 2015. “Potential Antarctic Ice Sheet retreat
4 driven by hydrofracturing and ice cliff failure.” *Earth Planet. Sci. Lett.* 412: 112–121. doi:
5 10.1016/j.epsl.2014.12.035.

6 Price, S. F., A. J. Payne, I. M. Howat, and B. E. Smith. 2011. “Committed sea-level rise for
7 the next century from Greenland ice sheet dynamics during the past decade.” *P. Natl. Acad.*
8 *Sci. USA* 108: 8978–8983. doi:10.1073/pnas.1017313108.

9 Rignot, E., J. L. Bamber, M. R. van den Broeke, C. Davis, Y. Li, W. J. van de Berg, and E.
10 van Meijgaard. 2008. “Recent Antarctic ice mass loss from radar interferometry and regional
11 climate modeling.” *Nat. Geosci.* 1: 106–110. doi:10.1038/ngeo102.

12 Schoof, C. 2007. “Ice sheet grounding line dynamics: steady states, stability, and hysteresis.”
13 *J. Geophys. Res.* 112 (F03S28). doi:10.1029/2006JF000664.

14 Schoof, C. and R. Hindmarsh. 2010. “Thin-film flows with wall slip: an asymptotic analysis
15 of higher order glacier flow models”. *Quart. J. Mech. Appl. Math.* 63(1): 73–114. doi:
16 10.1093/qjmam/hbp025.

17 Seroussi, H., H. B. Dhia, M. Morlighem, E. Larour, E. Rignot, and D. Aubry. 2012.
18 “Coupling ice flow models of varying orders of complexity with the Tiling method.” *J.*
19 *Glaciol.* 58: 776–786. doi:10.3189/2012JoG11J195.

20 Shapiro, N. M., and M. H. Ritzwoller. 2004. “Inferring surface heat flux distributions guided
21 by a global seismic model: particular application to Antarctica.” *Earth Planet. Sci. Lett.* 223:
22 213–224. doi: 10.1016/j.epsl.2004.04.011.

23 Shepherd, A., E. R. Ivins, A. Geruo, V. R. Barletta, M. J. Bentley, S. Bettadpur, K. H. Briggs,
24 D. H. Bromwich, et al. 2012. “A reconciled estimate of ice-sheet mass balance.” *Science*
25 338(6111): 1183–1189. doi:10.1126/science.1228102.

26 Slater, D. A., P. W. Nienow, T. R. Cowton, D. N. Goldberg, and A. J. Sole. 2015. “Effect of
27 near-terminus subglacial hydrology on tidewater glacier submarine melt rates.” *Geophys. Res.*
28 *Lett.* 42: 2861–2868. doi: 10.1002/2014GL062494.

1 Sohn, H. G., K. C. Jezek, and C. J. van der Veen. 1998. "Jakobshavn Glacier, west Greenland:
2 30 years of spaceborne observations." *Geophys. Res. Lett.* 25(14): 2699-2702. doi:
3 10.1029/98GL01973.

4 Stanley, S. J., A. Jenkins, C. F. Giulivi and P. Dutrieux. 2011. "Stronger ocean circulation and
5 increased melting under Pine Island Glacier ice shelf." *Nat. Geosci.* 4: 519–523. doi:
6 10.1038/ngeo1188

7 Tedesco, M., X. Fettweis, T. Mote, J. Wahr, P. Alexander, J. E. Box, and B. Wouters. 2013.
8 "Evidence and analysis of 2012 Greenland records from spaceborne observations, a regional
9 climate model and reanalysis data." *The Cryosphere* 7: 615-630. doi: 10.5194/tc-7-615-2013

10 The PISM Authors. 2014. "PISM, a Parallel Ice Sheet Model. User's Manual." Accessed
11 June 15, 2015. <http://www.pism-docs.org/wiki/lib/exe/fetch.php?media=manual.pdf>.

12 Thomas, H. R., W. Abdalati, E. Frederick, W. B. Krabill, S. Manizade, and K. Steffen. 2003.
13 "Investigation of surface melting and dynamic thinning on Jakobshavn Isbræ." *J. Glaciol.* 49
14 (165): 231–239. doi:10.3189/172756503781830764.

15 Thomas, R. H. 2004. "Force-perturbation analysis of recent thinning and acceleration of
16 Jakobshavn Isbrae, Greenland." *J. Glaciol.* 50(168): 57–66. doi:
17 10.3189/172756504781830321.

18 Tulaczyk, S., W. B. Kamb, and H. F. Engelhardt. 2000a. "Basal mechanics of Ice Stream B,
19 West Antarctica 1. Till mechanics". *J. Geophys. Res.* 105(B1):463–481. doi:
20 10.1029/1999JB900329.

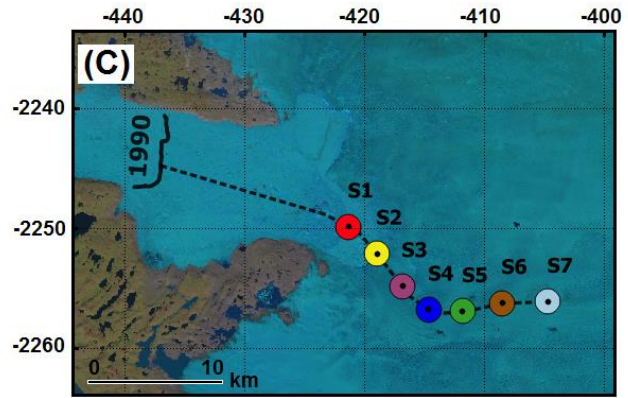
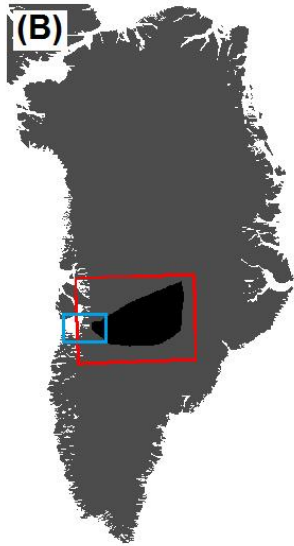
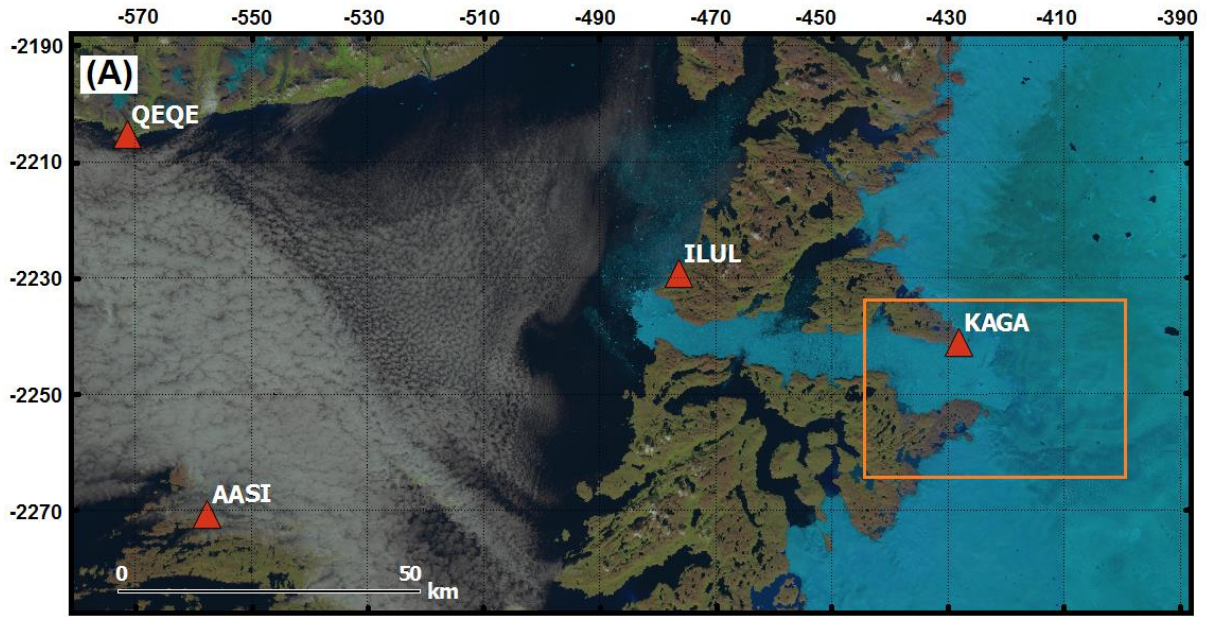
21 Tulaczyk, S., W. B. Kamb, and H. F. Engelhardt. 2000b. "Basal mechanics of Ice Stream B,
22 West Antarctica 2. Undrained plastic bed model". *J. Geophys. Res.* 105(B1): 483–494. doi:
23 10.1029/1999JB900328.

24 Van der Veen, C. J., J. C. Plummer, and L. A. Stearns. 2011. "Controls on the recent speed-up
25 of Jakobshavn Isbræ, West Greenland." *J. Glaciol.* 57 (204): 770–782.

26 Vieli, A., and F. M. Nick. 2011. "Understanding and Modeling Rapid Dynamic Changes of
27 Tidewater Outlet Glaciers: Issues and Implications." *Surv. Geophys.* 32: 437–458. doi:
28 10.1007/s10712-011-9132-4.

29 Weis M., R. Greve, and K. Hutter. 1999. "Theory of shallow ice shelves". *Continuum*
30 *Mechanics and Thermodynamics* 11(1): 15–50.

Winkelmann, R., M. A. Martin, M. Haseloff, T. Albrecht, E. Bueler, C. Khroulev, and A.
Levermann. 2011. “The Potsdam Parallel Ice Sheet Model (PISM-PIK) Part 1: Model
description.” *The Cryosphere* 5: 715–726. doi:10.5194/tc-5-715-2011.



1
2 Figure 1. (A) Landsat 8 image of Ilulissat fjord and part of Disko Bay acquired in August
3 2014. The dark orange triangles indicate the locations of the GPS stations (GPS data shown in
4 Fig. 5). The rectangle defined by light orange borders outlines the location of Fig. 1C. (B)
5 Grey filled Greenland map. The black filled rectangle highlights the JI basin used to compute
6 the mass loss (Fig. 4) and is identical to Khan et al. (2014). The rectangle defined by red
7 borders indicates the computational domain. The light blue border rectangle represents the
8 location of Fig. 1A. (C) Coloured circles indicate the locations plotted in Fig. 3. The thick
9 black line denotes the JI terminus position in the 1990s. The dotted black line represents the
10 flow-line location plotted in Fig. 6. The coordinates given in (A) and (C) are in polar-
11 stereographic projection units (km).

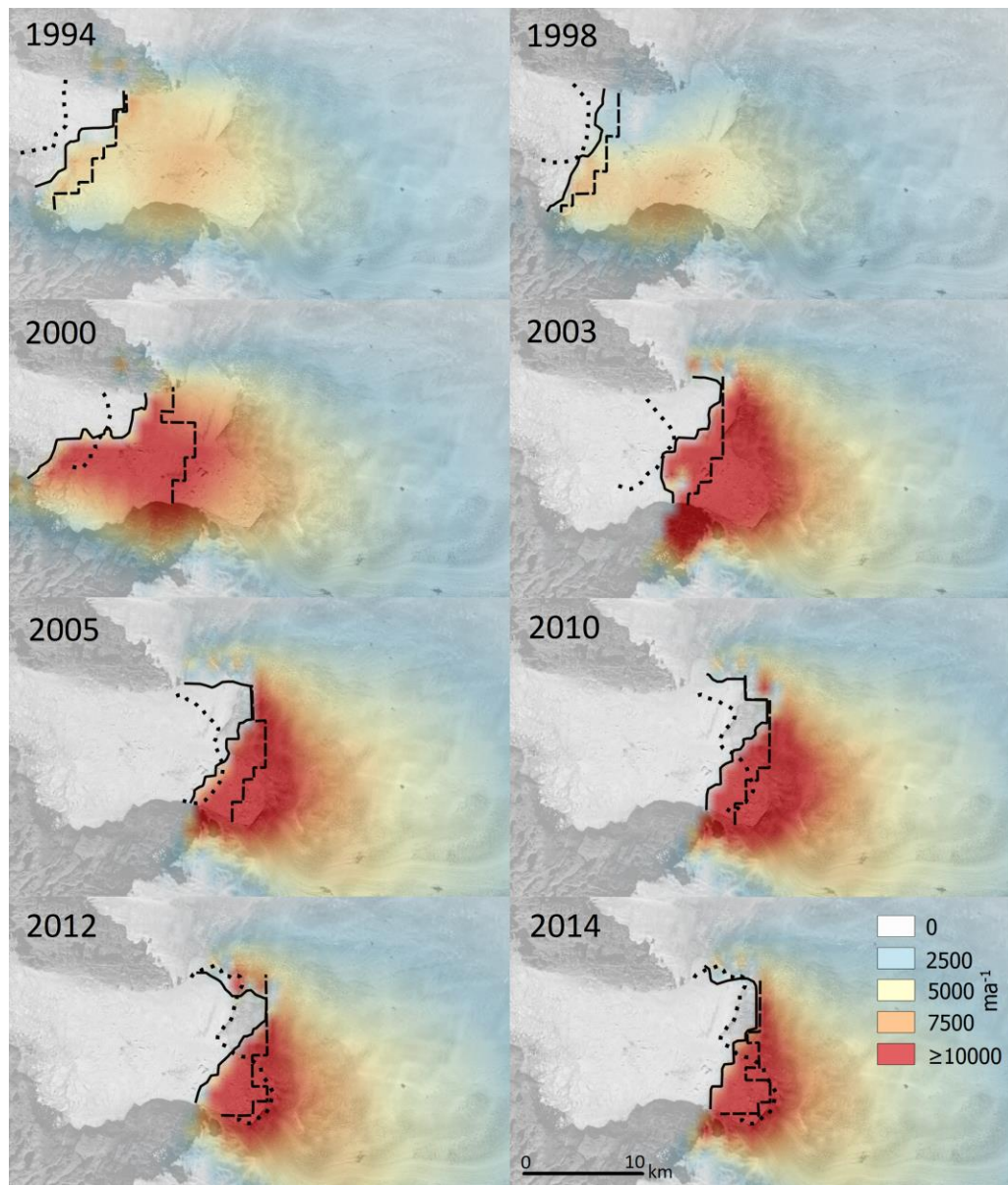


Figure 2. Modelled velocities at Jakobshavn Isbræ for December are shown for eight different years. The black line represents the modelled front positions, the black dotted line denotes the observed front position and the thick black dashed line represents the modelled grounding line position. The velocities are superimposed over a Landsat 8 image acquired in August 2014.

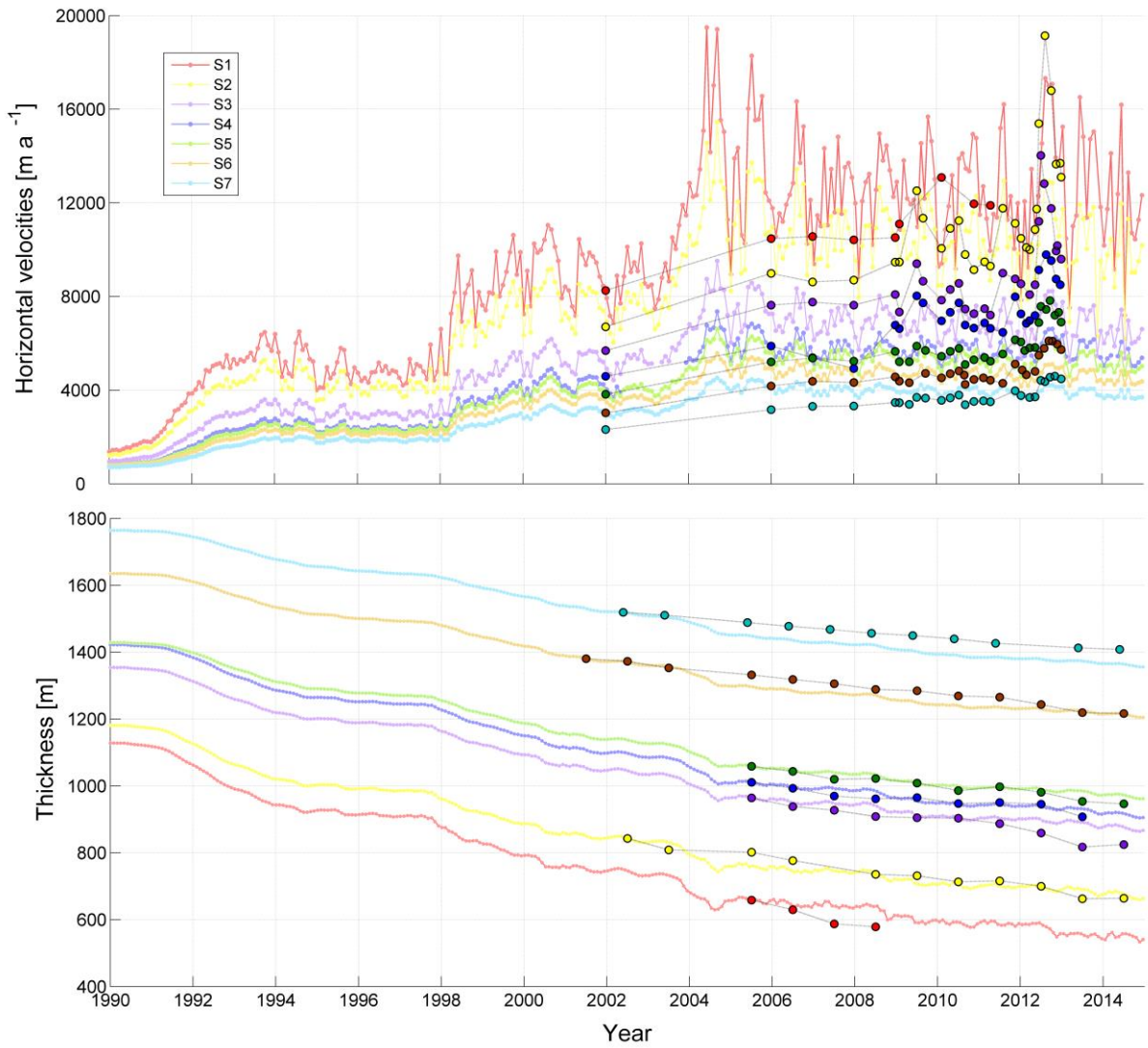


Figure 3. (A) Time series of modelled (filled circles) versus observed (filled circles with black edges) velocities (Joughin et al., 2010) (top figure) and ice thickness changes (Krabbil, 2014) (bottom figure) for the period 1990-2014 at locations (S1 to S7) shown in Fig. 1C. The same colour scheme is used for the modelled and the observed data. The observed velocities prior to 2009 are mean winter velocities and are largely consistent with our modelled winter estimates for the same period. The observed thickness has been adjusted to match the model thickness at the first available observation (i.e., by summing the modelled ice thickness corresponding to the first available observation with the observed thickness changes).

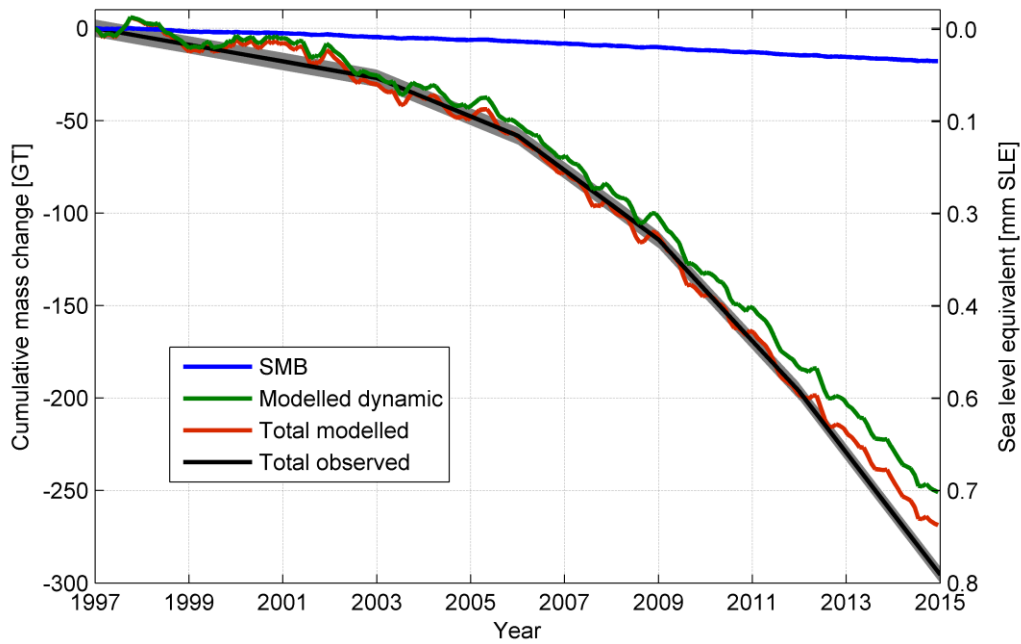


Figure 4. Modelled and observed cumulative mass change for Jakobshavn Isbræ. The blue curve represents the mass change due to SMB (Noël et al., 2015)) after the 1960-1990 baseline is removed. The green curve represents the modelled ice dynamics mass change (i.e., modelled mass change minus SMB change). The red curve represents the total modelled mass change including both SMB and ice dynamic changes. The black curve with grey error limits represents the total observed mass change including both SMB and ice dynamic changes. The modelled mass change for the period 1997-2014 is ~269 Gt and the observed mass change is ~296 Gt.

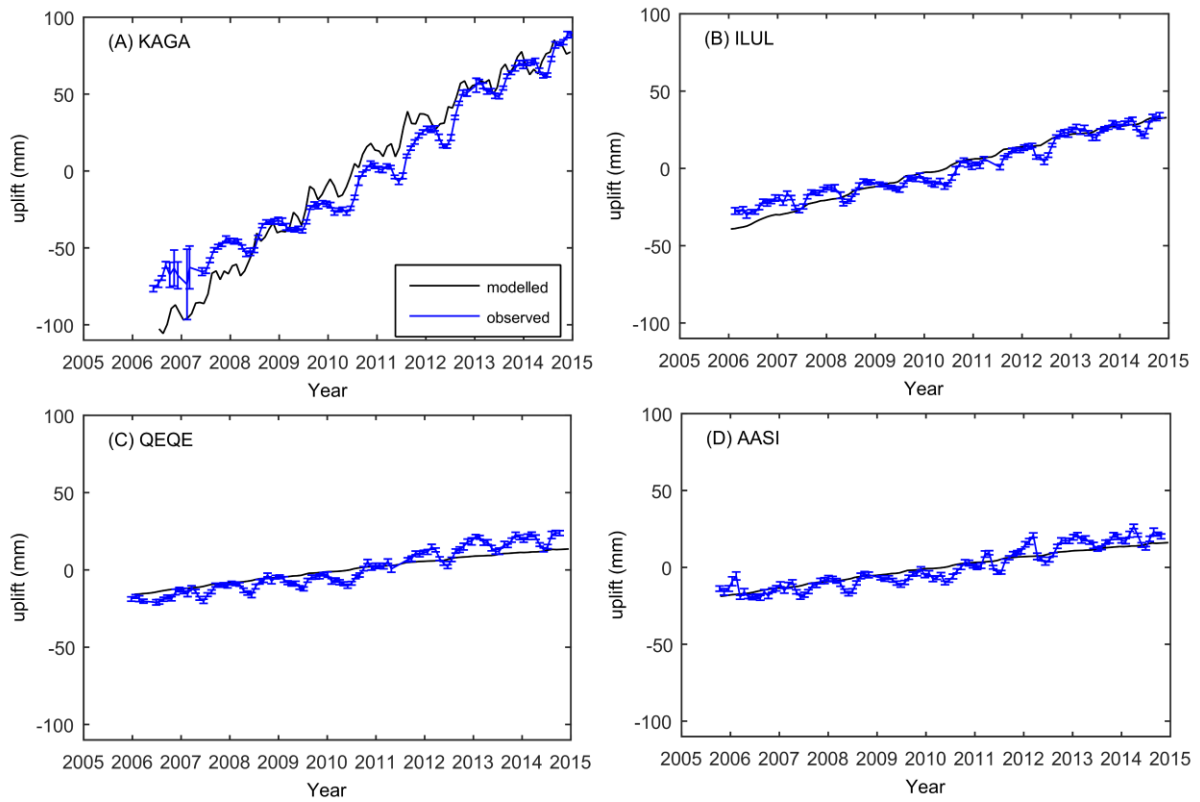


Figure 5. Observed versus modelled uplift in mm for the stations KAGA (A), ILUL (B), QEQE (C) and AASI (D). The positions of the four GPS stations are presented in Fig. 1A.

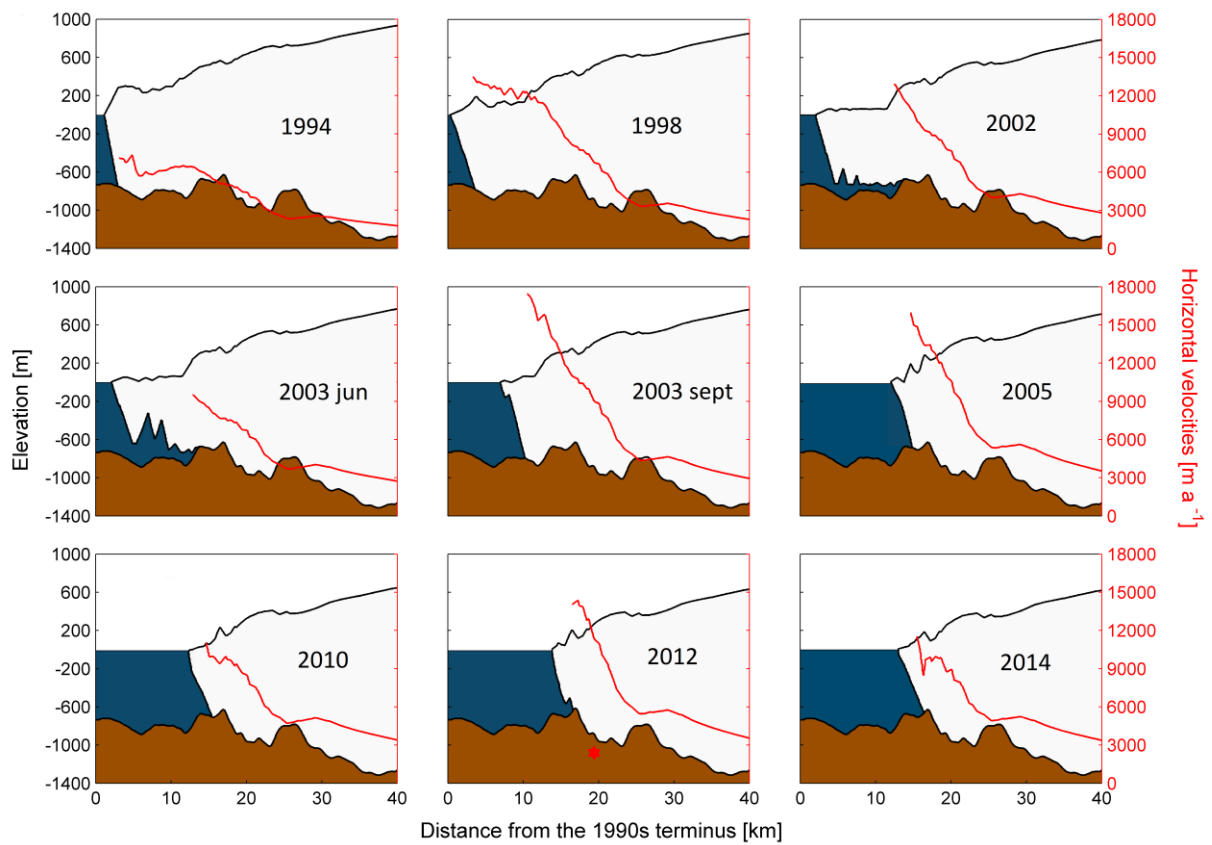


Figure 6. Modelled evolution of surface elevation (floating ice tongues thinner than 50 m are not shown) and horizontal velocities of Jakobshavn Isbræ for December along the flow-line shown in Fig. 1C. Note the acceleration in speed between 1994-1998 and between June 2003 and September 2003 corresponding to the final breakup of the floating tongue. The red star denotes the observed 2012 terminus position.

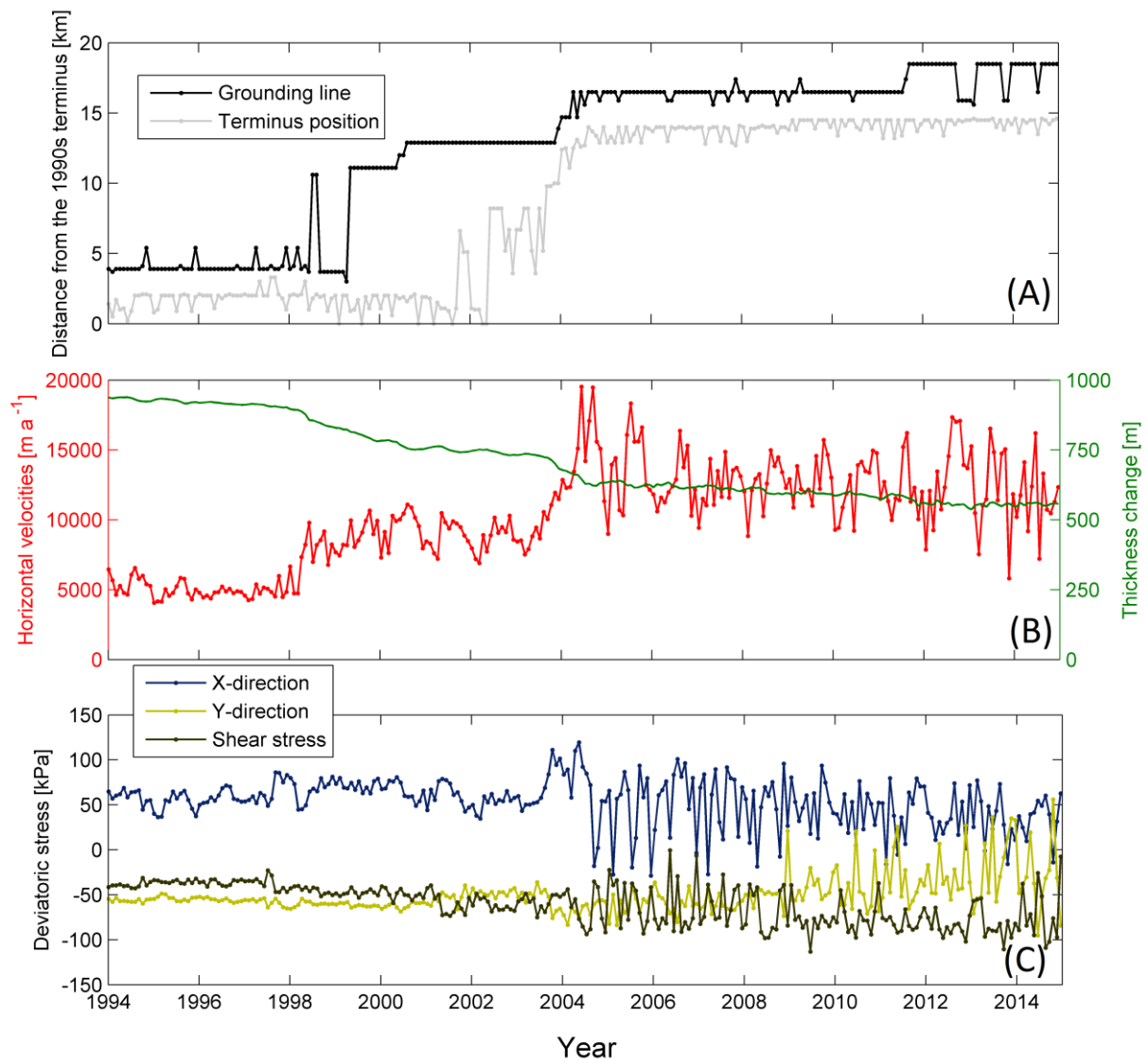


Figure 7. (A) Modelled grounding line and terminus position (floating ice tongues thinner than 50 m are not shown). (B) Modelled horizontal velocities and ice thickness changes at the point location S1 shown in Fig. 1C. (C) Modelled 2D deviatoric stresses (in the X direction, the Y direction, and the shear stress) at the point location S1 shown in Fig. 1C.